Determination of Site Information for Seismic Stations in Switzerland

Work Package 4: Pegasos Refinement Project

Donat Fäh, Stefan Fritsche,
Valerio Poggi, Gabriela Gassner-Stamm, Philipp Kästli,
Jan Burjanek, Peter Zweifel, Sascha Barman, John Clinton

Schweizerischer Erdbebendienst
ETH Zürich

Lori Keller
GeoExpert AG

Philippe Renault, Stefan Heuberger
SwissNuclear

Report

SED/PRP/R/004/20090831

1. Site-Characterization Project

1.1. Summary

This report summarizes the site characterization of more than 30 weak- and strong-motion stations in Switzerland. This includes the following elements: collection of all available data for the stations of interest: i.e., geological, geophysical, soil classification, geotechnical information, physiography of the site and data on sensor installation (e.g., tunnel, vault, building, free-field, etc.), available borehole information from locations near-by, and available standard penetration test (SPT) values in the area of the station. In addition, the fundamental frequency of resonance at the selected stations was determined using ambient vibrations, as well as the investigation of possible site effects due to topography or soft sediments. Some sites of seismic stations have been investigated in the past using geophysical methods. Measurements have been reassessed in order to retrieve average shear wave velocities in the upper 5 to at least 30m. The SP2 experts selected another 20 station sites for seismic measurements in Switzerland. The selection of the sites was based on the number of useful recordings at each site and their location in the Swiss foreland region. The initial plan to additionally perform measurements at selected seismic stations in Germany and France was not possible due to the limited time of the project and administrational issues. The measurements were made by the external contractor GeoExpert AG, using hybrid P-wave seismic surveys, S-wave seismic surveys and Multiple channel Analysis of Surface Waves (MASW). Control measurements by the Swiss Seismological Service (SED) at 3 sites (SULZ, SLE, BOURR) were used to assess the quality of results. The project team reviewed and validated all measurements of the 20 sites using the available data.

This report documents the work done in working package 4 of the PEGASOS Refinement Project (PRP) and provides the most important outcomes in three parts. The first part overviews the data and measurements, and summarizes the key results in tabular form. Appendix A consists of short summaries for the 20 investigated sites and measurements at the site ZUR that is not documented in publicly accessible reports. Appendix A presents the results and considerations that led to the interpretation of the average S-wave velocities. Appendix B includes three reports for the control measurements at the 3 sites SULZ, SLE and BOURR using ambient vibration array techniques.

This work package includes a compilation of a database that is accessible via the internet at:

http://histserver.ethz.ch/stations/stations.html

The database will be extended in the future and thus will continuously change in time. A snapshot at the end of August 2009 is provided on the DVD attached to this report. This DVD includes four folders containing further material in electronic form (figures and illustrations, extended station reports from the SED, reports from Geoexpert AG and literature).

1.2. Concept of the Project

Over the last few years, the Swiss Seismological Service (SED) has developed methods and concepts for the investigation and characterization of the sites of seismic instruments. Measurements and tests were mainly performed at sites in the Basel region as part of an INTERREG project (Fäh and Huggenberger, 2006). The general concept used here to characterize the sites is based on the outcome of the European project “Network of

Research Infrastructures for European Seismology" (NERIES) subproject "Geotechnical Site Characterization" (JRA4), which is dedicated to the development of reliable low-cost tools for geotechnical site characterization and the improvement of knowledge of recording site conditions throughout the Euro-Med region. In this project particular attention has been paid to the definition and collection of information regarding the general site condition and geographical location, the main features of the recordings, the geological and geomorphological setting of the area, the geological-geotechnical and geophysical surveys performed in the area and values of the available transfer functions and/or dispersion curves. The scheme defined during the NERIES project has been adapted and extended to our specific needs.
As in the past the SED had no systematic collection of seismic station site data, our project aimed to collect (1) geological and geotechnical information, (2) the physiography of the site, (3) data on sensor installation, (4) available borehole information from near-by locations, (5) available standard penetration tests (SPT) values, (6) fundamental frequency of resonance using ambient vibrations, (7) existing measurements and (8) noise spectra in order to investigate possible site effects due to topography or soft sediments. All these data are put into the online database. Over the course of the PEGASOS refinement project, the described information has been collected for a large number of seismic stations in Switzerland. Results from different site-investigation techniques have been (re-) assessed. This includes results from Spectral Analysis of Surface Waves (SASW), Multi channel Analysis of Surface Waves (MASW), ambient vibration array and ambient vibration H/V techniques, and P- and S-wave seismic surveys (surface and borehole measurements). Available Standard Penetration Test (SPT) and borehole information have been collected but not analyzed.
The contractor performing the measurements at 20 station sites for the PRP project is GeoExpert AG. Three investigation methods are used: 1) Shear-wave refraction tomography (used to check MASW), 2) Multiple channel Analysis of Surface Waves (MASW), 3) P-wave hybrid seismic data processing (combined reflection and refraction seismic surveys). The procedure for the interpretation of the results is described further on. The main output for the PRP project is the values of the average S-wave velocity in the upper 30m (vs30).
The availability of all collected site data is a big improvement compared to the PEGASOS project.

1.3. Stations selected for investigations

The PRP-SP2 experts selected the sites shown in Figure 1 for the measurement campaign. The selection of the sites was based on the number of useful recordings at each site and their location in the Swiss foreland region. The initial plan to additionally perform measurements at selected seismic stations in Germany and France was not possible due to the limited time of the project and administrational issues. Most of the instruments located on these sites are part of the Swiss Digital Seismic Network (SDSNet) and are equipped with broadband instruments, a few with short period 5s seismometers (ACB, TRULL, WEIN and STEIN). At some of the sites an accelerometer is operational in addition to the broadband instrument (BOUR, BNALP and SULZ). Station SKEH belongs to the Swiss Strong Motion Network (SSMNet).

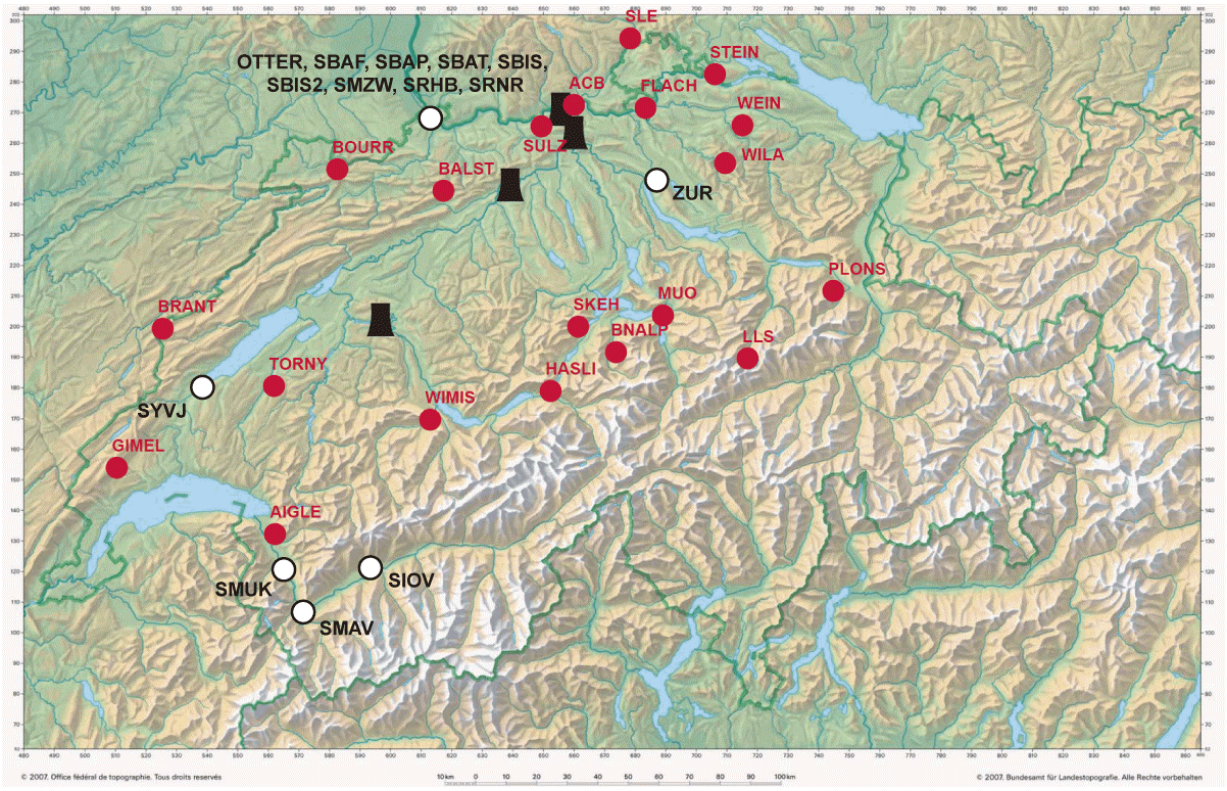

Figure 1: Selected sites for the measurement campaign (red dots) and sites investigated by the SED (white dots). (S. Heuberger, swissnuclear, 07.11.2008, modified by SED, 20.08.2009).

1.4. Seismic measurement at 20 sites

Many of the selected sites are in remote areas and are not accessible during wintertime. Most sites are located on rock, often in mountain areas and therefore on rough topography. The seismic instruments are placed in bunkers, galleries, small vaults, natural caves or small buildings. At some sites the rock is weathered or covered with a layer of loose sediments. The ground conditions are often very heterogeneous and the properties of the ground changes considerably within the measurement area and along the seismic lines. When possible, measurements were performed on two perpendicular seismic lines. For some sites, it was not possible to perform measurements directly at the site of the seismic station, and another site with similar ground conditions had to be selected. After selection of the profiles, the contractor GeoExpert applied, if possible, the following three investigation methods at each chosen site:

1. **P-wave hybrid seismics** (combined reflection and refraction seismics). This method was used to map the shallow soil conditions and bedrock along the seismic lines. The method allows the identification of strong lateral changes along the survey lines, so that only those parts of the profile most similar to the site of the seismic station could be selected for the estimation of the S-wave velocity profile. The measured P-wave velocities allowed the definition of a theoretical upper bound for the S-wave velocity by assuming a vp/vs-ratio of square root of 3. This upper bound was used to verify the measured S-wave profiles.
2. **Multiple channel Analysis of Surface Waves (MASW)**. In general the MASW results are used in order to derive S-wave velocity profiles. Dispersion curves are measured using the recorded vertical ground motion only. It was assumed that the measured curve corresponds to the fundamental mode Rayleigh wave. For rock sites

in particular, where there is an absence of layers of weathered material, this assumption cannot be verified. Where the higher mode Rayleigh waves are actually measured this would lead to an overestimation of S-wave velocities (see discussion for site SULZ in Appendix B). In addition to the fundamental mode, higher modes could be identified in some cases, but this information was not used in the inversion. For the inversion of velocity profiles, the assumption of a layered 1D medium is needed in order to interpret the measured dispersion curves. For profiles with strong lateral changes, the measured dispersion curves were often considerably different in the two directions of the same seismic line. A careful selection of the MASW profiles on the seismic lines was therefore necessary in some cases.

3. **Shear-wave refraction tomography** was used to check results obtained with MASW. The shear-wave refraction survey often resulted in velocities that were too high when compared to the velocities obtained from P-wave refraction (i.e., where the vp/vs ratio was too low). The reason for this might be wave conversion from P to S, such that the direct S-wave cannot be recognized properly.

For more details on the commercial software and analysis method used by GeoExpert, see their final report (GeoExpert, 2009).

A validation test for the above procedure was performed at the beginning of the measurement campaign. Ambient vibration array measurements were performed by the SED at 4 sites. While at site BNALP no useful dispersion curve could be measured, results at sites BOURR, SULZ and SLE could be used for validation (for details see reports in Appendix B). For the sites SULZ and BOURR, the results from MASW are confirmed by ambient vibration array measurements within the uncertainties of the methods (see reports in Appendix A). Due to the complex structure at SLE with strong lateral changes in geology, the location of the array is not representative of the site of the station. In fact, the array's position is above a thick layer of soft sediments not present at the station. However, the results obtained from MASW in this area of the sedimentary layer could be confirmed by ambient vibration array measurements within the uncertainties of the methods and of the difference in measurement location.

Each of the 20 sites is a special case and therefore required special considerations. For this reason the project team adopted the following working procedure:

1) Geoexpert AG proposed the seismic lines at each site. These were then discussed and approved by the project team. GeoExpert performed the measurement and processed the data using commercial software.
2) The project team discussed the outcome of the processing, proposed modifications and selected those parts of the seismic lines most similar to the site of the seismic station. For each site GeoExpert provided a final report that includes selected dispersion curves and inverted velocity profiles, interpolated S-wave sections from MASW, an estimation of the parameters vs5, vs10, vs20, vs30, vs40, vs50, and vs100 if possible, the results from P- and S-wave seismics, and a comparison of results obtained using the different methods, as well an evaluation of error. The average S-wave velocities were computed from the interpolated S-wave sections obtained with MASW.
3) The final computation of the average vs values was performed by the SED, using the inverted structural models and the collected information for the site. The average wave velocities were recomputed from the inverted structural models and might therefore differ from the values in the corresponding station report provided by GeoExpert. Beside average vs values for given depths, the average quarter wavelength velocity as a function of frequency is provided together with a standard deviation. The average values and standard deviation were derived from the set of available velocity profiles. The standard deviation does not represent the full uncertainties. A qualitative assessment of the quality of the average vs values is given in overview table C.

2. Data Presentation

2.1. Overview

Three documents with different levels of information are presented as outcome of this project:

1. **Overview tables** (paragraph 3)
2. **Station reports** for the 30 sites analyzed in this project (accessible via a web interface or as a pdf file from the DVD)
3. **Summaries** for the 20 selected sites for which measurements were performed within this project and of the site ZUR that is not documented in publicly accessible reports (appendix A). For these sites GeoExpert provided measurement reports. Appendix B includes three summaries for the control measurements at the 3 sites SULZ, SLE and BOURR using ambient vibration array techniques.

Overview tables
The overview tables (A, B and C) in paragraph 3 provide a summary for all sites and allow a comparison of the key data. The table is limited to the most important information regarding site location, housing, instrumentation and the station site. Furthermore the tables summarize the kind of experiments that have been carried out. Finally the average shear-wave velocities are given, including a qualitative rating of the quality.

Station reports
For the detailed information the SED created a station report for each site. These reports include an overview of all available data for a particular site. The reports are accessible via a web interface (see paragraph below) but are also presented as a pdf document on the DVD. The overview tables and station reports are extracts from the database (see below).

Summaries for the 20 selected sites
The summaries explain how the results of the different geophysical investigation methods performed by GeoExpert have been weighted and interpreted for each station site. These summaries are presented in appendix A. Similar documents regarding the results from ambient vibration array experiments for sites BOURR, SLE and SULZ are given in appendix B. These results were used as a validation test of measurement procedure for the 20 sites.

The aggregated data can be summarized in three different classes or types (see 2.3-2.5):

1. location of the station site, housing and instrumentation;
2. physiology of the station site: morphology, geological and geotechnical information, and stratigraphy;
3. experimental data.

For the first type, data were available for most sites on different databases at the SED. Further investigations have been made with respect to the housing of the instruments, particularly regarding the exact position of the sensors (e.g., horizontal/vertical distance to the surface) and the installation environment.
The presented data of the second type rely primarily on homogeneous data sources available for Switzerland, such as the digital version of the geological and geotechnical map of Switzerland. Stratigraphic data from boreholes was available for only few sites.

Not many boreholes exist at sufficiently close distance to the station sites. Furthermore most of them are destructive drillings.
With respect to the third type of data (experimental data) information is very heterogeneous and needed reassessment in most cases. Apart from the experiments performed during this project, single station ambient vibration H/V measurements were performed for almost all seismic stations that are presently operating in Switzerland. For some stations in the northern part of Switzerland ambient vibration array and seismic experiments have been carried out in recent projects. For stations in the foothills of the Alps and the Alps itself such measurements do not exist at all.

2.2. Database

The SED created a database allowing the retention of information of various types. The database is available via a web interface:
http://histserver.ethz.ch/stations/stations.html - login: mirador - password: mivella. The database will be extended in the future and will therefore continuously change in time.

2.3. Location of the station site, housing and instrumentation

Station		**Table**	**Station-Report**
Naming			
Code:	Three to five capital letters, specifying the instrument site	A,B,C	1
Name:	Instrument site name	A	1
Appendix:	Naming of the appendix of this report (an appendix is available for the 20 sites investigated with geophysical measurements during this project).	A	
Coordinates			
CH-X/Y:	X/Y-coordinate based on the reference system CH1903	A	1.1
Lat/Lon:	Lat/Lon based on the World Geodetic System 1984 (WGS1984)	A	1.1
Altitude:	Elevation according to the reference system CH1903	A	1.1
Instrumentation			
Instrument type	Broadband, Accelerometer, Short-Period (**yes/no)**	A	1.2 and 3
Housing			
Freefield	The instrument is placed in free-field conditions **(yes/no)** Very restrictive rules were applied	A	4
Below surface	Position of the sensor below the surface in meters	A	4
Type of structure	Basement, buried chamber, bunker, etc.	A	4
Location inside structure	On concrete basement, on rock, on soil etc.	A	4
Illustrations	Location sketch, overview and detail photographs		4

2.4. Site Characteristics

Morphology		**Table**	**Station-Report**
Classification (EC8/SIA261)	Ground classification according to the Eurocode 8 (EC8) and the norm 261 of the Swiss Engineers and Architects Society (SIA 261)	B	1.7
Description	Short description of the site's morphology (hill, slope, plane etc)	B	1.7
Terrain map	Google-terrain map		1.7
Geology/geotechnics			
Geological information	Detail of the digital geological map of Switzerland and description of the site location according to the map's legend (available in German only). **Reference map:** Geologische Karte der Schweiz (Elektronische Daten) . Pixelkarte / Hrsg: Bundesamt für Landestopographie = Carte géologique de la Suisse. Carte pixel / Ed.: Office fédéral de topographie. - Wabern : Bundesamt für Landestopografie, 2007.	B	2
Geotechnical information	Detail of the digital geotechnical map of Switzerland and description of the site location according to the map's legend (available in German only). **Reference map:** Geotechnische Karte der Schweiz (Elektronische Daten), hrsg. von der Schweizerischen Geotechnischen Kommission (Kartenmaterial). (Ausg. 2001) - Bern, Schweizerische Geotechnische Kommission, 2001	B	2
Borehole-stratigraphy:	All relevant borehole information available via cantonal GIS is included in the reports. The overview table indicates whether borehole data are available.	B partly	2.2.3
SPT-experiments	Reference of performed SPT-experiments. The overview table indicates whether SPT data are available.	C partly	2.3.2

2.5. Key Data and Experiments

Vs derived ➡ average wave velocities derived from the experiments performed		**Table**	**Station-Report**
Average Vs (table)	Average shear wave velocities (Vs5, 10, 20, 30, 40, 50, 100, 150, 200). Values in bracket represent extrapolations.	C	1.5
Vs 30 (Allen and Wald)	The authors propose an algorithm using topographic slope as proxi for Vs30. This value is given for all station sites, at the grid point closest to the station. The station-grid point distance is also presented. Reference: Allen, T. I., and Wald, D. J. (2007). Topographic Slope as a Proxy for Seismic Site Conditions and Amplification. Bulletin of the Seismological Society of America, Vol.97, No.5, pp.1379–1395,October 2007, doi:10.1785/0120060267		1.5.1
Quarter wavelength velocity plot (fig.)	Quarter wavelength velocity based on the available Vs-profiles		1.6

Ambient vibration H/V single station Method ➡ Fundamental frequency of resonance (f_0)		**Table**	**Station-Report**
f_0	Fundamental frequency of resonance from ambient vibration H/V single station methods. Three methods are applied to compute average H/V ratios. The first 2 are classical polarization analysis in the frequency domain, where the polarization is defined as the ratio between the quadratic mean of the Fourier spectra of the horizontal components and the spectrum of the vertical component. The methods are the one described in Fäh et al. (2001), and that used in the CAP and SESARRAY software developed during the SESAME project (Ohrnberger, 2004; Wathelet, 2005). The third method for H/V ratios tries to reduce the SH-wave influence by identifying P-SV-wavelets from the signal and taking the spectral ratio only from these wavelets (Fäh et al., 2001).	C	2.5.2
f_0 min.	Lower limit of the range for f_0	C	2.5.2
f_0 max.	Upper limit of the range for f_0	C	2.5.2
f_0 quality	Quality of a peak. Defined as the average value of two quality measures on the H/V curve according to Fritsche et al. (2008).	C	2.5.2

Ambient vibration array method ➡ Shear wave velocity profile		**Table**	**Station-Report**
Array location	Array diameter, distance to station, position of central station		2.5.3
Average Vs (table)	Average shear wave velocities (Vs5, 10, 20, 30, 40, 50, 100, 150, 200).		2.5.3
Vs-profiles (figure)	Shear wave velocity models		2.5.3
Dispersion-curves	Love and Rayleigh dispersion-curves		2.5.3

Seismic ➡ Shear and compressional wave velocity profiles		**Table**	**Station-Report**
Location of experiment	Length of the seismic line, position of the initial and final points of the seismic line.		2.5.4
Compressional and shear wave velocities (figure)	Compressional and shear wave velocity images along the seismic profiles.		2.5.4
Average Vs (table)	Average shear wave velocities (Vs5, 10, 20, 30, 40, 50, 100, 150, 200).		2.5.4
Vs and Vp-profiles (figure)	Shear and compressional wave velocity models.		2.5.4

MASW/SASW ➡ Shear wave velocity profiles		**Table**	**Station-Report**
Location of experiment	Length of SASW/MASW line, position of the initial and final points of the line		2.5.5

Averaged Vs (table)	Average shear wave velocities (Vs5, 10, 20, 30, 40, 50, 100, 150, 200).		2.5.5
Shear wave velocity profiles and sections (figure)	Shear wave velocity models.		2.5.5

2.6. Web-Interface of the Database

The web-interface creates the station reports on the basis of the data available for a specific station site. These reports include the site information available at present. The reports have the following structure:

1. Overview Data: Station, Location, Key Data
1.1 Coordinates
1.2 Instrumentation at Site
1.3 Regional Overview
1.4 Local Overview
1.5 vs (Derived)
1.6 Quarter Wavelength Velocity
1.7 Overview of Morphology
2. Experiments
2.1 Overview of Regional Experiments
2.2 Overview of Local Experiments
2.3 Geognostic Experiments
2.3.1 SPT/CPT
2.3.2 Borehole Stratigraphy
2.4 Geotechnical Laboratory Tests and Analysis
2.5 Geophysical In-Situ Tests
2.5.1 Overview and Key Data
2.5.2 Detailed Data: Ambient Vibration, Single Station Method
2.5.3 Detailed Data: Ambient Vibration, Array Method
2.5.4 Detailed Data: Seismics
2.5.5 Detailed Data: SASW/MASW
3. Station History
4. Housing

It is possible to access any station of the Swiss Seismological Service by adding the station code at the end of the URL:
http://histserver.ethz.ch/stations/stations.html?sta=XXXX
where XXXX is the station code. We suggest using program Firefox for optimal display of the reports.
The database is presently only populated by the stations reported here. This includes primarily the 20 selected sites for which measurement campaigns have been performed (see 1.3) and more than 10 sites of seismic stations that have been investigated by SED in the past. The 10 sites are mainly located in the Basel and Valais regions.

2.7. DVD

The database will be extended in the future and will therefore continuously change in time. A snapshot at the end of August 2009 is provided on the DVD attached to this report. The DVD has the following data structure and contents:

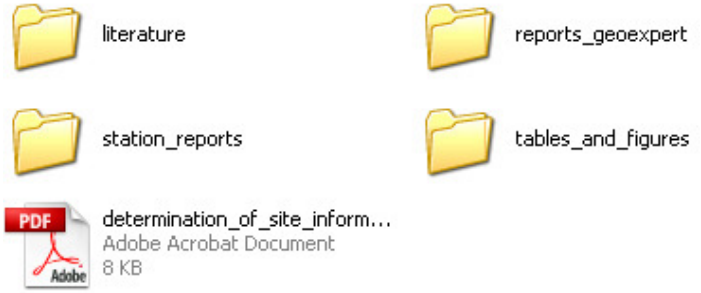

Beside the main document (this report), the DVD contains four folders:

literature: This folder contains all used or cited literature available in electronic form;
reports_geoexpert: reports produced by GeoExpert AG;
station_reports: station reports created from SED-database;
tables_and_figures: Contains a folder for each investigated site including two subfolders. The subfolder ILLUSTRATIONS includes all figures and illustrations produced for the station reports. The subfolder TEXT contains text files summarizing key data.

3. Overview Table

Table A1: Overview data																
Station			Coordinates					Instruments				Housing				Remarks
Code	Name	Appendix (Summary)	CH-X	CH-Y	Lat	Lon	Altitude	Broadband	Accelerometer	Short-Period	Nr. of Recordings	Freefield	Below surface (m)	Type of structure	Location in structure	
ACB	Achenberg	App. A.1	661360	271080	47.5876	8.25434	470			x			10	former military bunker	on concrete basement of the bunker	
AIGLE	Aigle	App. A.2	562638	132363	46.3416	6.95336	800	x					20-25	military bunker	on concrete basement of the bunker	
BALST	Balsthal digital	App. A.3	619375	242800	47.3358	7.69498	908	x					3	Buried chamber, small vault	on concrete basement	
BNALP	Bannalp	App. A.4	675200	191513	46.8705	8.42502	1540	x	x				20	leak water gallery	on concrete basement	
BOURR	Bourrigon	App. A.5	584263	249237	47.3938	7.23018	860	x	x				15-20	Military bunker	on concrete basement	
BRANT	Les Verrieres	App. A.6	526473	199000	46.9380	6.47298	1145	x					9	natural cave	on concrete base	
FLACH	Flaach	App. A.7	684970	269690	47.5724	8.5679	370			x		x		natural cave	on concrete base	
GIMEL	St. Georges / Gimel	App. A.8	509999	154267	46.5336	6.26545	1121	x					10	Former military bunker (A. 641) near St. George.	on concrete basement	
HASLI	Hasliberg/Brienz	App. A.9	654438	178650	46.7568	8.15117	1280	x					3	Former military bunker	On concrete basement in the backmost part of the bunker	
LLS	Linth-Limmern	App. A.10	719680	189649	46.8472	9.00783	1740	x	x				~20	Gallary near dam	niche in gallery	
Paragraph in station report			**1.1**					**1.2**				**4**				

Table A2: Overview data																
Station			Coordinates					Instruments				Housing				Remarks
Code	Name	Appendix (Summary)	CH-X	CH-Y	Lat	Lon	Altitude	Broadband	Accelerometer	Short-Period	Nr. of Recordings	Freefield	Below surface (m)	Type of structure	Location in structure	
MUO	Muotathal	App. A.11	691200	202538	46.9677	8.63706	1920	x					a few m	Military bunker	on concrete basement	
PLONS	Plons (SG)	App. A.12	747557	212735	47.0492	9.3807	1020	x				x	3	rock niche	on concrete base	
SKEH	Kerns-Hobiel	App. A.13	663460	194980	46.9029	8.27152	560		x				0.5	converter building	on concrete basement	
SLE	Schleitheim	App. A.14	679000	290968	47.7645	8.49236	648	x				x	4	Buried chamber	on concrete basement on the bottom of the chamber	
STEIN	Stein am Rhein	App. A.15	707425	280879	47.6697	8.86899	540			x			a few	wine cellar	In the cellar of the building on concrete base	
SULZ	Cheisacher digital	App. A.16	650675	264300	47.5275	8.11153	670	x	x			x	2	burried chamber	on concrete basement of the chamber	
TORNY	Torny/Romont	App. A.17	563338	180388	46.7737	6.95862	758	x					4	military bunker	on concrete basement	
WEIN	Weingarten	App. A.18	716510	265370	47.5287	8.98586	555			x			0	small house	in the basement of the building	
WILA	Wila	App. A.19	710850	252575	47.4147	8.90753	908	x					4	military bunker	on concrete basement of the bunker	
WIMIS	Wimmis	App. A.20	614200	168200	46.6649	7.62418	770	x					3	bunker	concrete basement	horizontal distance to free surface: ~ 3m; vertical distance: ~ 20m
Paragraph in station report			**1.1**					**1.2**				**4**				

Table A3: Overview data																	
Station			Coordinates					Instruments				Housing				Remarks
Code	Name	Appendix (Summary)	CH-X	CH-Y	Lat	Lon	Altitude	Broadband	Accelerometer	Short-Period	Nr. of Recordings	Freefield	Below surface (m)	Type of structure	Location in structure	
ZUR	Degenried	App. A.21	686275	247113	47.3692	8.58088	615	x	x			x	4.5	burried chamber	basement	
OTTER	Otterbach	-	612428	269691	47.5778	7.6038	298		x			x	0	container	inside the container	
SBAF	Basel-Friedhofgasse	-	611540	270351	47.5838	7.59202	248		x				3	house	in the cellar	
SBAP	Basel-PUK	-	609464	269085	47.5724	7.5644	263		x				4	residential house	in the center of the cellar	
SBAT	Basel-Tropenhaus	-	610769	267553	47.5586	7.5817	260		x				3	greenhouse	basement	
SBIS	Binningen Sternwarte	-	610832	265629	47.5413	7.5825	315		x				3	large house	in the cellar	Substituted by SBIS2 in 2008
SBIS2	Binningen Sternwarte	-	610908	265607	47.5411	7.5835	315		x			x	3	burried chamber	bottom of the chamber	Substitute for SBIS
SIOV	Sion-Valere	-	594260	120409	46.2351	7.36423	560		x			x	2	transformer-building	on the basement of the building	
SMAV	Martigny-Verdan	-	572870	105470	46.1002	7.08781	510		x				1	transformer-building	on concrete basement	
SMUK	Muraz-Kläranlage	-	561617	126221	46.2863	6.9406	388		x				0	Service building of municipal sewage plant, concrete building	on concrete basement	
SMZW	Muttenz-Waldhaus	-	615709	266341	47.5476	7.6473	272		x			x	0	hut	on concrete base	
SRHB	Riehen-Bäumlihof	-	613979	268972	47.5713	7.6244	260		x				2	small brickbuilding	on concrete basement	
SRNR	Reinach	-	612400	262261	47.511	7.60323	293		x			x	1	transformer-building	on the basement of the building	
SYVJ	Yverdon-Jordils	-	538819	180971	46.7771	6.63754	434		x				1	converter building	on concrete basement	
Paragraph in station report			1.1					1.2				4				

Station		Table B1: Site characteristics							
Code	Appendix (summary)	Morphology		Geology	Geotechnics	Site classification (EC8)	Site classification (SIA 261)	Groundwater level (m below surface)	Borehole stratigraphy (data avaliable)
		Classification	Description	**Geological unit** (Geologische Karte der Schweiz [Elektronische Daten] . Pixelkarte / Hrsg: Bundesamt für Landestopographie Wabern: Bundesamt für Landestopografie, 2007.)	**Geotechnical unit** Geotechnische Karte der Schweiz (Elektronische Daten), hrsg. von der Schweizerischen Geotechnischen Kommission (Kartenmaterial). (Ausg. 2001) - Bern, Schweizerische Geotechnische Kommission, 2001.				
ACB	App. A.1	slope	on the northern slop (about 150m above Rhein river)	Fluvioglaziale und glaziolakustrische Schotter (Hoch- und Niederterrassen); Ausseralpine Plattform; Mesozoische epivariszische Plattform; Flachliegende epivariszische Plattform (Schwaebische Alb, Dinkelberg, Vorbergzone, Plateau)	Bedeutende Lagen von Mergelschiefern und Mergelkalken; Fels	B	B	-	no
AIGLE	App. A.2	slope	on the slope of the main valley (400m above the bottom)	Malm bzw. Jura im Allgemeinen; Mittelpenninische Sedimentdecken und -schuppen; Klippen-Decke; Decke der Prealpes medianes plastiques	Dolomite und Rauwacken; z. T. mit Gipslagen; Fels	A	A	-	yes
BALST	App. A.3	flat	on the border of a plateau	Malm; Faltenjura; Interner Jura; Faltenjura s.str.	Kalke allgemein; Massige Ausbildung, häufig mit mergeligen Zwischenlagen, z.T. mit kieseligen Kalken und Grünsandsteinen; Fels	A	A	-	no
BNALP	App. A.4	top of cliff	-	Unterkreide; Helvetische Sedimentdecken s.str.; Axen-Decke; Westliche Axen-Decke	Kalke allgemein; Massige Ausbildung, häufig mit mergeligen Zwischenlagen, z.T. mit kieseligen Kalken und Grünsandsteinen; Fels	A	A	-	no
BOURR	App. A.5	flat	plateau on jurassic chain	Malm; Faltenjura; Interner Jura; Faltenjura s.str.	Kalke allgemein; Massige Ausbildung, häufig mit mergeligen Zwischenlagen, z.T. mit kieseligen Kalken und Grünsandsteinen; Fels	B	B	-	no
BRANT	App. A.6	flat	in a cave below plane	Malm; Faltenjura; Interner Jura; Faltenjura s.str.	Kalke allgemein; Massige Ausbildung, häufig mit mergeligen Zwischenlagen, z.T. mit kieseligen Kalken und Grünsandsteinen; Fels	A	A	-	no
FLACH	App. A.7	step slope	step slope near Rhein river	Aquitanien (USM); Molassebecken; Mittellaendische Molasse; Flachliegende mittellaendische Molasse	Mergel mit Einschaltungen von schwach verfestigten Sandsteinen; z.T. überwiegend, und vereinzelt von Konglomeraten oder Muschelsandsteinen; Fels	B	B	-	no
GIMEL	App. A.8	on a cliff/rock face	steep slope in front of a plane	Malm; Faltenjura; Interner Jura; Faltenjura s.str.	Kalke allgemein; Massige Ausbildung, häufig mit mergeligen Zwischenlagen, z.T. mit kieseligen Kalken und Grünsandsteinen; Fels	A	A	-	yes
HASLI	App. A.9	on a cliff/rock face	on top of a mountain ridge	Malm; Helvetische Sedimentdecken s.str.; Axen-Decke; Westliche Axen-Decke	Kalke allgemein; Massige Ausbildung, häufig mit mergeligen Zwischenlagen, z.T. mit kieseligen Kalken und Grünsandsteinen; Fels	A	A	-	no
LLS	App. A.10	steep slope	in a tunnel in the (rock) slope below lake Limmeren	Malm; Autochthon - Parautochthon, Infrahelvetische Decken; Autochthones und Parautochthones Mesozoikum; Autochthon-Parautochthon des Aar-Gastern-Massives (N- u. W-Rand)	Kalke allgemein; Massige Ausbildung, häufig mit mergeligen Zwischenlagen, z.T. mit kieseligen Kalken und Grünsandsteinen; Fels	A	A	-	no
Paragraph in station report		**1.7**		**2.1**	**2.2**	**1.7**			**2.3.2**

Station		Table B2: Site characteristics							
		Morphology		Geology	Geotechnics				
Code	Appendix (summary)	Classification	Description	**Geological unit** (Geologische Karte der Schweiz [Elektronische Daten] . Pixelkarte / Hrsg: Bundesamt für Landestopographie Wabern: Bundesamt für Landestopografie, 2007.)	**Geotechnical unit** Geotechnische Karte der Schweiz (Elektronische Daten), hrsg. von der Schweizerischen Geotechnischen Kommission (Kartenmaterial). (Ausg. 2001) - Bern, Schweizerische Geotechnische Kommission, 2001.	Site classification (EC8)	Site classification (SIA 261)	Groundwater level (m below surface)	Borehole stratigraphy (data avaliable)
MUO	App. A.11	mountain peak	on top of Fronalpstock	Unterkreide; Helvetische Sedimentdecken s.str.; Saentis-Decke; (Saentis-)Drusberg-Decke (der Zentralschweiz)	Bedeutende Lagen von Mergelschiefern und Mergelkalken; Fels	A	A	-	no
PLONS	App. A.12	slope	on the western slope of the Seeztal	Perm (Verrucano); Helvetische Sedimentdecken s.str.; Verrucano und Trias der östlichen helvetischen Decken s.str. (nicht differenziert);	Tonschiefer bis Phyllite; Oft sandig, mit Einlagerungen von Sandsteinen und Brekzien bis Konglomeraten; Fels	A	A	-	no
SKEH	App. A.13	hilly	on small ridge	Schuttkegel; Helvetische Sedimentdecken s.str.; Wild horn-Decke; östliche Wildhorn-Decke und Randkette	Bedeutende Lagen von Mergelschiefern und Mergelkalken; Fels	C	D	-	no
SLE	App. A.14	hill	in former stone quarry	Keuper; Ausseralpine Plattform; Mesozoische epivariszische Plattform; Flachliegende epivariszische Plattform (Schwaebische Alb, Dinkelberg, Vorbergzone, Plateau)	Mergel und Schiefertone bis Tonschiefer; Mit Kalk-, Dolomit- und Sandsteinbänken, stellenweise mit Lagen von Gips- und Anhydritgesteinen; Fels	B	B	-	no
STEIN	App. A.15	slope	in the slope of a hill	Langhien - Serravallien (Tortonien) (OSM); Molassebecken; Mittellaendische Molasse; Flachliegende mittellaendische Molasse	Mergel mit Einschaltungen von schwach verfestigten Sandsteinen; z.T. überwiegend, und vereinzelt von Konglomeraten oder Muschelsandsteinen; Fels	B	C	-	no
SULZ	App. A.16	hill	on top of a hill	Dogger; Ausseralpine Plattform; Mesozoische epivariszische Plattform; Flachliegende epivariszische Plattform (Schwaebische Alb, Dinkelberg, Vorbergzone, Plateau	Kalke allgemein; Massige Ausbildung, häufig mit mergeligen Zwischenlagen, z.T. mit kieseligen Kalken und Grünsandsteinen; Fels	A	A	-	no
TORNY	App. A.17	flat	flat, small hills	Moraene, mit Wall; inkl. rezente Moraene; Molassebecken; Mittellaendische Molasse; Flachliegende mittellaendische Molasse	Sande bis Silte; Meist tonig (Lehme), t.T. Kalkhaltig (Löss), oft mit Geschieben (Grundmoränen) oder Schutt, fein bis grob, gemischt mit Sand, Silt und Ton (Obermoränen); Lockere Oberflächenbildungen	B	B	-	yes
WEIN	App. A.18	hill	in the slope of a hill	Langhien - Serravallien (Tortonien) (OSM); Molassebecken; Mittellaendische Molasse; Flachliegende mittellaendische Molasse	Konglomerate; Schwach bis mittelstark verfestigt, mit reichlich bis vorwiegend Sandstein-und Mergellagen; Fels	B	B	-	yes
WILA	App. A.19	hilly area	on foot of a hill	Langhien - Serravallien (Tortonien) (OSM); Molassebecken; Mittellaendische Molasse; Flachliegende mittellaendische Molasse	Konglomerate; Schwach bis mittelstark verfestigt, stets begleitet von Sandstein- und Mergellagen; Fels	B	B	-	yes
WIMIS	App. A.20	foot of a hill	on the border of plane (at foot of a rocky hill)	Malm bzw. Jura im Allgemeinen; Mittelpenninische Sedimentdecken und -schuppen; Klippen-Decke; Decke der Prealpes medianes plastiques	Kiese und Sande, meist sauber; Bisweilen mit tonig-siltigen Über-deckungen oder Einlagerungen, sowie ausgedehnte Geröllablagerungen (heutige Bachablagerungen); Lockere Oberflächenbildungen	A	A	-	no
Paragraph in station report		**1.7**		**2.1**	**2.2**	**1.7**			**2.3.2**

Station		Table B3: Site characteristics							
		Morphology		Geology	Geotechnics				
Code	Appendix (summary)	Classification	Description	**Geological unit** (Geologische Karte der Schweiz [Elektronische Daten] . Pixelkarte / Hrsg: Bundesamt für Landestopographie Wabern: Bundesamt für Landestopografie, 2007.)	**Geotechnical unit** Geotechnische Karte der Schweiz (Elektronische Daten), hrsg. von der Schweizerischen Geotechnischen Kommission (Kartenmaterial). (Ausg. 2001) - Bern, Schweizerische Geotechnische Kommission, 2001.	Site classification (EC8)	Site classification (SIA 261)	Groundwater level (m below surface)	Borehole stratigraphy (data avaliable)
ZUR	App. A.21	in the slope of a large hill	hill slope	Langhien - Serravallien (Tortonien) (OSM); Molassebecken; Mittellaendische Molasse; Flachliegende mittellaendische Molasse	Mergel mit Einschaltungen von schwach verfestigten Sandsteinen; z.T. überwiegend, und vereinzelt von Konglomeraten oder Muschelsandsteinen; Fels	B	B	-	yes
OTTER	-	small hill	flat	Alluvionen; Quartaer; Grosse Alluvialebenen	-	B	C	4.6	yes
SBAF	-	plane	on alluvial plane of the Rhein river	Alluvionen; Quartaer; Grosse Alluvialebenen	-	B	C	6	yes
SBAP	-	terrace	flat	Fluvioglaziale und glaziolakustrische Schotter (Hoch- und Niederterrassen); Quartaer; Grosse Alluvialebenen	Kiese und Sande, sauber oder siltig; Bisweilen etwas verkittet (Schotter der Eiszeit); Lockere Oberflächenbildungen	B	C	20	yes
SBAT	-	flat	alluvial river terrace	Fluvioglaziale und glaziolakustrische Schotter (Hoch- und Niederterrassen); Quartaer; Grosse Alluvialebenen	Kiese und Sande, sauber oder siltig; Bisweilen etwas verkittet (Schotter der Eiszeit); Lockere Oberflächenbildungen	B	C	17	yes
SBIS	-	flat	terrace	Chattien (USM); Ausseralpine Plattform; Tertiaere Graeben; Oberrhein-Graben	Kiese und Sande, sauber oder siltig; Bisweilen etwas verkittet (Schotter der Eiszeit); Lockere Oberflächenbildungen	B	C	25	yes
SBIS2	-	flat	terrace	Chattien (USM); Ausseralpine Plattform; Tertiaere Graeben; Oberrhein-Graben	Kiese und Sande, sauber oder siltig; Bisweilen etwas verkittet (Schotter der Eiszeit); Lockere Oberflächenbildungen	B	C	25	yes
SIOV	-	slope	valley between two hills (Valère and Tourbillon)	Trias; Unterpenninische Sedimentdecken und -schuppen, Ophiolithe; Zone von Sion-Courmayeur; Pierre-Avoi-Einheit (bzw. Unite des Cols)	Quarzite; Massig oder plattig bis schiefrig; Fels	A	A	-	no
SMAV	-	flat	alluvial plane, on the foot of the valley slope	Alluvionen, Quartaer, Grosse Alluvialebenen	Sande bis Silte; Meist tonig (Lehme), t.T. Kalkhaltig (Löss), oft mit Geschieben (Grundmoränen) oder Schutt, fein bis grob, gemischt mit Sand, Silt und Ton (Obermoränen); Lockere Oberflächenbildungen	B	C	-	yes
SMUK	-	flat	alluvial plane	Alluvionen; Quartaer; Grosse Alluvialebenen	Kiese und Sande, meist sauber; Bisweilen mit tonig-siltigen Über-deckungen oder Einlagerungen, sowie ausgedehnte Geröllablagerungen (heutige Bachablagerungen); Lockere Oberflächenbildungen	C	D	-	no
SMZW	-	flat	alluvial plane	Muschelkalk; Ausseralpine Plattform; Mesozoische epivariszische Plattform; Flachliegende epivariszische Plattform (Schwaebische Alb, Dinkelberg, Vorbergzone, Plateau	Kiese und Sande, sauber oder siltig; Bisweilen etwas verkittet (Schotter der Eiszeit); Lockere Oberflächenbildungen	B	C	11.5	yes
SRHB	-	flat	alluvial plane	Alluvionen; Quartaer; Grosse Alluvialebenen	Kiese und Sande, sauber oder siltig; Bisweilen etwas verkittet (Schotter der Eiszeit); Lockere Oberflächenbildungen	B	B	16	yes
SRNR	-	flat	alluvial/glacial plane	Fluvioglaziale und glaziolakustrische Schotter (Hoch- und Niederterrassen); Ausseralpine Plattform; Tertiaere Graeben; Oberrhein-Graben	Kiese und Sande, sauber oder siltig; Bisweilen etwas verkittet (Schotter der Eiszeit); Lockere Oberflächenbildungen	B	B	7	yes
SYVJ	-	flat	alluvial plane	Torf; Quartaer; Grosse Alluvialebenen	Tonige Silte bis tone; Bisweilen mit Einlagerungen von Sanden bis Kiesen (Seebodenlehme, Schwemmlehme, Gehängelemme); Lockere Oberflächenbildungen	S2	F	-	yes
Paragraph in station report		**1.7**		**2.1**	**2.2**	**1.7**			**2.3.2**

Station		Table C1: Key data														Performed experiments					
		Fundamental frequency of resonance (f_0 Quality: p=poor, m=medium, g=good, v=very good)				V_s derived (Quality of V_s-determination: h=high, m=moderate, l=low)															
Code	Appendix (summary)	f_0	f_0 min.	f_0 max.	f_0 Quality	Quality	V_s 5	V_s 10	V_s 20	V_s 30	V_s 40	V_s 50	V_s 100	V_s 150	V_s 200	S-wave refraction and reflection seismics	P- wave reflection and refraction seismics	Spectral Analysis of Surface Waves (SASW)	Multiple channel Analysis of Surface Waves (MASW)	Ambient vibration array techniques	Standard Penetration Test (SPT)
ACB	App. A.1	1.31	1.22	1.56	g	m	524	502	576	(658)	(713)	(752)	-	-	-	yes	yes	-	yes	-	-
AIGLE	App. A.2	1.29	1.19	1.64	m	l-m	1370	1338	1303	(1243)	(1292)	(1416)	-	-	-	yes	yes	-	yes	-	-
BALST	App. A.3	1.36	1.23	1.52	p	m	1298	1287	1265	1348	1472	(1561)	-	-	-	yes	yes	-	yes	-	-
BNALP	App. A.4	no peak	-	-	-	m	1574	1497	1500	1654	1778	1882	(2174)	-	-	yes	yes	-	yes	yes, but no result	-
BOURR	App. A.5	1.66	1.38	1.94	m	m-h	515	562	619	693	(773)	(845)	-	-	-	yes	yes	-	yes	yes	-
BRANT	App. A.6	no peak	-	-	-	m	901	825	947	1079	1184	1260	(1453)	-	-	yes	yes	-	yes	-	-
FLACH	App. A.7	5.41	4.56	6.01	v	m-h	437	411	535	610	(666)	(762)	-	-	-	yes	yes	-	yes	-	-
GIMEL	App. A.8	4.51	3.59	5.44	m	h	1467	1392	1399	1496	1562	(1606)	-	-	-	yes	yes	-	yes	-	-
HASLI	App. A.9	1.59	1.33	2.18	m	m-h	1535	1421	1455	1603	1722	1811	(2027)	-	-	yes	yes	-	yes	-	-
LLS	App. A.10	5	3.53	7.16	m	l-m	2920	2949	2885	3011	(3081)	(3125)	-	-	-	yes	yes	-	yes	-	-
Paragraph in station report		**2.5.2**				**1.5**										**2.5.4**	**2.5.4**	**2.5.5**	Report Geoexpert AG	**2.5.3**	**2.3.1**

Station		Table C2: Key data														Performed experiments					
		Fundamental frequency of resonance (f_0 Quality: p=poor, m=medium, g=good, v=very good)				V_s derived (Quality of V_s-determination: h=high, m=moderate, l=low)															
Code	Appendix (summary)	f_0	f_0 min.	f_0 max.	f_0 Quality	Quality	V_s 5	V_s 10	V_s 20	V_s 30	V_s 40	V_s 50	V_s 100	V_s 150	V_s 200	S-wave refraction and reflection seismics	P- wave reflection and refraction seismics	Spectral Analysis of Surface Waves (SASW)	Multiple channel Analysis of Surface Waves (MASW)	Ambient vibration array techniques	Standard Penetration Test (SPT)
MUO	App. A.11	1.61	1.41	1.89	m	m-h	967	928	986	1086	1193	1269	(1460)	-	-	yes	yes	-	yes	-	-
PLONS	App. A.12	1.52	1.31	1.64	m	h	1844	1770	1742	1810	1890	1943	(2060)	-	-	yes	yes	-	yes	-	-
SKEH	App. A.13	1.9	1.55	2.28	m	l	152	179	227	(275)	(320)	(354)	-	-	-	yes	yes	-	yes	-	-
SLE	App. A.14	4	1.52	6.83	m	h	693	671	656	686	(736)	-	-	-	-	yes	yes	-	yes	yes	-
STEIN	App. A.15	2.31	2.09	2.57	m	h	262	273	342	387	(434)	(468)	-	-	-	yes	yes	-	yes	-	-
SULZ	App. A.16	0.89	0.82	1.07	m	h	922	949	991	1028	(1053)	(1070)	-	-	-	yes	yes	-	yes	yes	-
TORNY	App. A.17	2.24	1.96	2.54	p	h	385	439	570	691	777	(841)	-	-	-	yes	yes	-	yes	-	-
WEIN	App. A.18	4.67	3.61	5.9	v	l-m	569	539	612	(682)	(744)	(789)	-	-	-	yes	yes	-	yes	-	-
WILA	App. A.19	4.94	4.55	5.39	g	m	467	498	603	683	(747)	(793)	-	-	-	yes	yes	-	yes	-	-
WIMIS	App. A.20	1.43	1.21	1.72	m	l-m	1055	1119	1311	1443	1569	1664	(1900)	-	-	yes	yes	-	yes	-	-
Paragraph in station report		2.5.2				1.5										2.5.4	2.5.4	2.5.5	Report Geoexpert AG	2.5.3	2.3.1

Station		Table C3: Key data														Performed experiments					
		Fundamental frequency of resonance (f_0 Quality: p=poor, m=medium, g=good, v=very good)				V_s derived (Quality of V_s-determination: h=high, m=moderate, l=low)															
Code	Appendix (summary)	f_0	f_0 min.	f_0 max.	f_0 Quality	Quality	V_s 5	V_s 10	V_s 20	V_s 30	V_s 40	V_s 50	V_s 100	V_s 150	V_s 200	S-wave refraction and reflection seismics	P- wave reflection and refraction seismics	Spectral Analysis of Surface Waves (SASW)	Multiple channel Analysis of Surface Waves (MASW)	Ambient vibration array techniques	Standard Penetration Test (SPT)
ZUR	App. A.21	6.34	5.93	6.73	m	m	310	374	529	635	727	806	(1031)	-	-	yes	-	-	-	yes	-
OTTER	-	0.8	0.64	0.95	m	h	220	277	371	418	446	469	550	(604)	(656)	yes	-	yes	-	yes	yes
SBAF	-	0.99	0.64	1.58	v	h	249	268	331	379	408	429	497	569	(651)	yes	-	-	-	yes	yes
SBAP	-	1.32	0.81	1.68	v	h	217	260	335	383	412	(432)	(505)	(627)	(761)	-	-	-	-	yes	yes
SBAT	-	0.89	0.82	1.02	v	h	314	320	359	380	394	404	472	541	-	yes	-	yes	-	yes	yes
SBIS	-	0.72	0.51	0.84	v	m-h	277	300	350	378	401	427	562	668	(756)	-	-	-	-	yes	yes
SBIS2	-	0.72	0.51	0.84	v	m-h	277	300	350	378	401	427	562	668	(756)	-	-	-	-	yes	yes
SIOV	-	0.99	0.84	1.34	g	l	1215	1272	1412	1473	1552	1697	(2434)	-	-	-	-	-	-	yes	-
SMAV	-	1.1	0.91	1.25	g	h	259	269	335	329	431	461	(551)	-	-	-	-	-	-	yes	-
SMUK	-	0.4	0.36	0.6	v	m	282	282	282	282	(285)	(327)	-	-	-	-	-	-	-	yes	-
SMZW	-	3.02	2.37	3.4	g	h	415	444	469	484	495	515	802	(1039)	(1222)	yes	-	yes	-	yes	yes
SRHB	-	0.67	0.58	0.76	m	h	419	427	444	464	(486)	(504)	(583)	-	-	-	-	-	-	yes	yes
SRNR	-	0.57	0.47	0.67	v	h	501	501	510	523	541	(571)	(694)	-	-	-	-	-	-	yes	yes
SYVJ	-	0.93	0.8	1.15	v	h	190	211	240	261	277	289	341	428	(521)	yes	-	-	-	yes	-
Paragraph in station report		2.5.2				1.5										2.5.4	2.5.4	2.5.5	Report Geoexpert AG	2.5.3	2.3.1

4. Literature

GeoExpert ag (2009). Seismic Shear Wave Velocity Determination and Hybrid Seismic Surveying at 20 Swiss Seismological Service Stations in Switzerland. Summary Report to swissnuclear.

GeoExpert ag (2009). Seismic Shear Wave Velocity Determination and Hybrid Seismic Survey at the SED-Stations ACB, AIGLE, BALST, BNALP, BOURR, BRANT, FLACH, GIMEL, HASLI, LLS, MUO, PLONS, SLE, STEIN, SULZ, TORNY, WEIN, WILA, WIMIS and SKEH. Report to Swissnuclear: PEGASOS Refinement Project: SP2 Ground Motion Characterization.

Schweizerischer Erdbebendienst (2009). Station Reports. Snapshots of the instrument site characteristion database for SED-stations ACB, AIGLE, BALST, BNALP, BOURR, BRANT, FLACH, GIMEL, HASLI, LLS, MUO, OTTER, PLONS, SBAF, SBAP, SBAT, SBIS, SBIS2, SIOV, SKEH, SMAV, SMUK, SMZW, SRHB, SLE, SRNR, STEIN, SULZ, TORNY, WEIN, WILA, WIMIS, SYVJ and ZUR. Internal Reports.

Stamm, G., Burjanek, J. and D. Fäh (2009). Array-measurements at the broadband-site BOURR. Internal report, Schweizerischer Erdbebendienst, ETH Zürich.

Stamm, G. and Fäh, D. (2009). Array-measurements at the broadband-site SLE. Internal report. Schweizerischer Erdbebendienst, ETH Zürich.

Stamm, G., Burjanek, J. and D. Fäh (2009). Array-measurements at the broadband-site SULZ. Internal report, Schweizerischer Erdbebendienst, ETH Zürich.

Appendix A:
Summaries

A.1 Station ACB

The sensor of station ACB is located in a bunker in rock, about 10-15m below the surface. S-wave measurements were performed along 2 sections. Both sections are about 50m away from the sensor, and therefore the results obtained from the geophysical measurements need some interpretation. On section 1, the seismic S-wave profile and the MASW results indicate sedimentary layers at both ends of the profile. For this reason only the results from sub-arrays of the central part of section 1 were used to compute the mean values of vs from 5 to 30m. In section 2, thicker layers of sediments are observed in the NW part. MASW results could not be interpreted in the SE part of section 2. For the selected parts of the section, the average value of the S-waves in the uppermost layer is in the velocity range of 500-600m/s, with a thickness of about 25m. From the 40m sub-arrays, and more reliably from the 96m arrays (useful seismic lines m1-, m2+, m2-), the average S-velocity of the first non-weathered rock layer is in the order of 1000-1400m/s.

The H/V spectral ratio at site ACB has two clear peaks, a stronger one at around 1.3 Hz and a smaller peak in the frequency range of about 5-6 Hz. Due to the observed S-wave values in the surface part of the structure, close to station ACB, the stronger peak must be associated to a layer of soft rock with low S-wave velocity. Assuming a mean velocity of this rock layer of about 1200 m/s (with a possible range of 1000-1400 m/s), we estimate a thickness of around 230 m (with a range of about 190 – 270 m), including surface sediments and weathering. The estimate of the S-wave velocity of this “soft” bedrock is supported somewhat by the evidence of a narrow-band wave-train with velocity of 1200m/s, clearly observable in the dispersion plot from MASW analysis performed using the entire array length (96m) of the sections M1+ and M2- (see page 17 of the report by GeoExpert for site ACB, Fig 3.3f and Fig 3.3g). The deeper rock layers need to have S-wave velocities larger than about 2500 m/s in order to generate the amplitude in the H/V peak at 1.3 Hz. The second peak in the H/V spectral ratio at station ACB (at around 5-6 Hz) might be explained by the layer found with MASW (25m with average S-wave velocity of about 500-600m/s), which consists of gravel layers and weathered rock material.

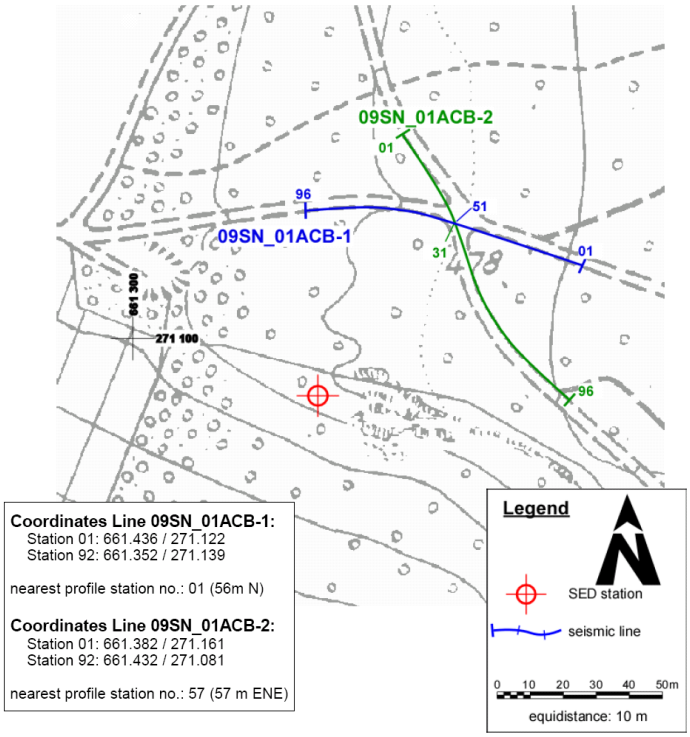

Figure A.1.1. Measurements at site ACB.

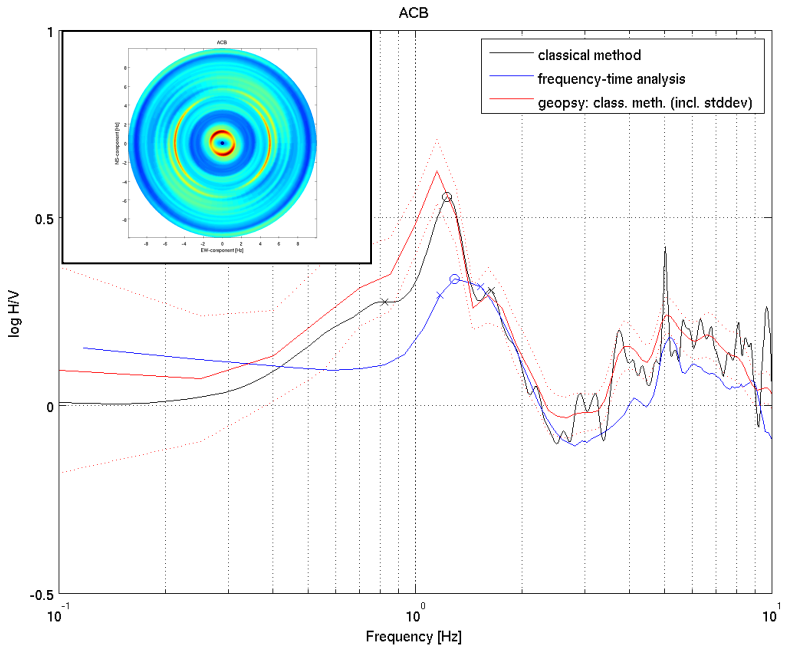

Figure A.1.2. H/V spectral ratios at the site of seismic station ACB.

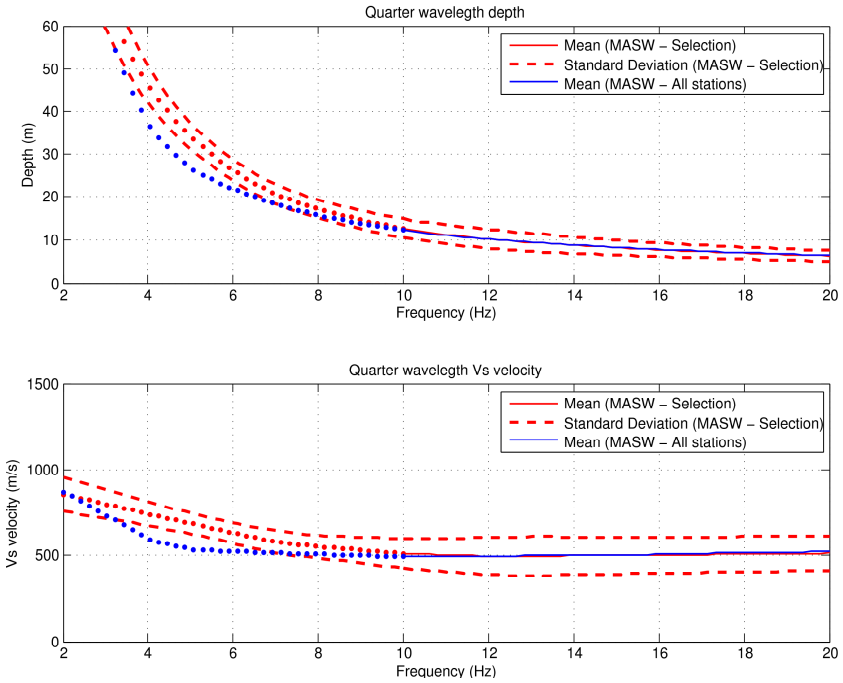

Figure A.1.3. Quarter wavelength velocity for site ACB obtained with MASW. For the vs5 to vs30 computation, the red curve is used. The blue curve is the average over the entire profile, including the sedimentary layers that are not present at station ACB.

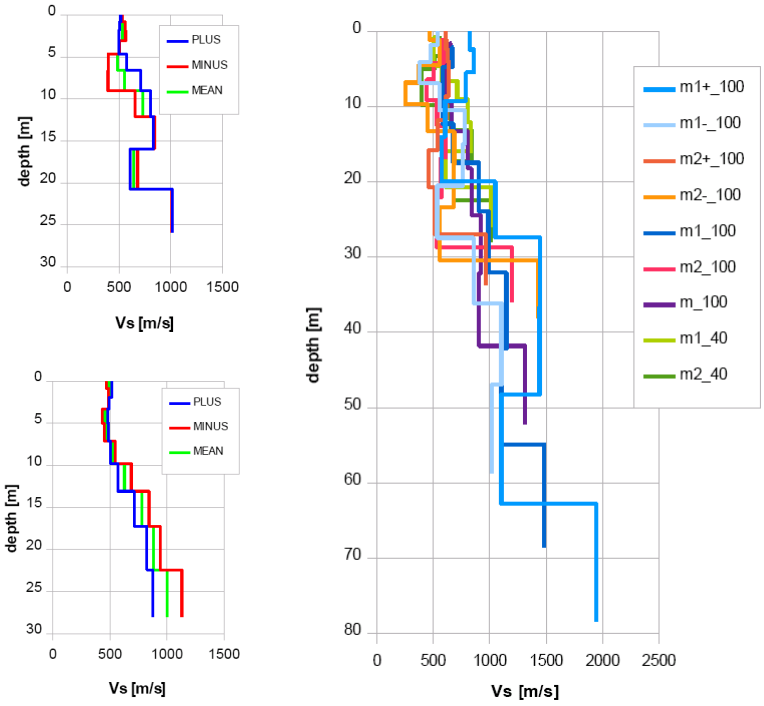

Figure A.1.4. Structural models at site ACB obtained from MASW. For more details, see the report of GeoExpert related to the site ACB.

A.2 Station AIGLE

The sensor of station AIGLE is located on the concrete basement at the rear of a bunker, about 20-25 m below the surface. The bunker is located in the flank of a Jurassic sediment ridge with Malm limestones. Active S-wave measurements at this site were performed along two sections that are more than 20m from the station site. The lines of the seismic survey are placed partly on loose talus covering the Jurassic (Malm) sediment ridge. This is particularly valid for seismic profile 1, which crosses an area with loose material in the north-western part of the section. This area is excluded from the derivation of vs5 to vs30. Due to problems with the software used by GeoExpert there were difficulties in inverting for velocity profiles that explain all measured dispersion curves from MASW. The velocities were generally larger along section 2 than those measured along section 1; even when only measurements outside the area with loose surface material were considered. This was confirmed with P-seismics, but not with S-wave seismics. Due to the problems with some inversions, only the profiles that explain the measured dispersion curves and that are outside the area with loose surface material were selected for the vs5 to vs30 calculation. The selected inverted profiles show a layer of weathered rock of about 10-15m. The range of velocities measured for the non-weathered rock shows considerable scatter. By comparing the quarter wavelength velocity for site AIGLE obtained with MASW from selected profiles in sections 1 and 2, and for the whole 96m array of section 2 we recognize a discrepancy between the two results. This is due to a difficulty in correctly picking the dispersion curves, due to the poor quality and large scatter of the acquired data. The low velocity values of the selected shorter profiles appear to be unreasonable. We therefore suggest the use of the whole 96m array only.

The H/V spectral ratio at site AIGLE has only a very weak and insignificant peak at about 1.2-1.6 Hz. The generally very flat H/V curve is typical for rock sites.

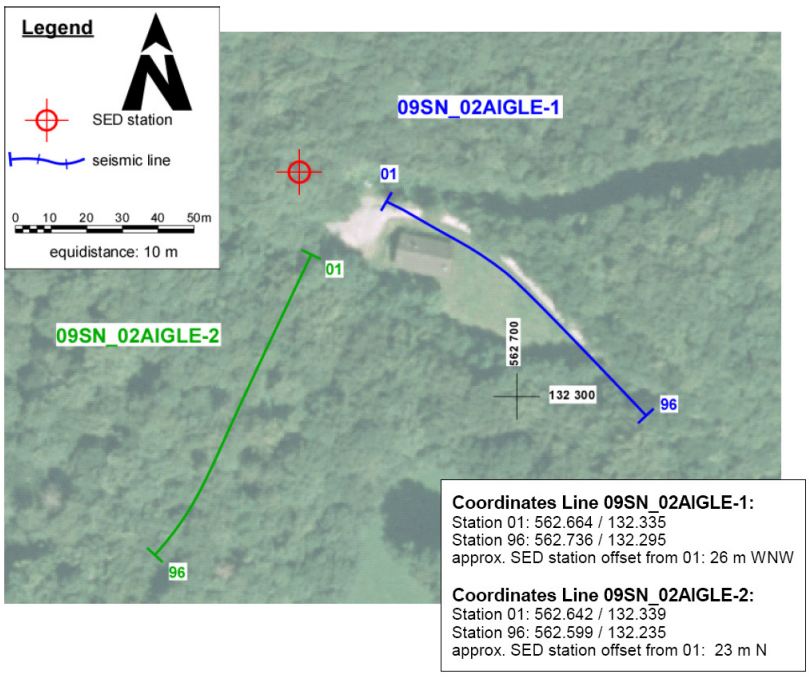

Figure A.2.1. Measurements at site AIGLE.

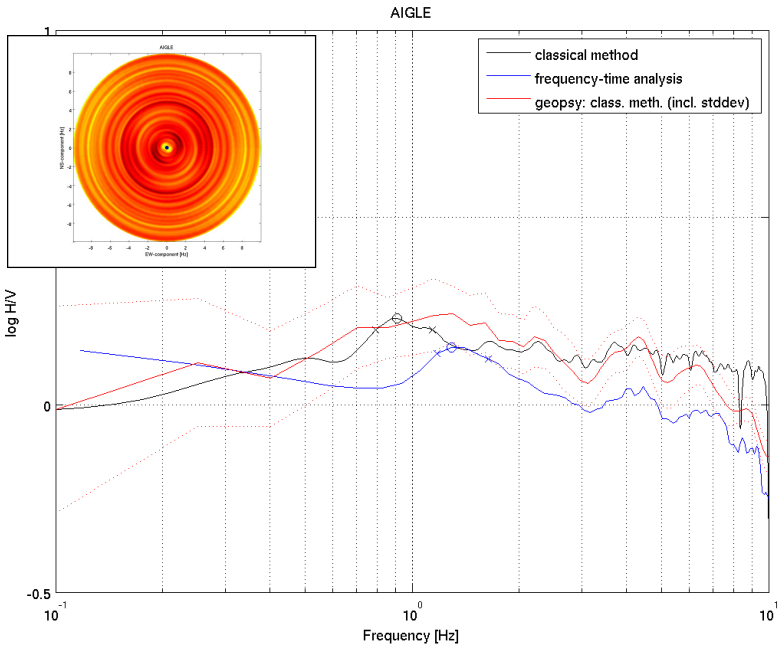

Figure A.2.2. H/V spectral ratios at the site of seismic station AIGLE. The station is about 20-25m below the surface.

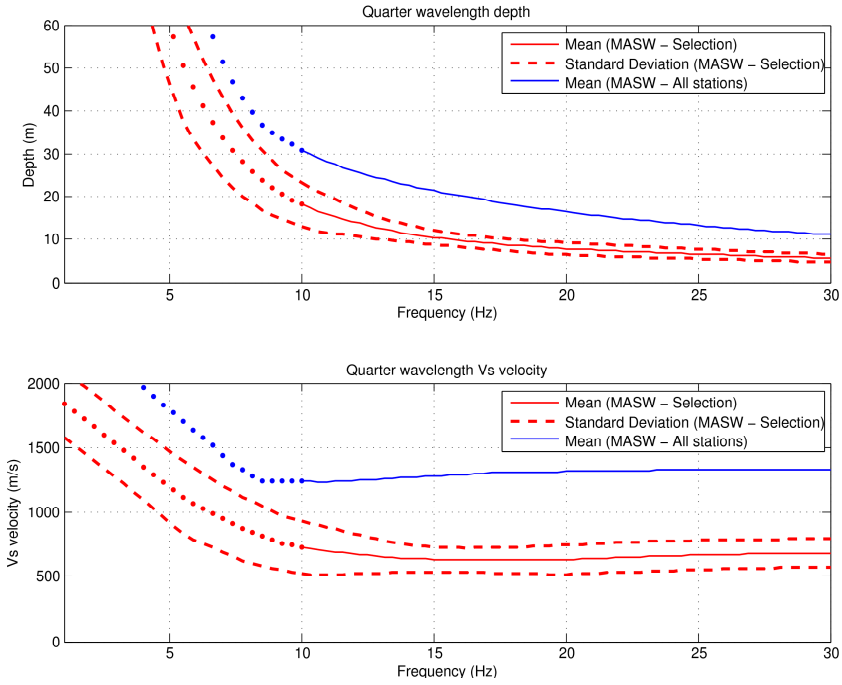

Figure A.2.3. Quarter wavelength velocity for site AIGLE obtained with MASW from selected profiles in section 1 and 2, and for the whole of section 2. The discrepancy between the two results is due to a difficulty in correctly picking the dispersion curves, caused by the poor quality and large scatter of the acquired data. The low velocity values of the selected profiles appear to be unreasonable. We therefore suggest the use of the whole 96 m array of section 2 only.

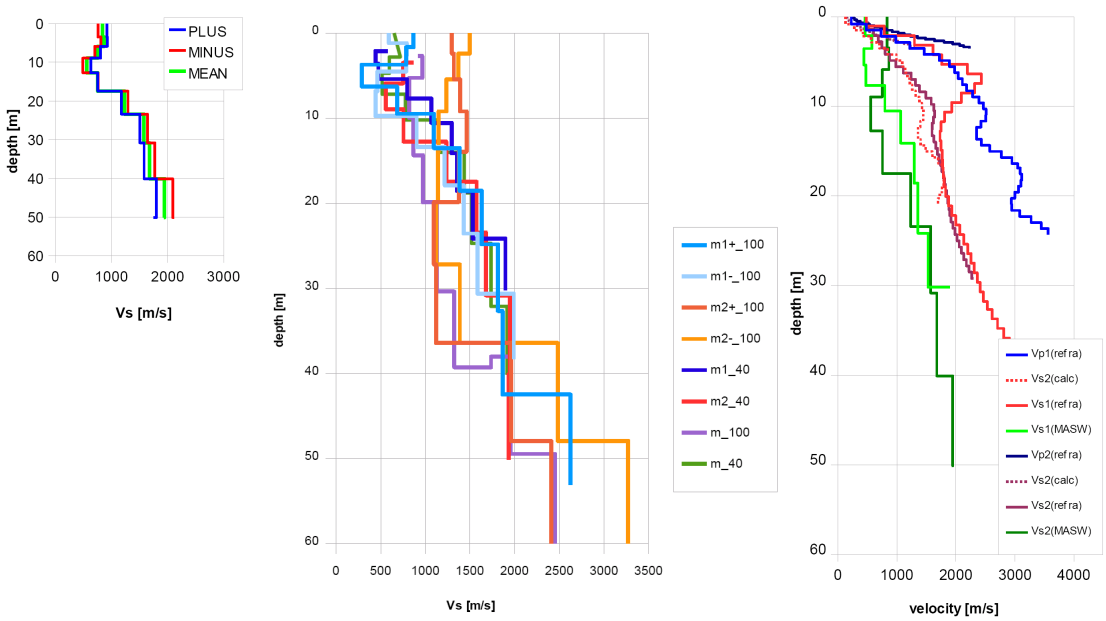

Figure A.2.4. Structural models at site AIGLE without removing structures that do not explain the measured dispersion curves. For more details, see the report of GeoExpert related to the site AIGLE.

A.3 Station BALST

The sensor of station BALST is located in a vault in the rock at the edge of a plateau, about 3 m below the surface. The plateau is part of the Jura ridge with karst Jurassic (Malm) sediments, encircled by older (Dogger) and younger (USM) sediments. S-wave measurements were performed on 2 sections. The first section was very close to station BALST, the second section was about 20m away. The MASW measurements, the P-wave hybrid seismics and the geological observations at the site indicate several sinkholes (limestone with karst formations). On section 1, a sinkhole is seen in the western part of the section showing a layer with reduced shear velocities of around 400m/s. In section 2 the influence of sinkholes and karst formations is visible almost along the entire section with the exception of the southern part. Because H/V spectral ratios at station BALST show no significant peak up to a frequency of 30 Hz (not shown here) and from the geographic position of seismic station BALST, we have assumed that the site is on rock, without influence from the sinkholes. For this reason, only the results from the arrays outside the influence of the sinkhole are used to compute the values for vs5 to vs30. Nevertheless the dispersion curves are rather different for different sections, which results in a large scatter of inverted velocity profiles and in a large standard deviation for the quarter wavelength velocity. The results obtained for the 96m long arrays also show considerable difference between the two sections and in the plus and minus direction as well. These long arrays are influenced by the sinkholes and the average velocity is smaller than for the selected profiles. This again results in a large standard deviation for the quarter wavelength velocity. Lower velocities on section 2, seen with MASW, are also found with P- and S-wave seismics, and the long 85m MASW profiles. Measured S-wave velocities from seismics for depths below about 5m are not reliable, because they are too high when compared to S-wave velocities derived from measured P-wave velocities. P- and S-wave seismics indicate a surface layer of weathered material, which is seen with MASW on some of the inverted profiles, especially in locations of sinkholes.
The H/V spectral ratio at site BALST has only a very weak and insignificant peak at about 1.2-1.5 Hz, which indicates good quality rock conditions.

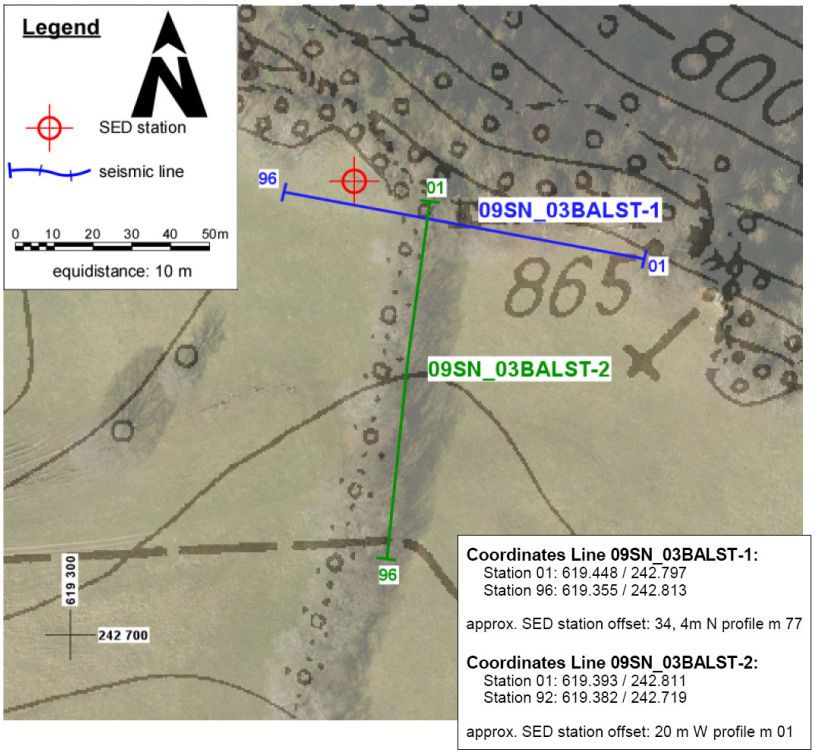

Figure A.3.1. Measurements at site BALST.

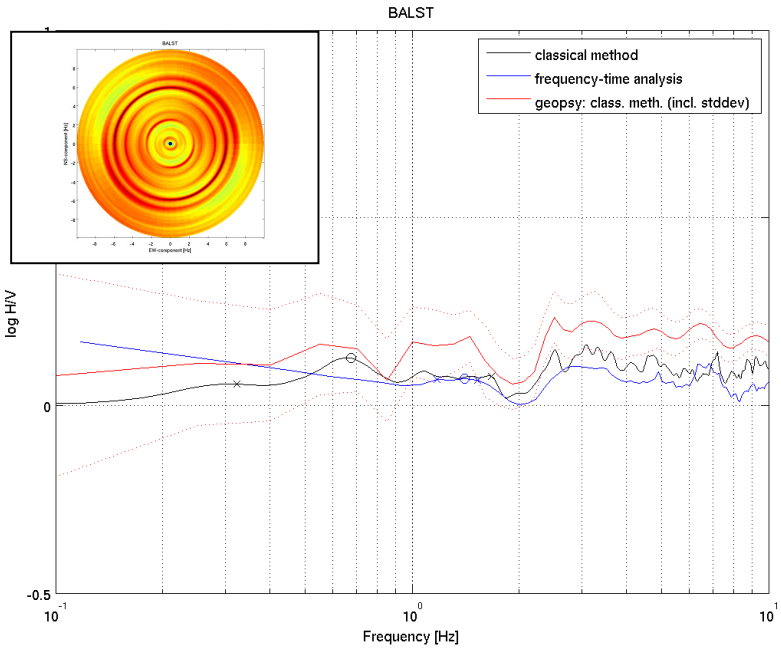

Figure A.3.2. H/V spectral ratios at the site of seismic station BALST.

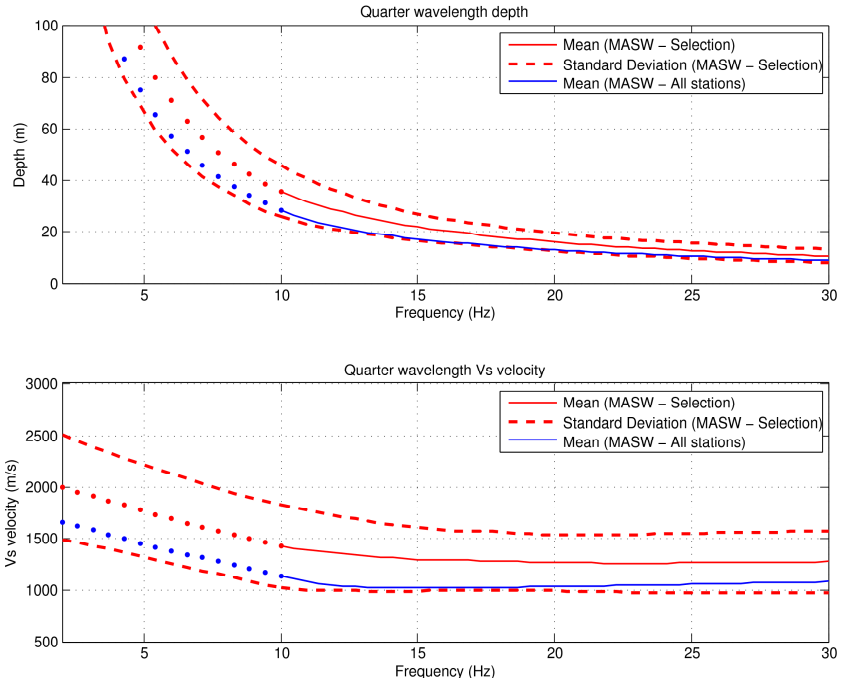

Figure A.3.3. Quarter wavelength velocity for site BALST obtained with MASW.

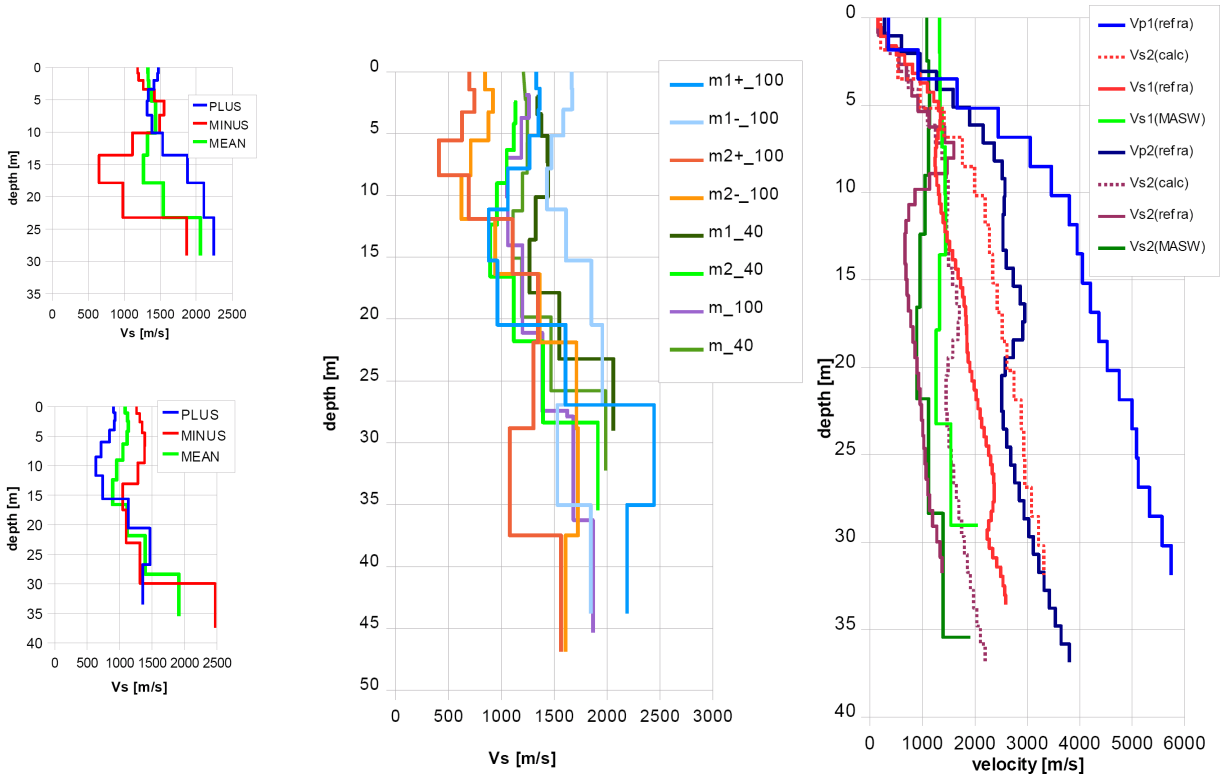

Figure A.3.4. Structural models at site BALST obtained from MASW and seismic measurements. For more details, see the report of GeoExpert related to the site BALST.

A.4 Station BNALP

The sensor of station BNALP is located in a leak water gallery, about 20 m below the surface. The gallery is located in Lower Cretaceous sedimentary rocks. Ambient vibration array measurements were performed at two locations, however no useful dispersion curve could be obtained. Active S-wave measurements at this site were performed on two sections. Section 1 is closer to the position of the station BNALP. The velocities obtained from MASW on section 1 were generally higher than those on section 2, even when only measurements with high phase velocities on section 2 were used for comparison. Slightly lower velocities on section 2 are also found with P- and S-wave seismics in the upper 10m of the structure, as well as on the long 96m MASW profile. The seismic profile on section 2 crosses a shallow depression filled with loose material and is very close to the dam. Most probably due to the presence of the depression and the dam, dispersion curves could not be clearly identified and a large scatter of results was obtained with MASW. For this reason we excluded section 2 from the derivation of vs5 to vs30. Considerably different velocities were also measured on the different arrays in seismic section 1. In most cases velocities are above 1500m/s and many phase velocity curves are almost non-dispersive. This indicates the absence of layers with strongly weathered rock. The measured values for the average S-wave velocity from seismics are comparable to the results obtained with MASW. Measured S-wave velocities from seismics are also consistent with S-wave velocities derived from measured P-wave velocities. We have selected the MASW results from the small arrays of section 1 for the determination of vs5 to vs30.

The H/V spectral ratio at site BNALP has no peak. The generally very flat H/V curve is a typical feature for rock sites.

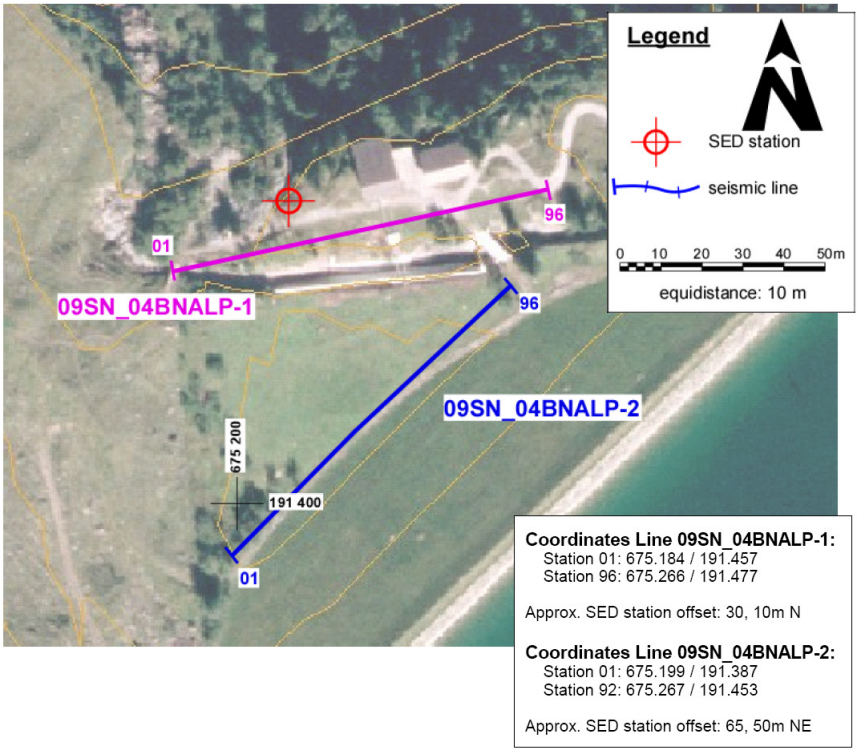

Figure A.4.1. Seismic measurements at site BNALP.

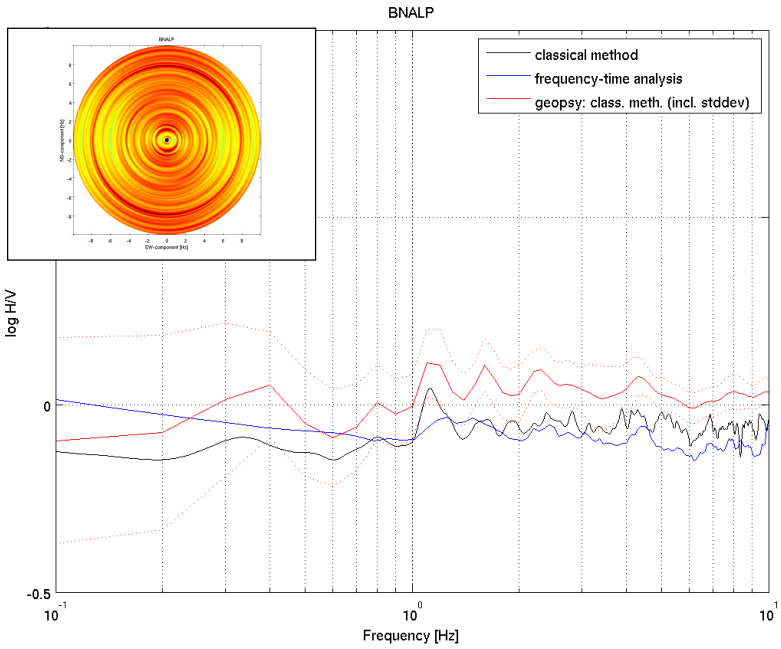

Figure A.4.2. H/V spectral ratios at the site of seismic station BNALP. The station is about 20 m below the surface.

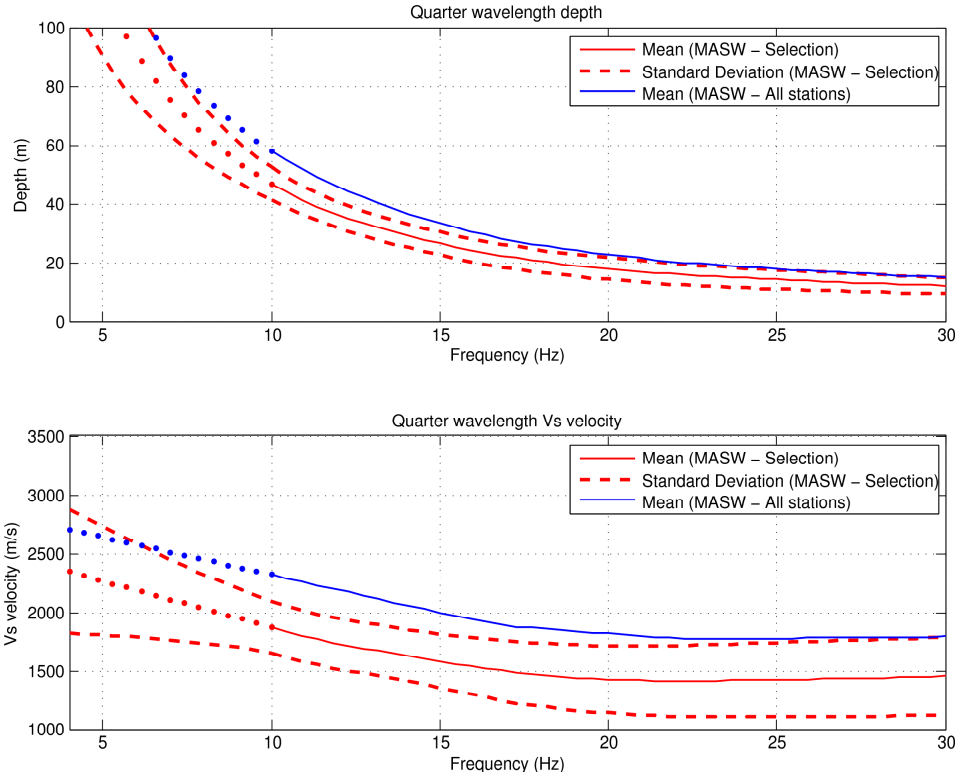

Figure A.4.3. Quarter wavelength velocity for site BNALP obtained with MASW. For the vs5 to vs30 determination, the mean of the different MASW sections on profile 1 is used.

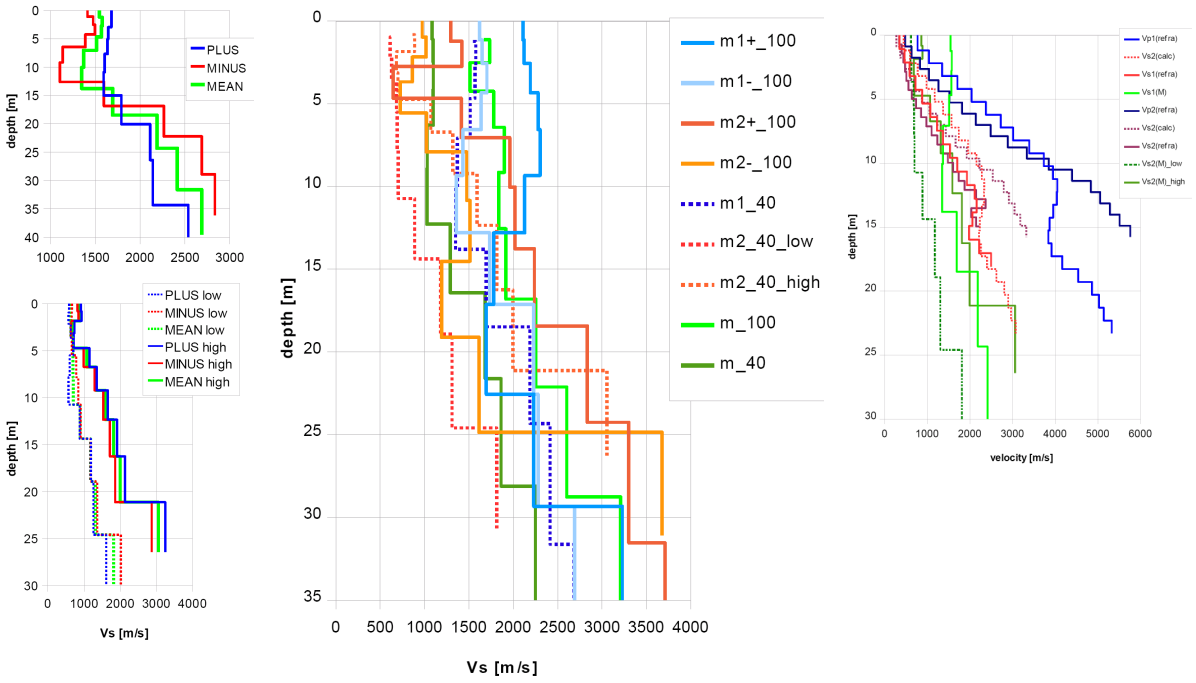

Figure A.4.4. Structural models at site BNALP. For more details, see the report of GeoExpert related to the site BNALP.

A.5 Station BOURR

Station BOURR is located 15-20 m below the surface in the south-east flank of a small hill, about 2 km east of the town of Bourrignon. The bedrock consists of a massive calcium-carbonate formation of late Jurassic age (Malm), occasionally alternating with marl layers. The rock formation is covered with a layer of weathered material and soils of variable thickness. The topography is highly irregular, with a terrace structure modeled by the action of water. Due to the irregularity of the terrain, it was not possible to perform the measurements at the same location as the seismic station BOURR. The arrays and seismic section are about 80-100m away from the sensor, and the obtained results from the geophysical measurements therefore need some interpretation.

As part of the validation test, ambient vibration array measurements were performed at the same site as the active seismic survey. Ambient vibration measurements were set up with two arrays, one on each terrace (see the results in the report for BOURR in Appendix B). The array on the lower terrace could only resolve the shallower soft sediments, which is not of interest for the characterization of the site of the seismic station. The array on the upper terrace better resolves the rock velocity profile. In this case, the upper part (due to soil formations) has been removed from the final interpretation because soils are not present on the flank of the hill.

Active S-wave measurements at this site were performed along one section at the base of the hill. MASW results were used to characterize the S-wave velocity. The section with only thin surface sediments was selected to characterize the structure. MASW for the long profiles resulted in an improved resolution at depth when compared to the smaller profiles. The results from MASW are confirmed by ambient vibration array measurements within the uncertainties of the methods, taking into account the difference in measurement location.

Ambient noise H/V spectral ratios from the BOURR station recordings reveal a stable peak at around 1.7 Hz, which is also visible in all the stations of the two arrays. This peak might be assigned to a first rock layer. Assuming an average S-wave velocity of 1100-1400 m/s, the thickness of this layer should be in the range of 165-210 m. As observable from the peak H/V amplitude, the velocity contrast to the deeper rock layers is not very strong.

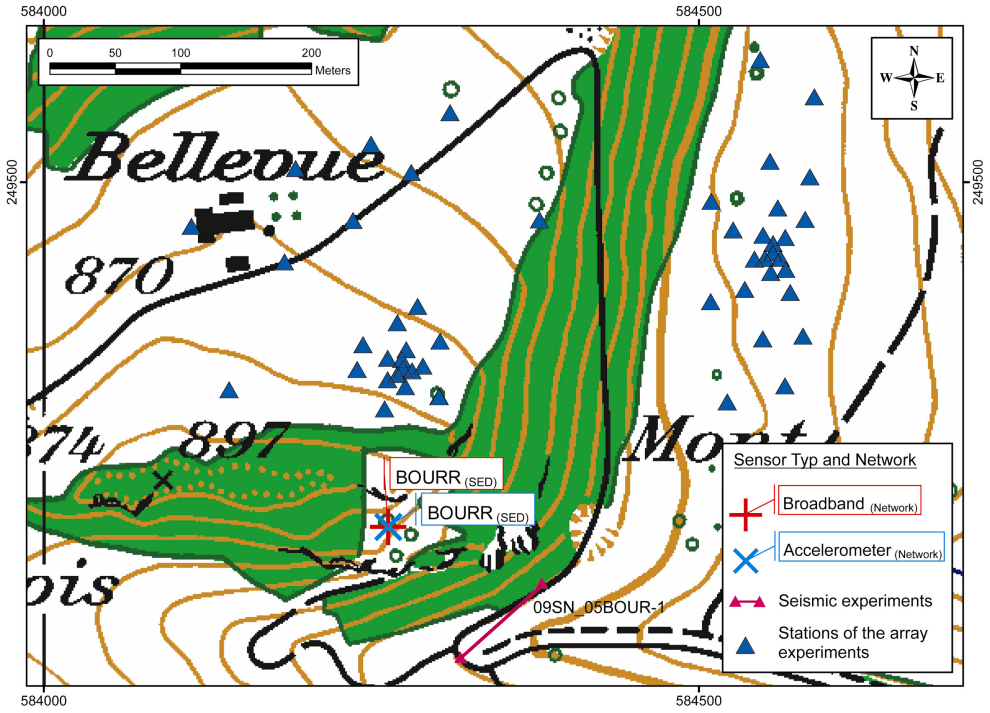

Figure A.5.1. Measurements at site BOURR.

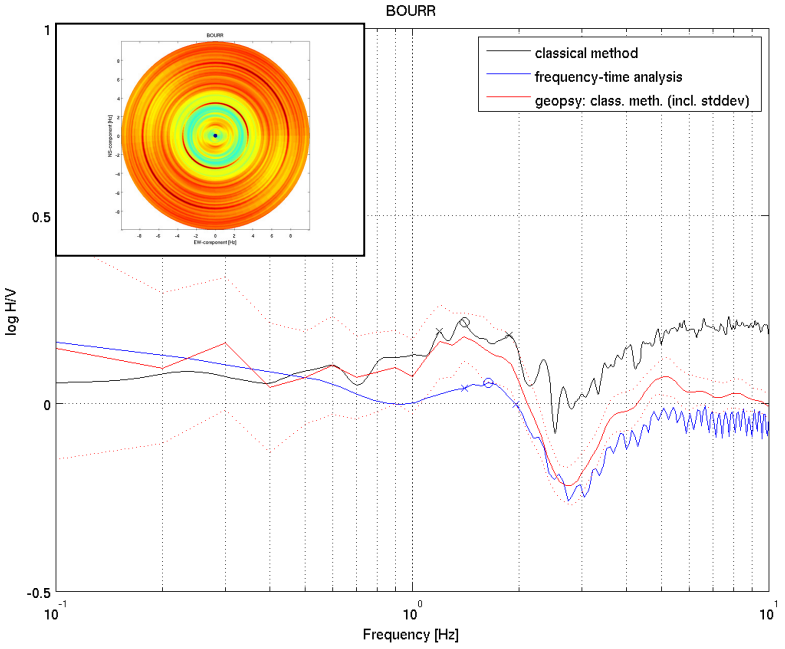

Figure A.5.2. H/V spectral ratios at the site of seismic station BOURR. The station is about 15-20m below the surface.

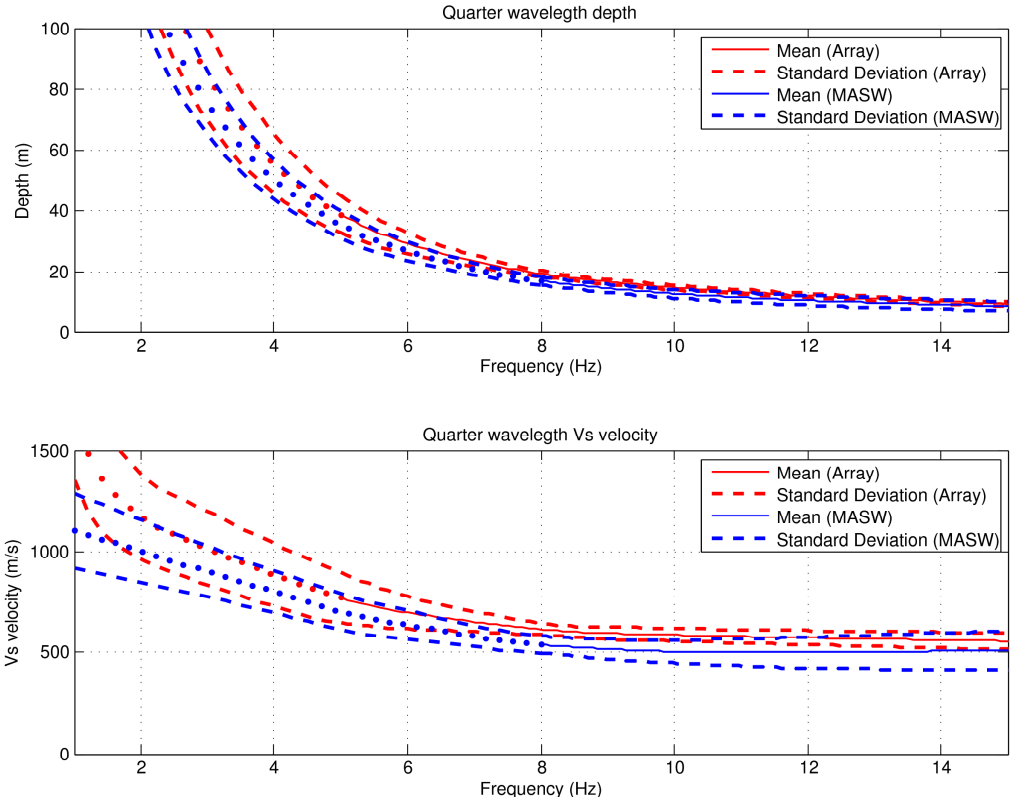

Figure A.5.3. Quarter wavelength velocity for site BOURR obtained with MASW and ambient vibration array techniques. For the computation of vs5 to Vs30 the results from the array measurements were used.

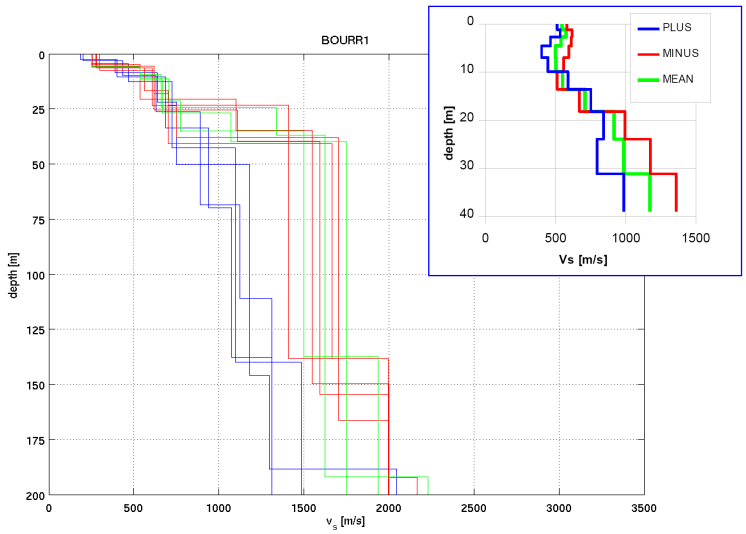

Figure A.5.4. Structural models at site BOURR measured from ambient vibrations on the upper terrace (left), and with MASW at the base of the hill. The blue structures in the left figure use the H/V spectrum in the inversion and are therefore selected to characterize the rock velocity. The upper part with soft sediments (6m) is removed for the determination of the quarter wavelength velocity of the ambient vibration results in Figure A.5.3.

A.6 Station BRANT

The sensor of station BRANT is located inside a natural cave, on a Jurassic (Malm) karst sediment plateau. The sensor is about 9 m below the surface. Active S-wave measurements at this site were performed along two perpendicular sections. The first section is at about 20m from the seismic station. In parts of the section the soil thickness may span over a few meters and increases towards the southwest. The inverted profiles from this part of the section, with increased thickness of softer sediments or weathered rock, are not used for the v5 to vs30 estimation. The second section is very close to the site of the sensor.
P- and S-wave seismics indicate a surface layer of weathered material, which is not resolved with MASW. The measured vp and vs velocities from seismic measurements are consistent for both sections for depths to about 10m. The S-wave velocity in the first 10 meters increases gradually to about 1000-1500 m/s.
The average S-wave velocity obtained with MASW is very similar for the two sections. Dispersion curves are better identified on section 2. The dispersion curves on the long 96m profile have the tendency to result in a higher phase velocity at given frequency. All the selected short profiles were used for the vs5 to vs30 calculation.
The H/V spectral ratio at site BRANT has no peak. The generally very flat H/V curve is typical for rock sites.

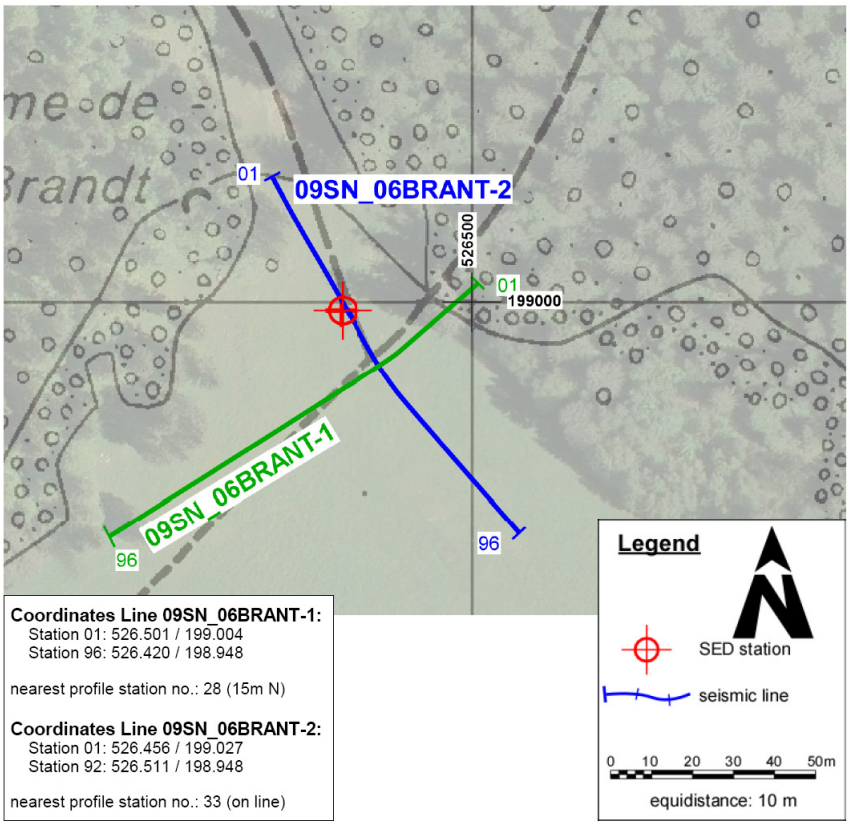

Figure A.6.1. Measurements at site BRANT.

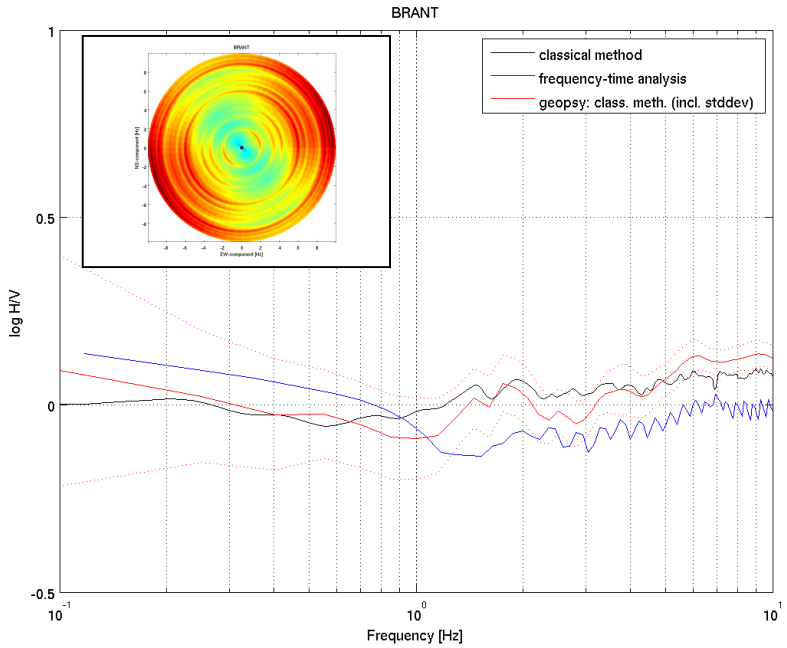

Figure A.6.2. H/V spectral ratios at the site of seismic station BRANT. The station is about 9m below the surface.

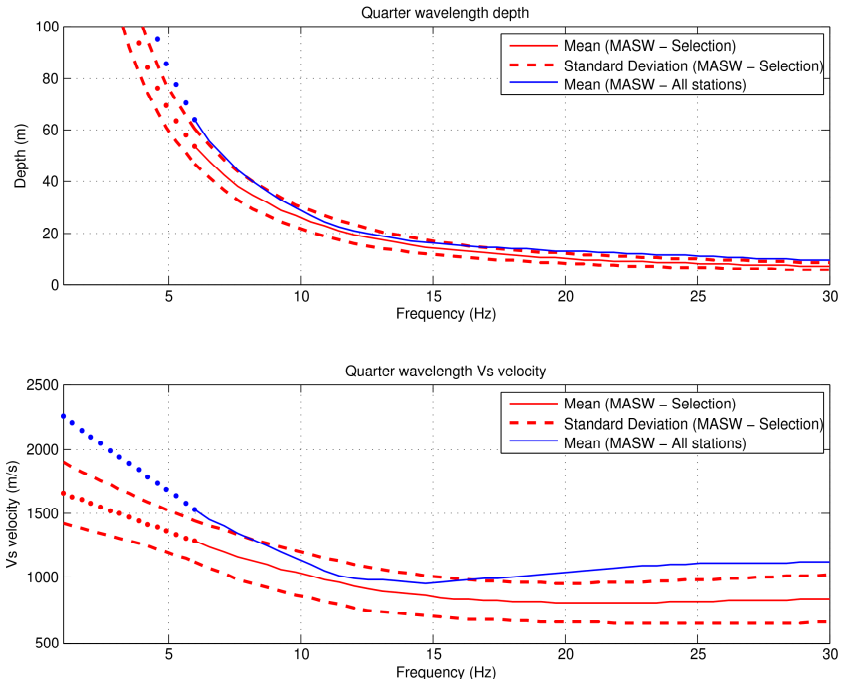

Figure A.6.3. Quarter wavelength velocity for site BRANT obtained with MASW from the small profiles in section 1 and 2, and for the whole sections. All the selected short profiles were used for the vs5 to vs30 calculation.

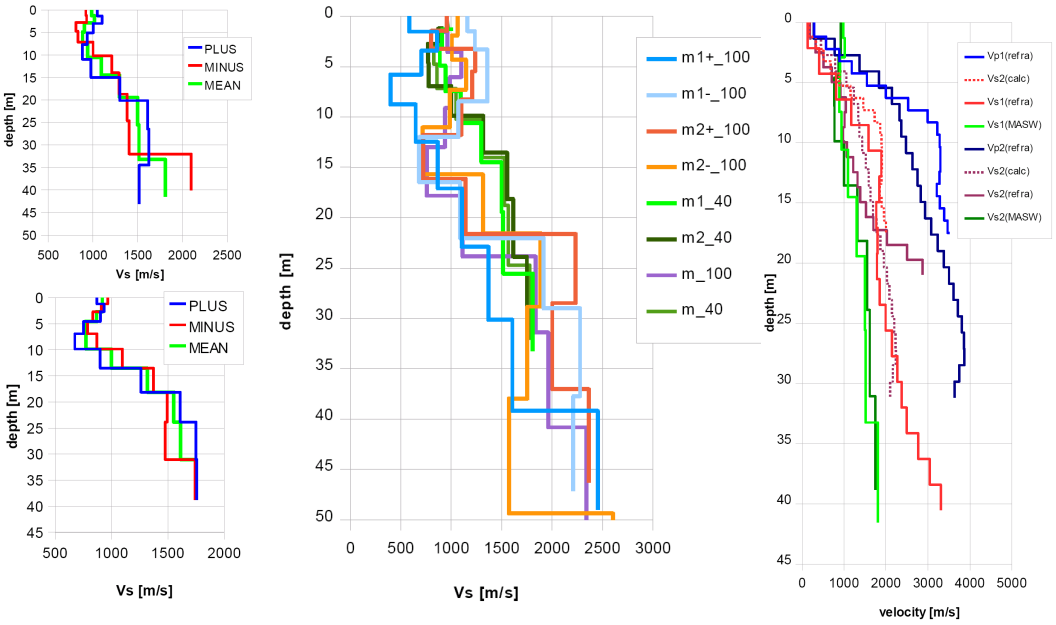

Figure A.6.4. Structural models at site BRANT. For more details, see the report of GeoExpert related to the site BRANT.

A.7 Station FLACH

The sensor of station FLACH is located on rock in a small natural cave in the flank of a hill. The rock is composed mostly of layered sandstones, marl and conglomerates. Surface material consists of unconsolidated, loose scree. Geophysical techniques were applied at site FLACH although not directly at the station site. S-wave measurements were performed on 2 sections. The end of the first MASW section is about 30m away from the sensor. The second section is more than 100m away and is located on the top of the hill. The seismic P-wave profiles indicate no strong lateral variations in velocity, and softer layers are visible over the entire profile with thicknesses in the range of 3 to 5m. Because both the MASW and S-wave seismic results did not show strong lateral variation in velocities, the results from the entire profiles were used to compute the values for vs5 to vs30. The average value of the S-waves obtained with MASW in the uppermost layers is around 400-500m/s. The thickness of this layer is about 10m. Below this layer velocities are gradually increasing to the first non-weathered rock layer at around 15m depth. The results from the 100m arrays show that the average S-velocity of the first non-weathered rock layer is of the order of 800-1000m/s. The layer thickness is around 20-25m. The results from S-wave seismic measurements below depths of 5m correspond to the results obtained with MASW. There is some indication of a phase in the range of 800-1200m/s in some of the dispersion plots that support this interpretation.

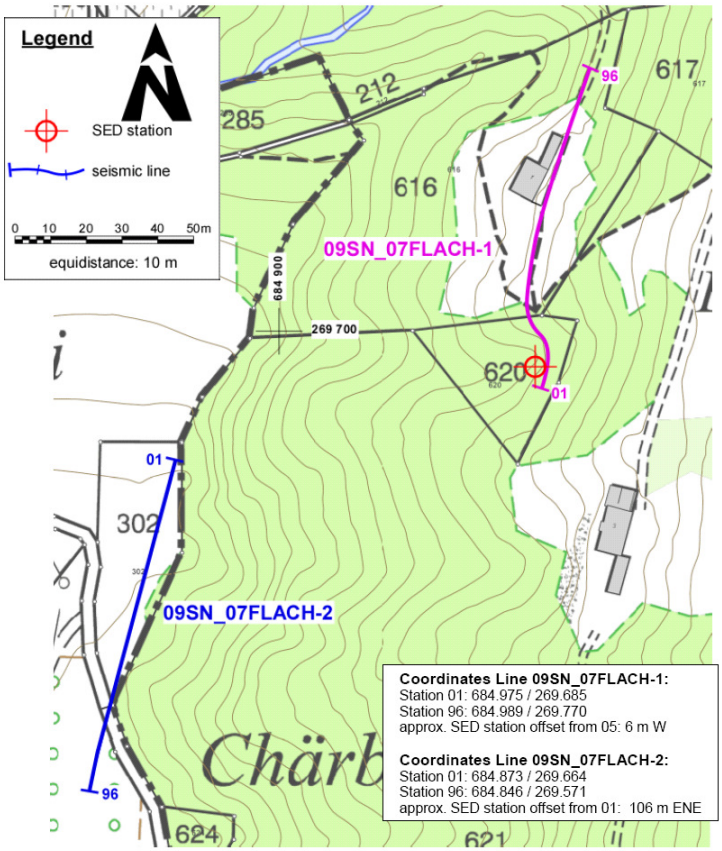

Figure A.7.1. Measurements at site FLACH.

The H/V spectral ratio at site FLACH has two peaks, a clear peak at around 5 Hz and a weak peak at 0.8 Hz. Assuming a mean velocity of the first layer of about 700m/s (uppermost layers plus first layer of non-weathered rock), with a thickness of about 35-40m, results in a fundamental frequency of resonance around 5 Hz, which can explain the clearly visible H/V peak. The H/V spectral ratio around this frequency shows a polarization in the EW direction, perpendicular to strike of the hill. This might indicate an influence of the topography at this site. The interpretation of the H/V peak at 5Hz would require a strong velocity increase at a depth of about 35-40m. The peak at the lower frequency might then be associated to a second velocity contrast between rock layers. Assuming an average velocity in the range 1500-1800 m/s for the entire layer above this contrast would result in a thickness in the range 460-570m.

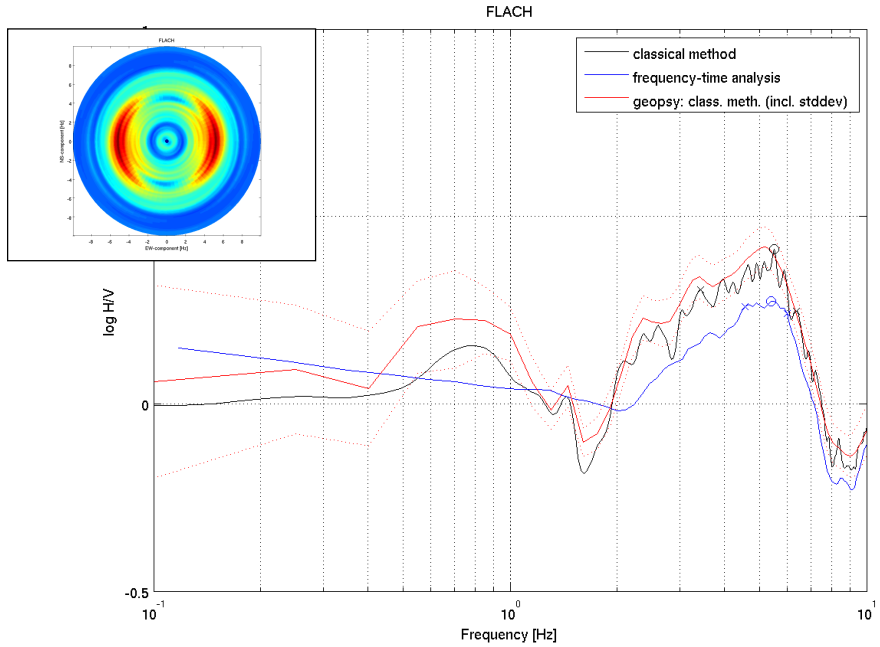

Figure A.7.2. H/V spectral ratios measured at the site of seismic station FLACH. The seismic instrument is located close to surface in a small natural cave.

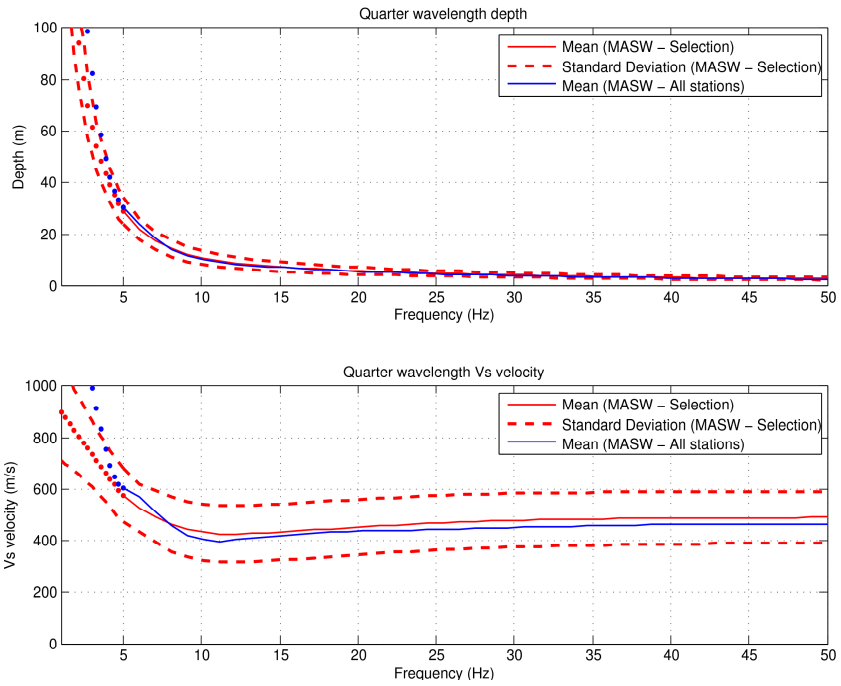

Figure A.7.3. Quarter wavelength velocity for site FLACH obtained from MASW, using selected smaller arrays (red) and the long 100m arrays (blue). For the Vs5 to vs30 calculation the whole lines are taken.

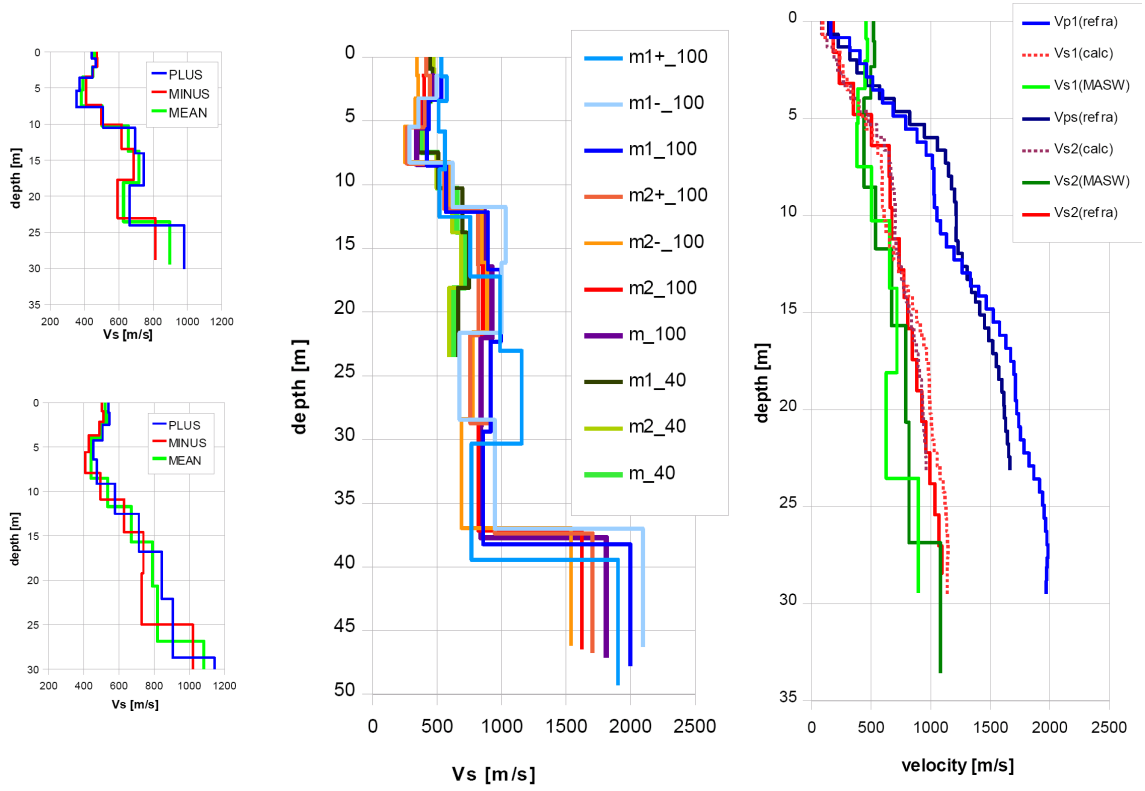

Figure A.7.4. Structural models close to site FLACH. For more details, see the report of GeoExpert related to the site FLACH.

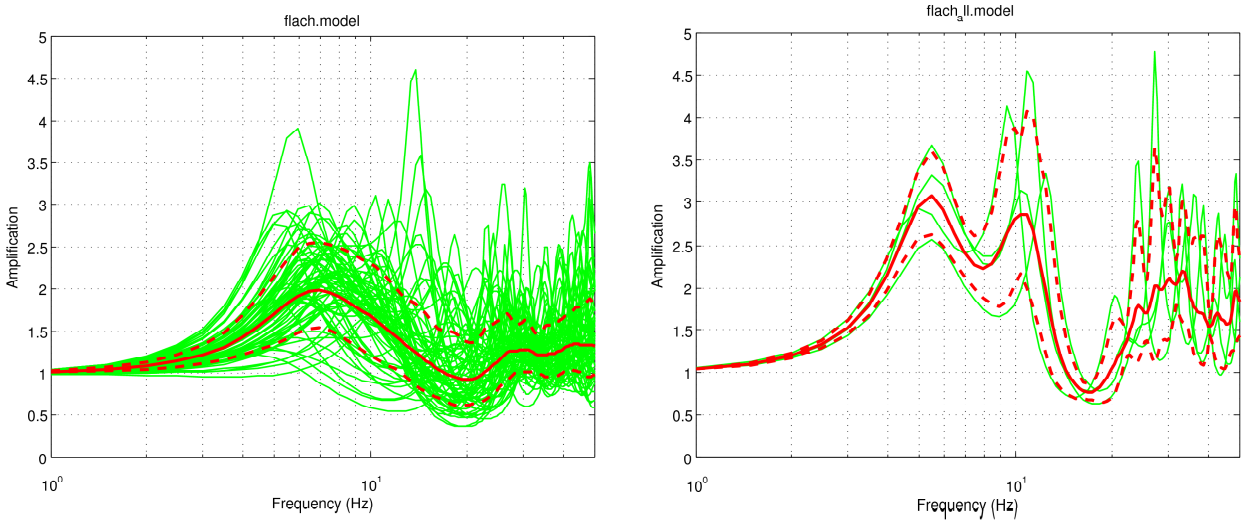

Figure A.7.5. SH amplification functions from Vs profiles obtained with MASW technique, using selected smaller arrays (a) and the long 100 arrays (b). The latter is preferable, due to the reliability of the inverted profiles and the good match of its fundamental frequency with the measured one. Average values are in red solid lines, standard deviations in red dashed lines.

A.8 Station GIMEL

The sensor of station GIMEL is located in a military cavern in a Lower Cretaceous sediment unit covering the widespread Malm rock plateau in the Jura. The sensor is about 10 m below the surface at the base of a cliff. Active S-wave measurements at this site were performed along two sections. The first section is on the Cretaceous cliff above the seismic station. In parts of the section the soil thickness may span over a few meters. The second section is also on the cliff, perpendicular to the first section, and more than 30m from the seismic station GIMEL.

P- and S-wave seismics indicate a surface layer of weathered material that is not resolved with MASW. The measured vp and vs velocities from seismics are consistent for section 1, for depths down to about 10m, whereas on section 2 the measured S-wave velocity seems to be too high when compared to the measured P-wave values.
The S-wave velocity in the first few meters increases gradually to about 1400-1600 m/s. This first rock layer is seen in all dispersion plots obtained with MASW. The dispersion curve shows only small variations in wave velocity dispersion. The average S-wave velocity obtained with MASW is very similar for the two sections. All the small profiles were therefore used for the vs5 to vs30 calculation.

The H/V spectral ratio at site GIMEL has only a small, insignificant peak at around 4.5Hz. The generally very flat H/V curve is typical for rock sites.

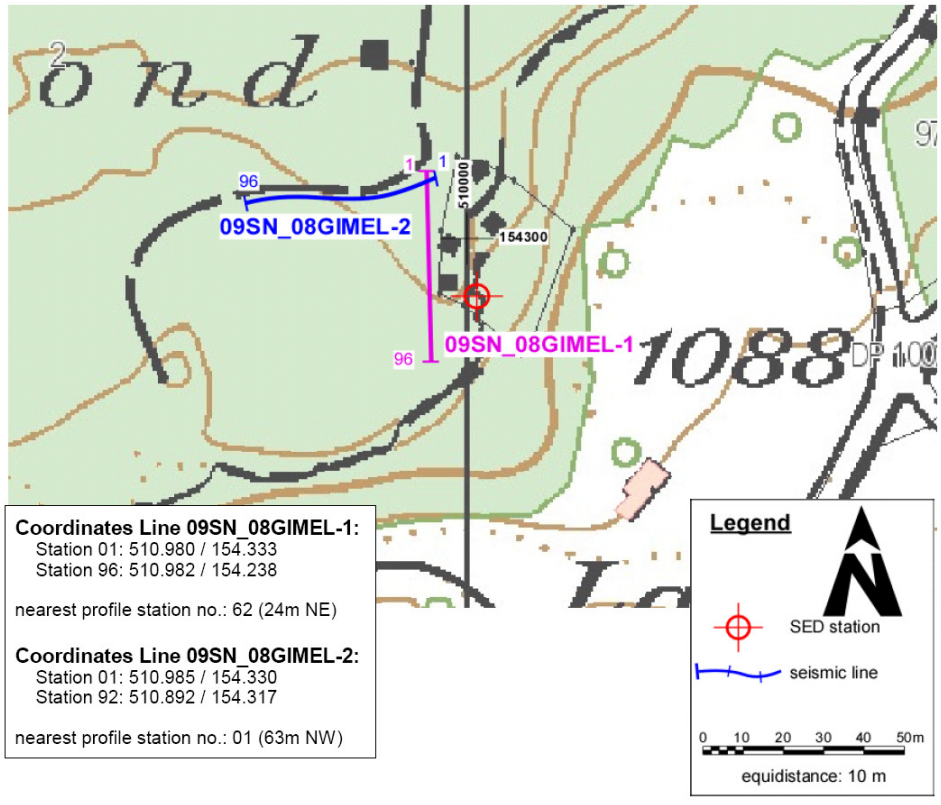

Figure A.8.1. Measurements at site GIMEL.

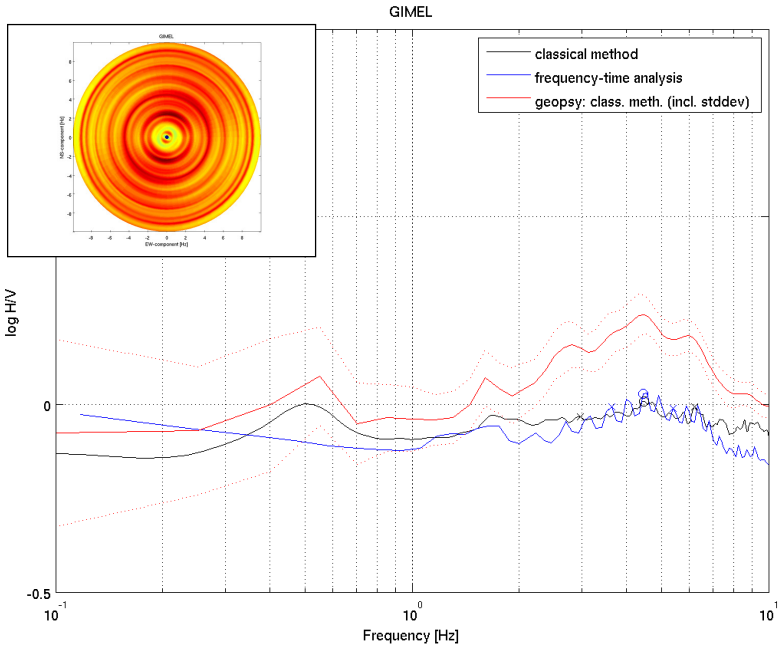

Figure A.8.2. H/V spectral ratios at the site of seismic station GIMEL. The station is about 10m below the surface.

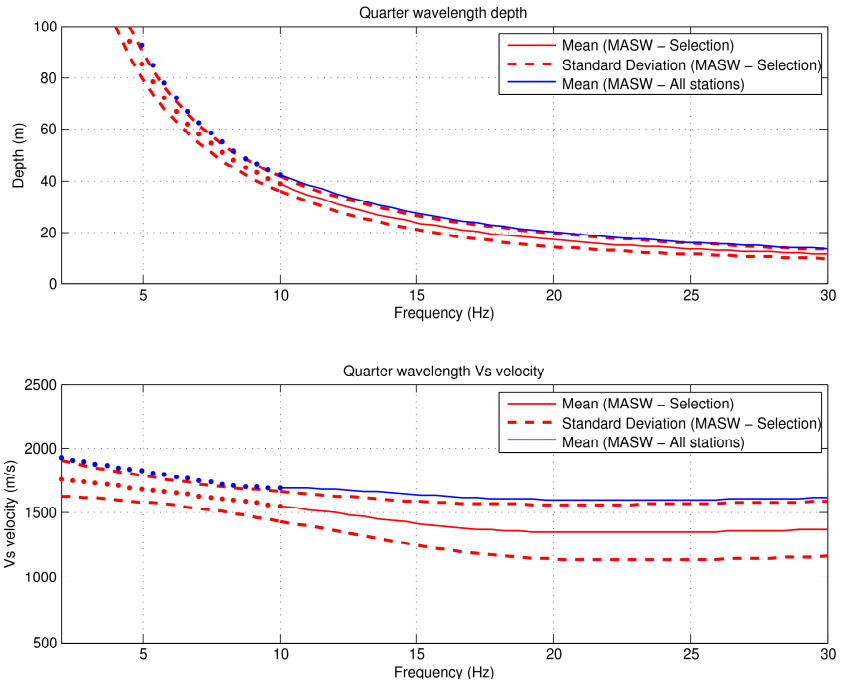

Figure A.8.3. Quarter wavelength velocity for site GIMEL obtained with MASW from the small profiles in section 1 and 2, and for the whole sections. For the determination of the vs5 to vs30 the small profiles were taken.

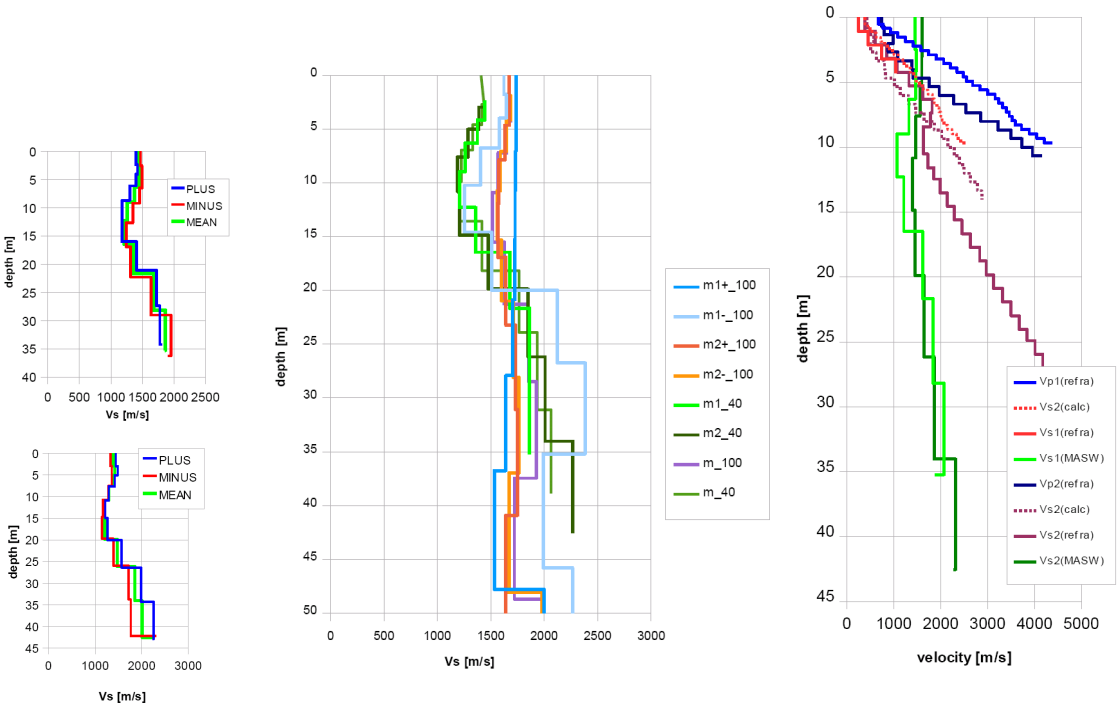

Figure A.8.4. Structural models at site GIMEL. For more details, see the report of GeoExpert related to the site GIMEL.

A.9 Station HASLI

The sensor of station HASLI is located on the concrete at the rear of a bunker, about 3 m below the surface. The bunker is located on the top of a Jurassic (Malm) sediment ridge. The rocks consist of hard, massive limestone. Active S-wave measurements at this site were performed on two sections. The seismic profile on section 2 crosses a shallow depression filled with loose material. The area of the depression was excluded from the derivation of vs5 to vs30. The dispersion curves have only small changes in phase velocity, in most cases with velocities always above 1500m/s. This indicates the absence of weathered rock layers. The velocities obtained with MASW on section 1 were higher than those on section 2, even when only measurements outside the depression were used. Lower velocities on section 2 are also found with P- and S-wave seismics and the long 85m MASW profiles. The measured S-wave velocities from seismics are not reliable because they are too high when compared to S-wave velocities derived from measured P-wave velocities. We cannot decide if the location of station HASLI is more similar to section 1 or the rock part of section 2, or alternatively, corresponding to the high values obtained from the long MASW profiles. For this reason we combine the results from both profiles, in a selected range, to define vs5 to vs30.
The H/V spectral ratio at site HASLI has only a very weak peak around 1.6 Hz, which might be due to changes in the velocity of the bedrock at greater depth. The generally very flat H/V curve is typical for rock sites. A strong phase can be identified in most dispersion curve images with phase velocity around 1600-2000m/s.

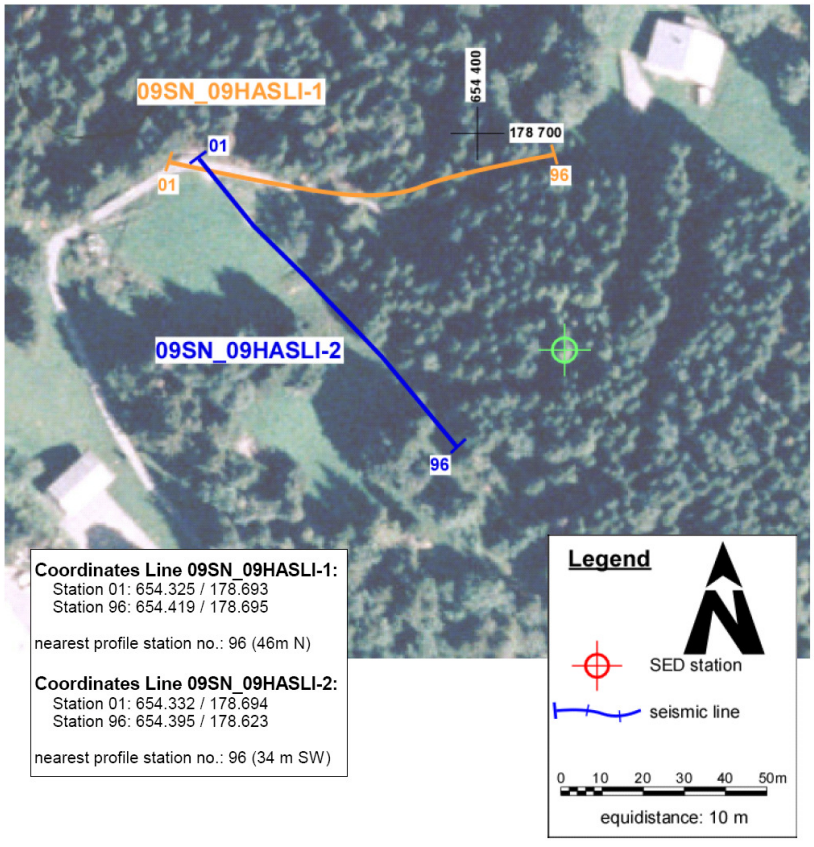

Figure A.9.1. Measurements at site HASLI.

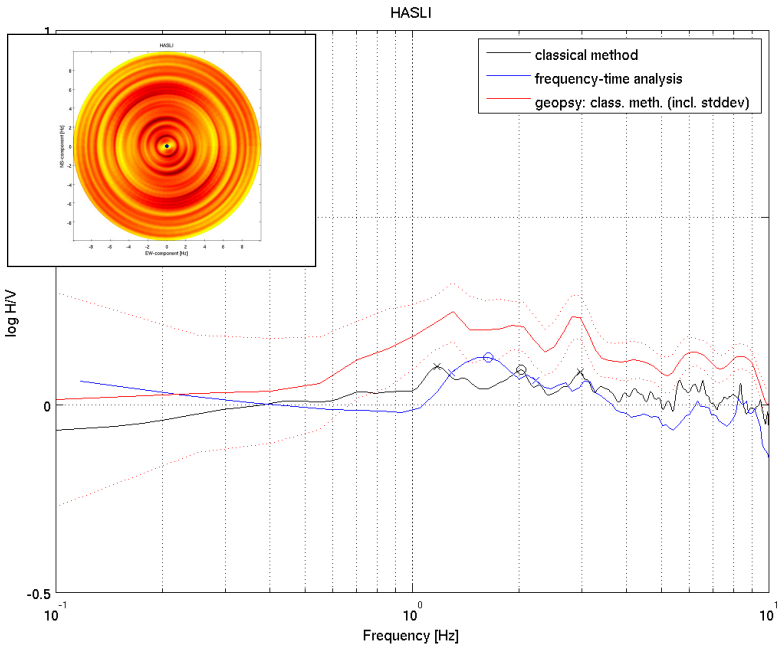

Figure A.9.2. H/V spectral ratios at the site of seismic station HASLI. The station is about 3 m below the surface.

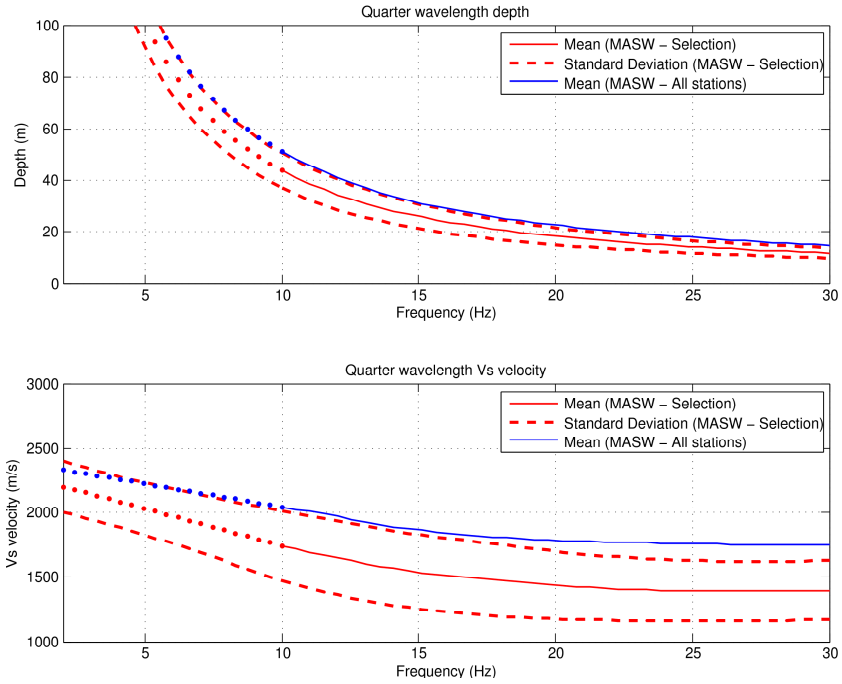

Figure A.9.3. Quarter wavelength velocity for site HASLI obtained with MASW using a combination of profiles 1 and 2. Velocity profiles obtained using all receivers appear to be high. For this reason, vs5 to vs 30 are estimated from the velocity profiles of the selected smaller array configurations only.

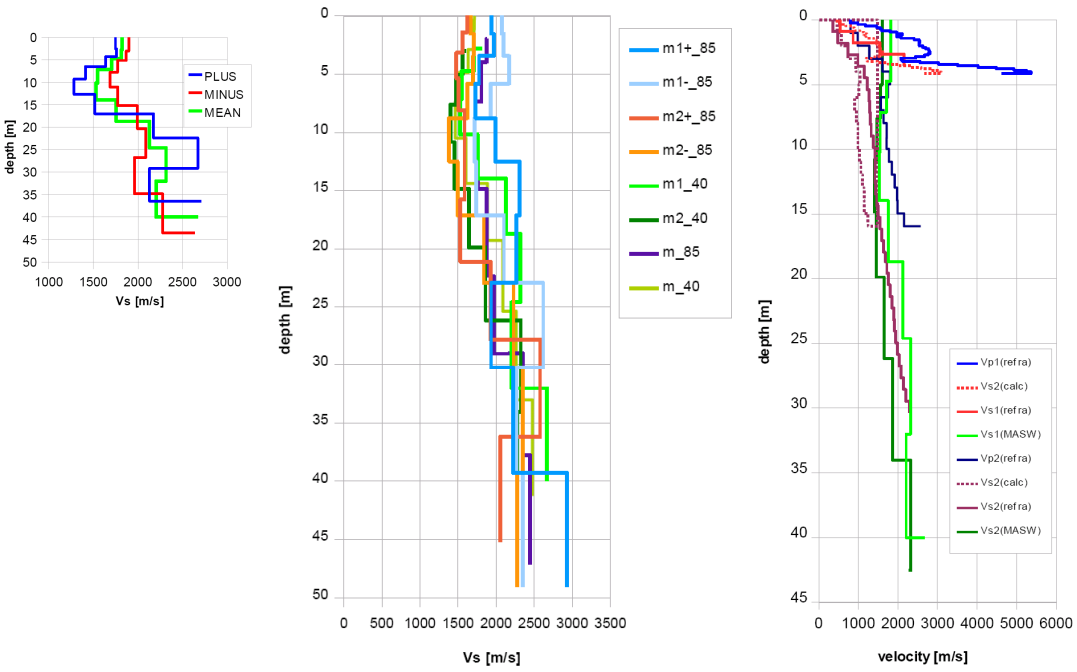

Figure A.9.4. Structural models for site HASLI. For more details, see the report of GeoExpert related to the site HASLI.

A.10 Station LLS

Station LLS is located 20m below the surface in a gallery in hard layered limestone sediments near the Linth-Limmern dam. The gallery is in the south-western flank of a steep rock face of about 700m in height. Active measurements at this site were performed in the gallery, which violates the assumptions for the inversion of the phase velocity curves and creates uncertainties in the interpretation of the seismic profiles. All results obtained with MASW show an almost non-dispersive phase with velocities around 2800-3000m/s. There are several possibilities to interpret this phase; one possibility would be as a direct S-wave train or another as a direct P-wave train. On one hand P-wave hybrid measurements indicate a P-wave velocity of about 2500-3000m/s in the upper 5m, which would then require S-wave velocities in the range 1400-1700m/s. On the other hand, the S-wave refraction seismic results in S-wave velocities in the range 2500-3000m/s in the upper 5m. The reason for this might also be wave conversion from P to S, such that the direct S-wave cannot be recognized. Due to the fact that the phase can be seen in MASW for frequencies as low as 50Hz, which corresponds to wavelengths in the range 50-60m, and that the P-wave velocity is increasing to velocities above 4000m/s at a depth larger than 10m, preference is given to the interpretation that an S-wave train is observed. The interpretation of the phase seen in the dispersion plot as the fundamental mode is somehow arbitrary. The exact problem would have to be treated with cylindrical symmetry.

Ambient noise H/V spectral ratios from the LLS station recordings reveal several small peaks around 1.5, 3.5 and 5 Hz. Whereas the peak at 1.5Hz is polarized in SW direction, perpendicular to strike of the rock face, the peaks at 3.5 and 5 Hz are polarized in the NS direction. A minimum in the H/V ratio is seen at around 7-9 Hz. These observations are not typical for rock- sites and might be due to topographic effects and/or the influence of the nearby dam and lake (the dam is striking in the SE direction and the lake is striking in the NS direction), and the machinery operating at these sites.

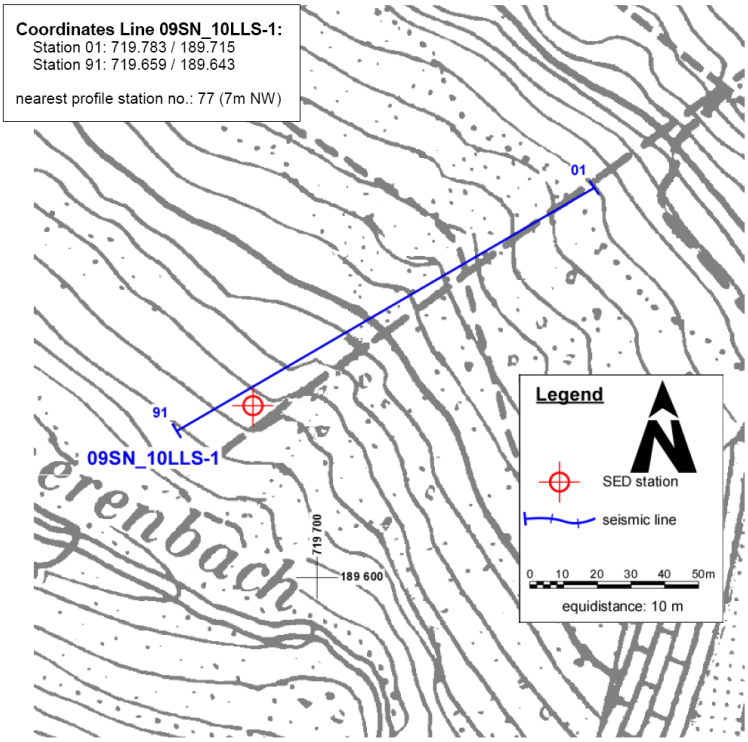

Figure A.10.1. Measurements at site LLS.

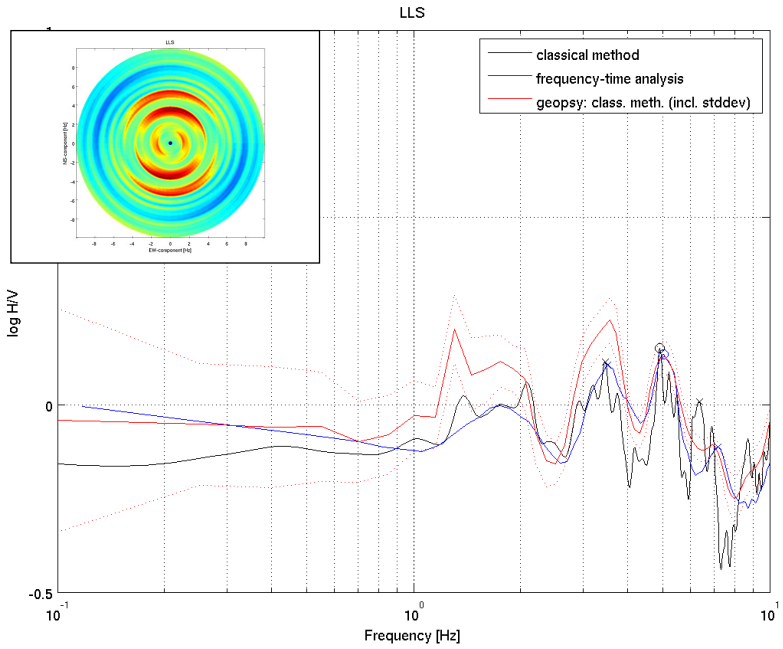

Figure A.10.2. H/V spectral ratios at the site of seismic stations LLS. The station is about 20m below the surface.

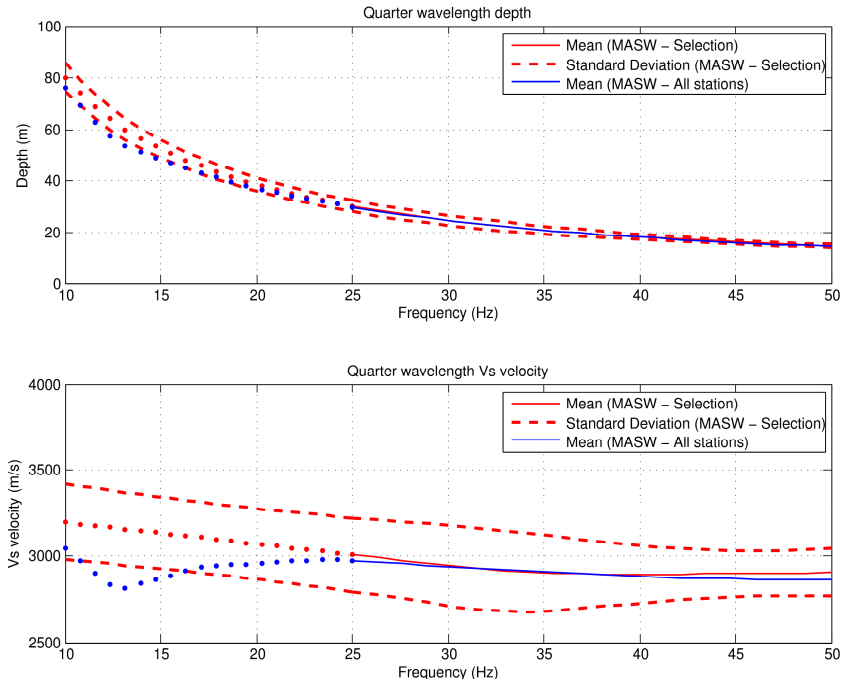

Figure A.10.3. Quarter wavelength velocity for site LLS obtained with MASW. For the vs5 to vs30 determination, the mean of the selected MASW small arrays is used.

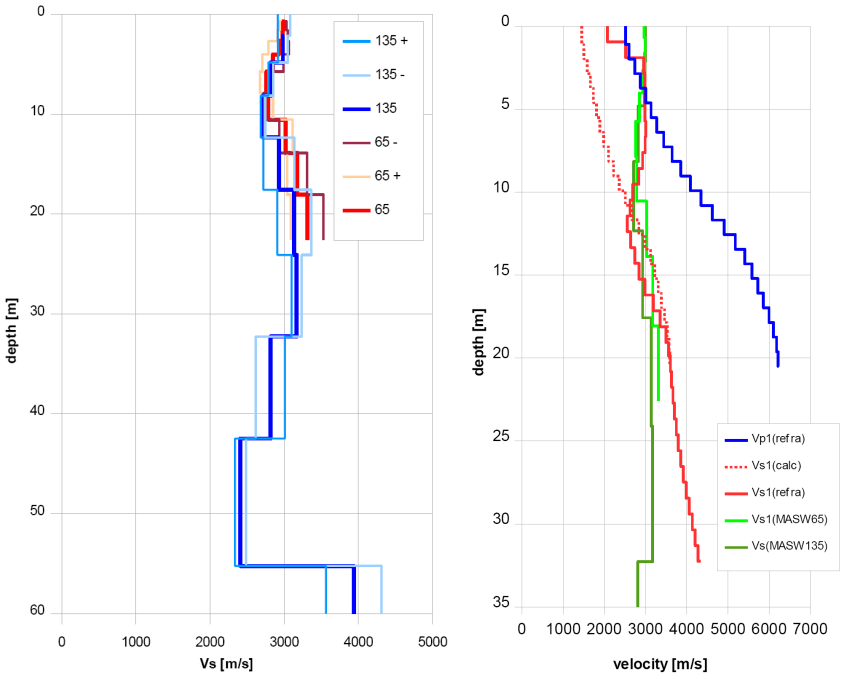

Figure A.10.4. Structural models at site LLS measured with MASW and seismic methods in the tunnel. For more details, see the report of GeoExpert related to the site LLS.

A.11 Station MUO

The sensor of station MUO is located in a bunker in rock at the edge of a small plateau on the top of a mountain, a few meters below the surface. The bunker is in a massive formation of Lower Cretaceous limestone. Active S-wave measurements at this site were performed on two sections. Due to the topography at the site, the position of the station MUO is about 25 and 50m away from the two profiles.
P- and S-wave seismics indicate a surface layer of weathered material, which is not resolved with MASW. The measured vp and vs velocities from seismics are consistent for both sections, for a depth range down to about 5m. The S-wave velocity in the first 10m meters increases gradually to 1000 m/s. MASW cannot resolve this gradient. The measured S- waves velocities below 5m depth derived from seismic and MASW are slightly too high when compared to S-wave velocities derived from measured P-waves.
The average S-wave velocity obtained with MASW is slightly smaller on section 1. Dispersion curves have only small variations of the phase velocity; some of the phase velocity curves are almost non-dispersive. All the smaller profiles were used for the vs5 to vs30 calculation. The dispersion curves on the long 96m profile have the tendency to result in slightly higher phase velocity at given frequency.

The H/V spectral ratio at site MUO is has a small peak at about 1.6 Hz. This peak shows a polarization in the NE-SW direction that might be related to some topographic effect. A series of smaller peaks in the H/V ratio show the same polarization with some azimuth variations. These general features of polarization indicate that the rock-slope is unstable and moving in SW direction.

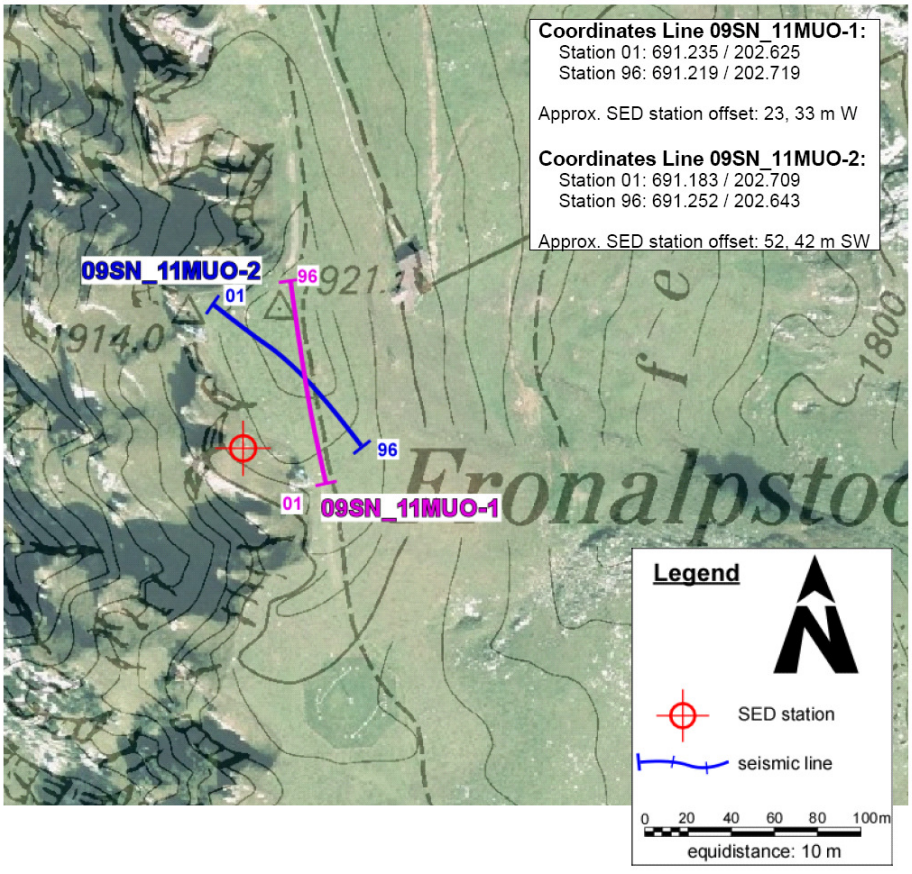

Figure A.11.1. Measurements at site MUO.

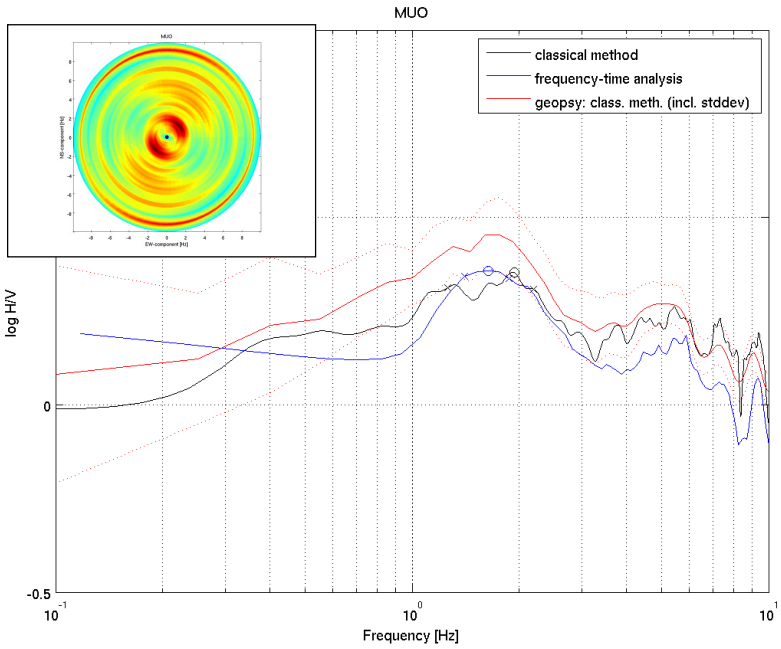

Figure A.11.2. H/V spectral ratios at the site of seismic station MUO. The H/V peak at about 1.5Hz might indicate a topographic effect. A clear polarization is seen in the radial plot. The general features of polarization indicate that the rock-slope is unstable and moving in SW direction.

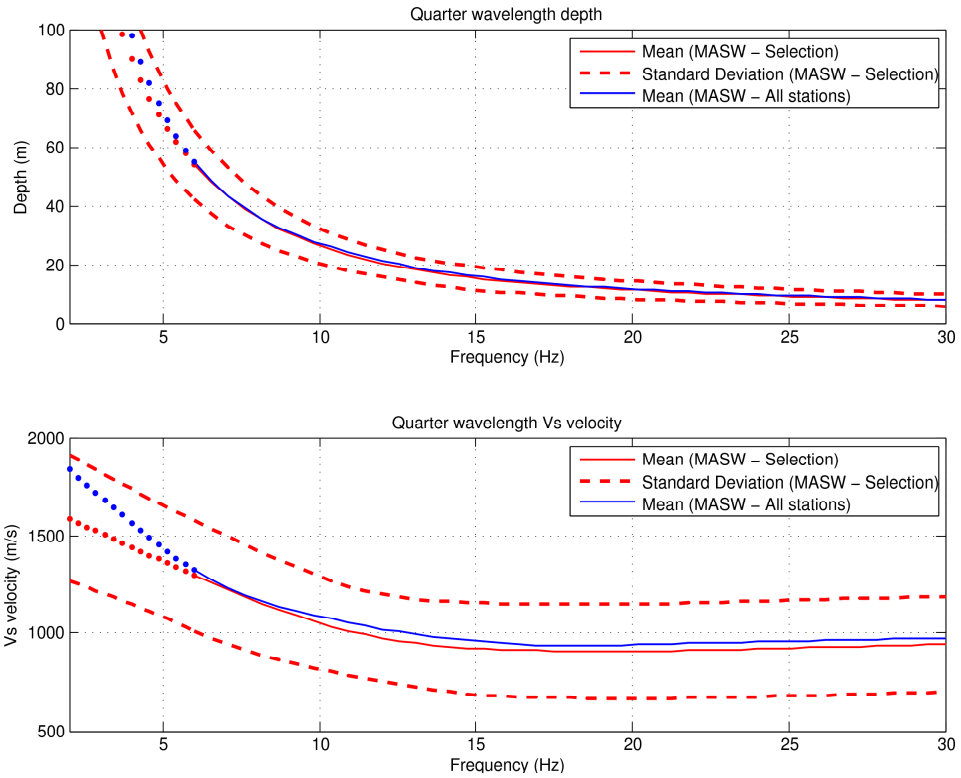

Figure A.11.3. Quarter wavelength velocity for site MUO obtained with MASW using profiles 1 and 2. For the vs5 to vs30 determination, all the small configurations of lines 1 and 2 have been used.

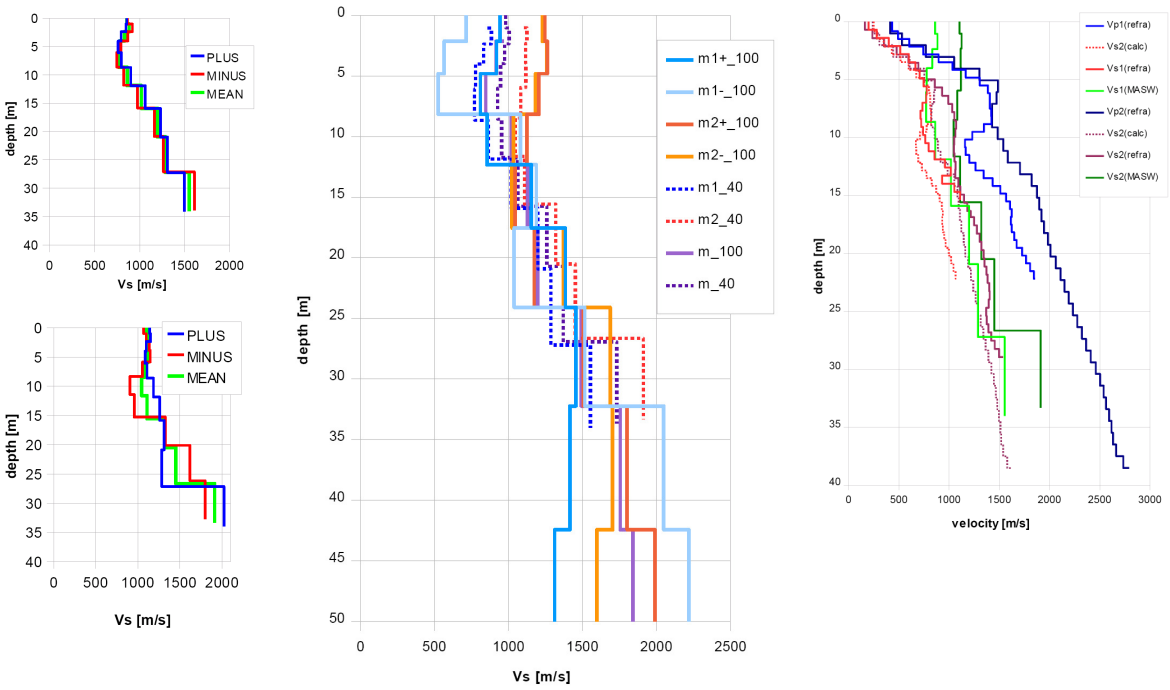

Figure A.11.4. Structural models at site MUO. For more details, see the report of GeoExpert related to the site MUO.

A.12 Station PLONS

The sensor of station PLONS is located in a rock niche, about 3 m below the surface in Permian sedimentary rock (Verrucano). S-wave measurements were performed on 2 sections. The first section is very close to stations PLONS, the second section is about 20m away. On section 2, the MASW measurements and P-wave hybrid seismics show a depression with soft material overlying the bedrock. This layer is about 10-15m thick with shear velocities lower than 600m/s. Its influence is visible along the entire length of section 2. The lower velocities that are seen with MASW and P-wave seismics on section 2 cannot be identified with S-wave seismics. Because H/V spectral ratios at station PLONS show no significant peak up to a frequency of 30 Hz (not shown here) and from the position of seismic station PLONS being clearly on rock, outside the depression, we have taken only the results from the small arrays on section 1 to compute the values for vs5 to vs30. For the MASW results on this section the dispersion curves are rather similar, showing only small changes in the phase velocity over the measured frequency range. Phase velocities are mostly in the range 1600-2200 m/s. The results obtained for the 96m long arrays are similar to those obtained with the small arrays.

The H/V spectral ratio at site PLONS has two small peaks, one slightly above 1 Hz and the second around 4Hz. The peak at 4Hz shows a polarization in the NS direction. It was identified as a disturbance from installations in the nearby dam and lake to the south of the stations PLONS (Chapfensee).

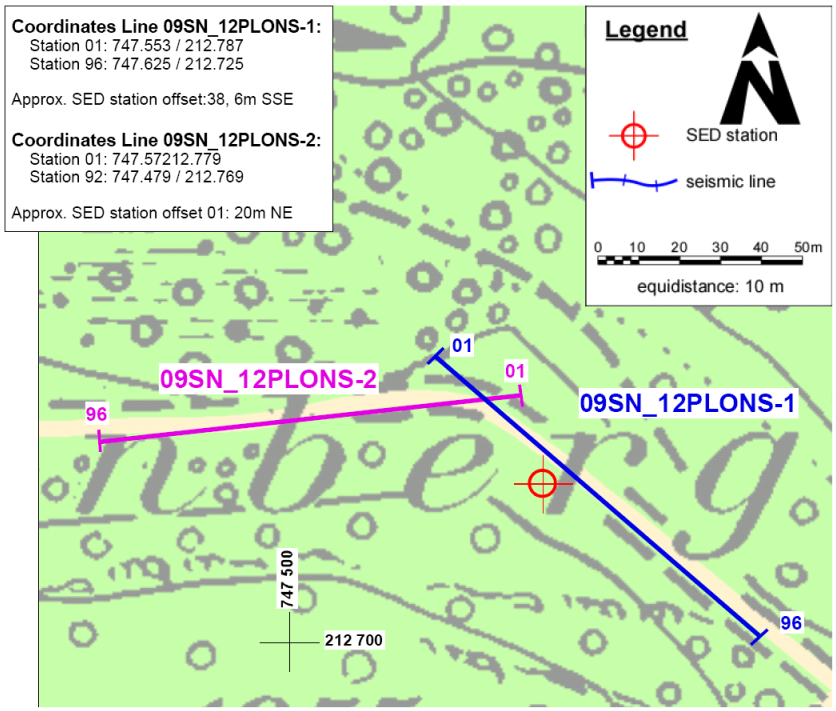

Figure A.12.1. Measurements at site PLONS.

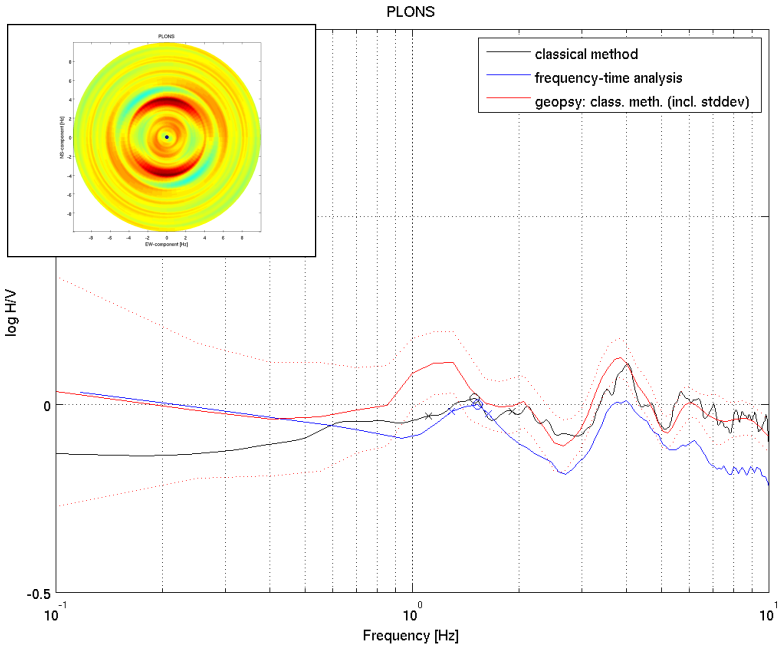

Figure A.12.2. H/V spectral ratios at the site of seismic station PLONS.

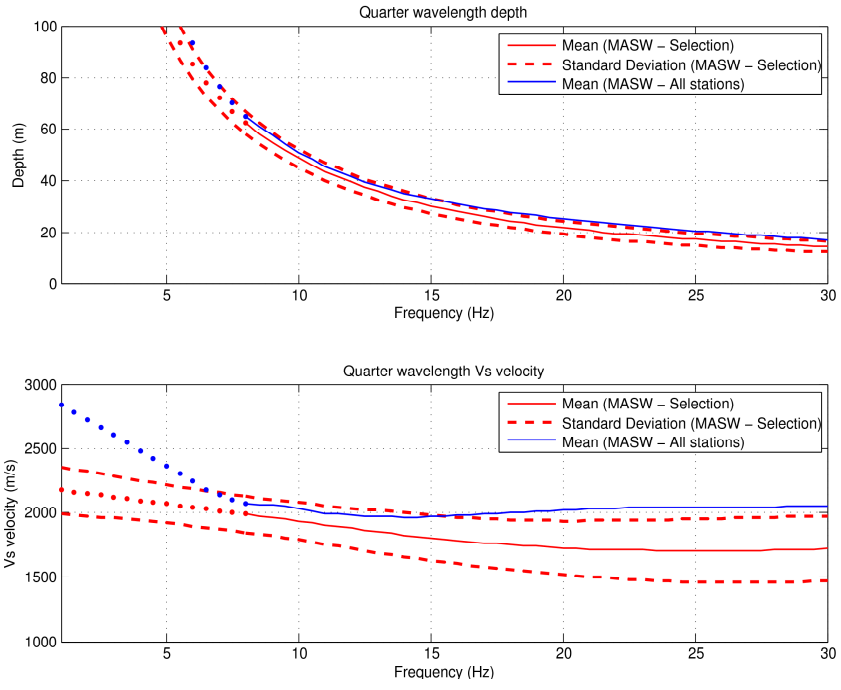

Figure A.12.3. Quarter wavelength velocity for site PLONS obtained with MASW.

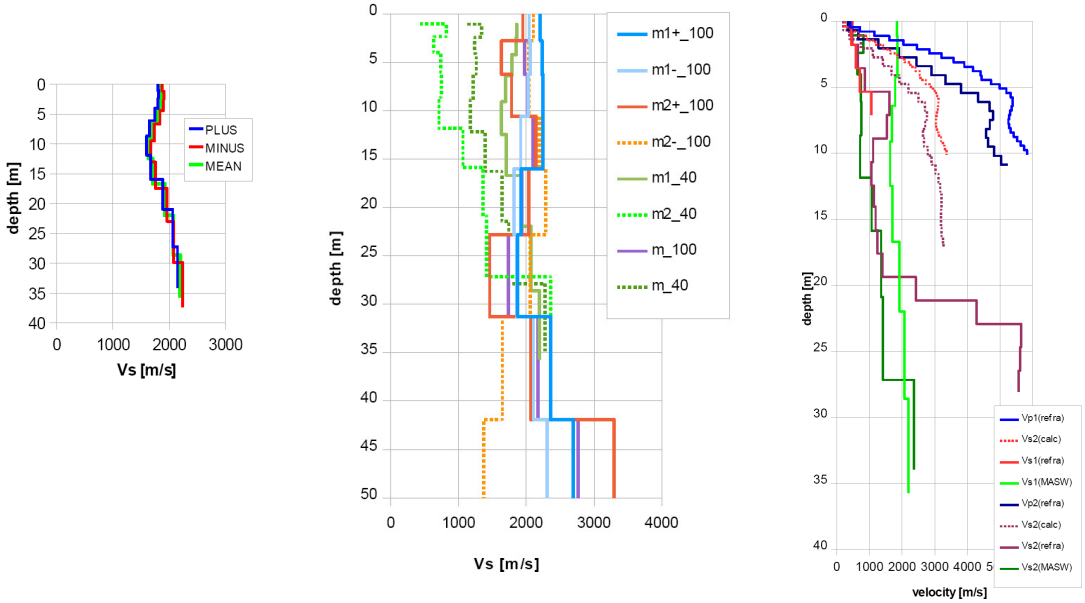

Figure A.12.4. Structural models at site PLONS. For more details, see the report of GeoExpert related to the site PLONS.

A.13 Station SKEH

Station SKEH is part of the Swiss Strong Motion Network. SKEH is situated on a relatively flat ridge of Cretaceous and Tertiary sediments. The sediments are composed of massive sandstones and limestones. A quaternary alluvial fan of unknown thickness covers the solid rock.

Geophysical techniques were applied along two sections at site SKEH. The first MASW section is very close to the site of SKEH, the second section is about 10m away from the sensor. The seismic P- and S- wave profiles are very similar, softer layers are visible along the entire profile with thicknesses in the range of about 2 to 5m. At 10m in depth, an S-wave velocity of more than 1000m/s is estimated from seismic measurements, reaching 2000m/s at 20 m. These values are high when compared to similar geological units. The P- and S- wave profiles are consistent.

The average S-wave structures obtained with MASW on the two sections are similar, however they are very different from the results obtained from the S-wave seismics. S-wave velocities obtained with MASW increase gradually and do not reach 1000m/s in the upper 30 m. The data quality and dispersion curves for MASW are not good, which resulted in large scatters and unclear dispersion-curve plots. This might be due to the influence of buildings, or subsurface structures such as pipes. The velocities of the surface sediments of some profiles are slightly lower than others, which might be due to the presence of a peat layer. The quarter wavelength velocity for site SKEH was obtained from MASW, using the results from sections 1 and 2 together, in the selected range from an offset of 30 to 60 m. It was not possible to use the results from the 95 m arrays, due to the relatively poor quality of dispersion data.

For the structural models SH amplification functions were computed and compared to the H/V spectral ratio measured at site SKEH. The H/V spectral ratio at site SKEH has a broad low-amplitude peak at around 2-4 Hz. In some of the MASW arrays we can probably identify a phase at a higher frequency with S-wave velocity around 1200-1400m/s that might be related to the non-weathered rock layer.

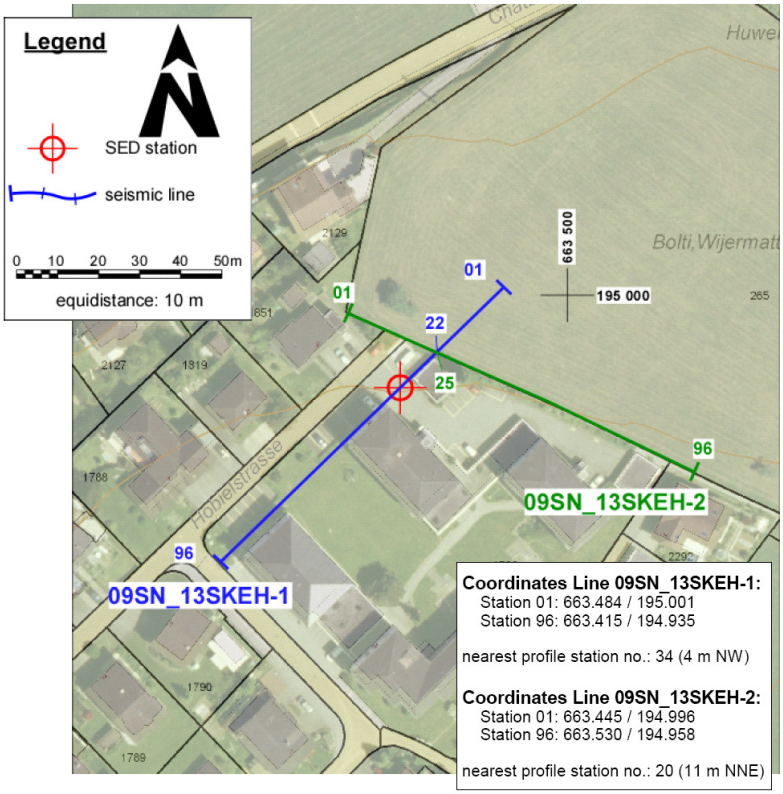

Figure A.13.1. Measurements at site SKEH.

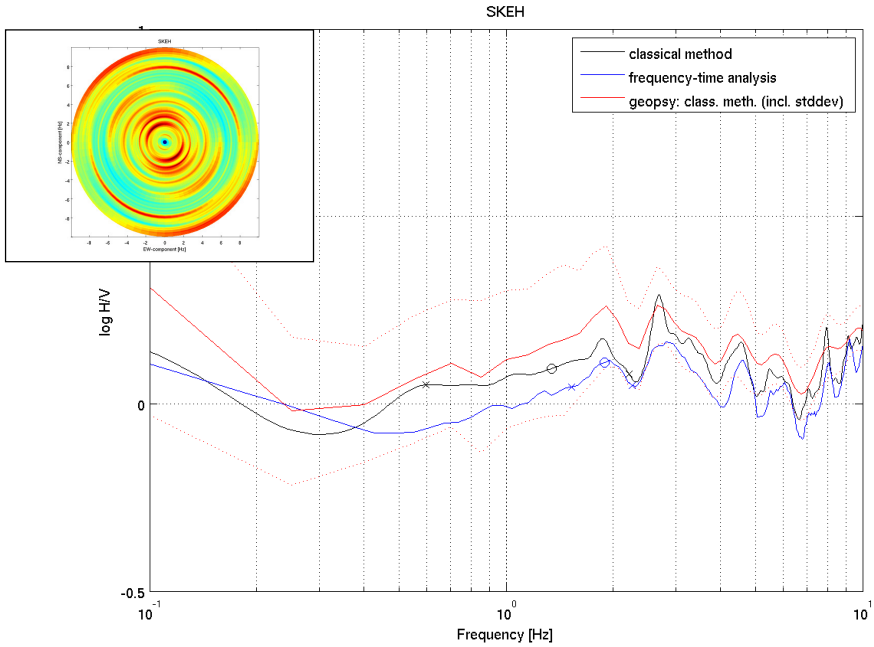

Figure A.13.2. H/V spectral ratios measured at the site of seismic station SKEH.

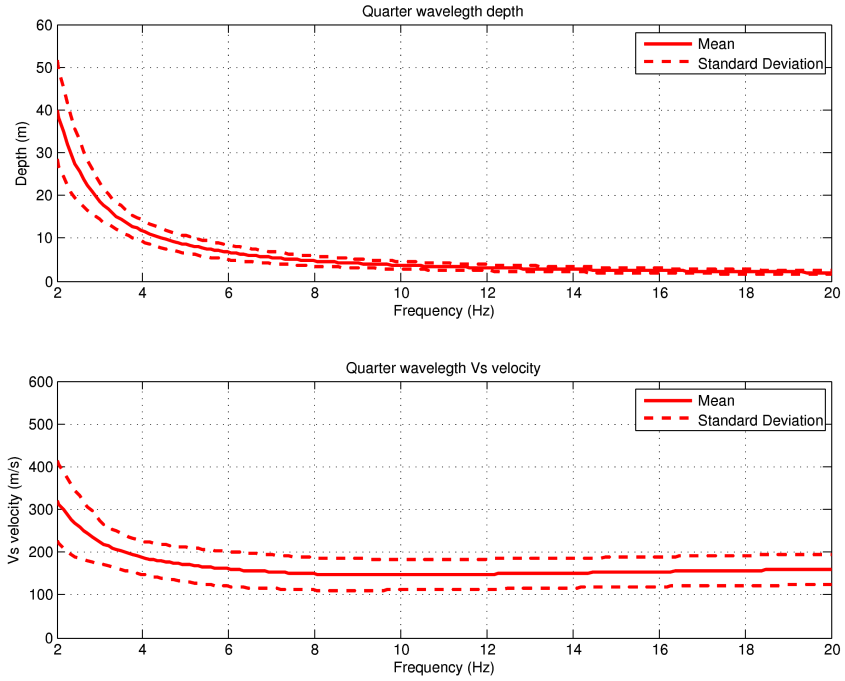

Figure A.13.3. Quarter wavelength velocity for site SKEH obtained from MASW, using the results from sections 1 and 2 together, in the selected range from offset 30 to 60 m. It was not possible to use the results from the 95 m arrays, due to the relatively poor quality of dispersion data. For the Vs5 to vs30 calculation, an average between profiles 1 and 2 is taken from the previously mentioned selected range.

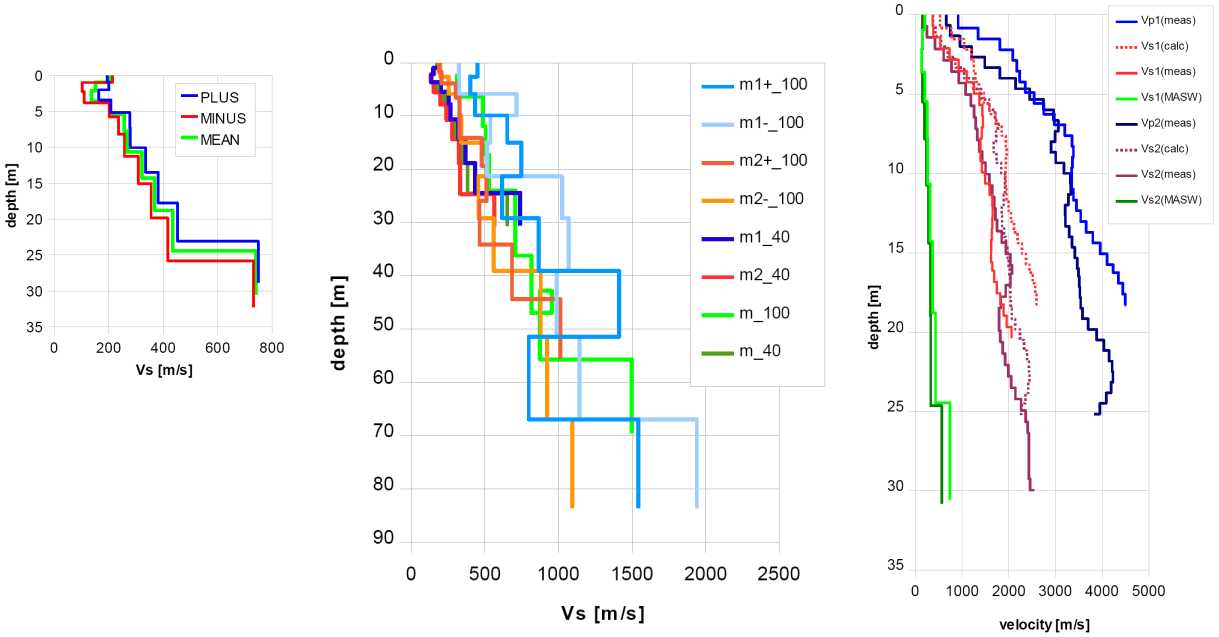

Figure A.13.4. Structural models for site SKEH obtained from MASW and seismic methods (right). For more details, see the report of GeoExpert related to the site SKEH.

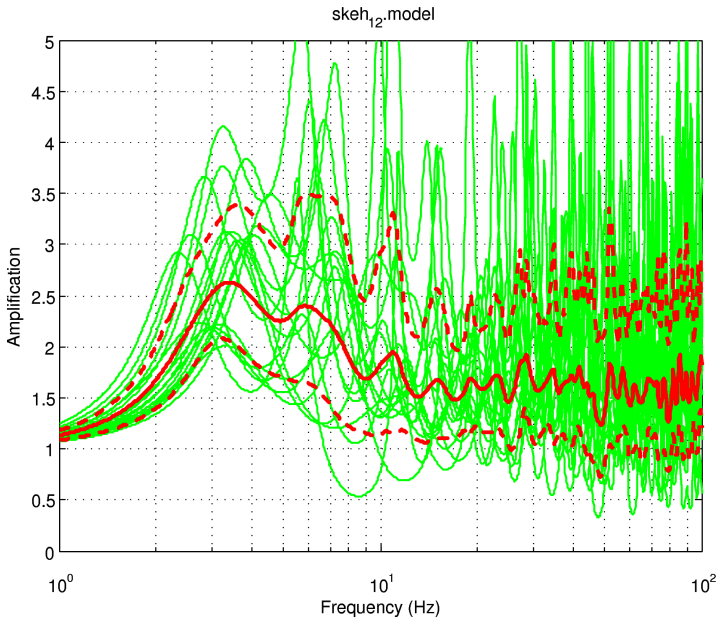

Figure A.13.5. SH amplification functions from Vs profiles obtained with the MASW technique, using a combination of sections 1 and 2. The uncertainties in the inverted profiles are reflected in the scattering of the amplification functions, especially at high frequencies (> 10 Hz). Average values are shown by the solid red line and standard deviations by the dashed red lines.

A.14 Station SLE

The sensor of station SLE is located in an ancient quarry, on the base of a buried chamber at about 4m in depth. Several geophysical techniques were applied at site SLE. For the Vs information MASW results are used. The shear-wave refraction survey resulted in velocities that were too high when compared to the velocities obtained from P-wave refraction (i.e., the vp/vs ratio was too low). The reason for this might be wave conversion from P to S, such that the direct S-wave cannot be recognized. As part of the validation test, ambient vibration array measurements were performed at the same site as the active seismic survey (see the results in the report for SLE in Appendix B). The ambient vibration array measurement was successful. However, due to the complex structure, with strong lateral changes in geology, the location of the array is not representative for the site of station SLE. In fact, the array's position is actually above a thick layer of soft sediments not present at the station. The results obtained from MASW in this area of the sedimentary layer are confirmed by ambient vibration array measurements within the uncertainties of the methods and due the difference in measurement location.

MASW measurements were performed on one section. The closest point of the section is about 20m away from the sensor. The P-wave hybrid seismics and MASW results indicate sedimentary layers at both ends of the profile. For this reason only the results from the central part of section were used to compute the values for vs5 to vs30. For the selected part of the section, the average value of the S-waves in the uppermost layer is about 620-680 m/s. The thickness of this layer is about 25m. The average S-velocity of the first non-weathered rock layer can be estimated from the MASW results over the entire section and the ambient vibration array measurements, and lies in the range of 1000-1500m/s.

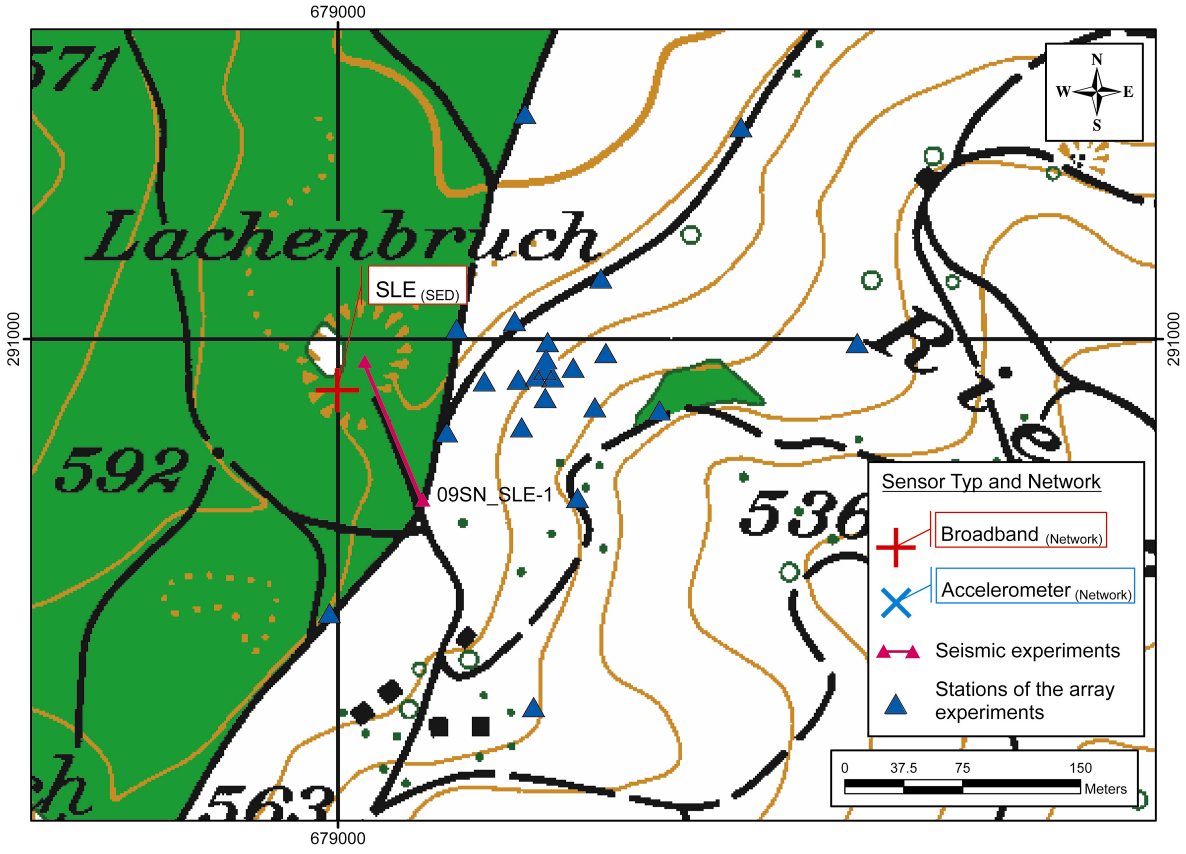

Figure A.14.1. Measurements at site SLE.

The H/V spectral ratio at site SLE has a broad peak in the frequency range of about 1.5-7 Hz without a clear maximum. Due to the rather high S-wave values in the surface part of the structure close to station SLE and the presence of outcropping rock, the peak must be associated to a layer of weathered bedrock. Assuming a mean velocity of this bedrock layer of about 620-680m/s with a thickness of about 25m results in a fundamental frequency f0 around 6.5 Hz, which is in the upper range of the estimated f0 value from H/V. Alternatively, there might be the possibility of a first peak in the H/V ratio that can be seen at around 1.5Hz and a second peak in the range 3-7 Hz. The peak at lower frequency might be associated to the first non-weathered rock layer (170-250m thickness). Due to the non-unique interpretation of the H/V peak(s) we did not modify the structure obtained from MASW for the computation of vs5 to vs30.

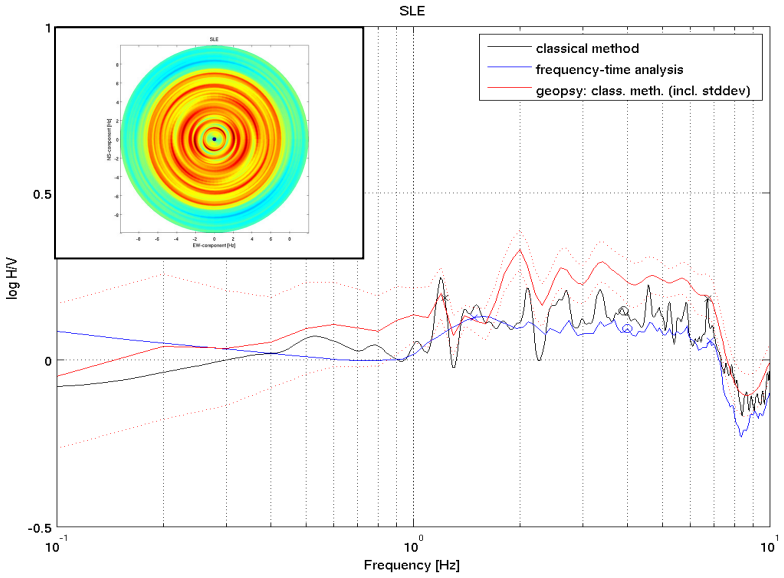

Figure A.14.2. H/V spectral ratios measured at the site of seismic station SLE. The seismic instrument is located on the base of a buried chamber at about 4m in depth.

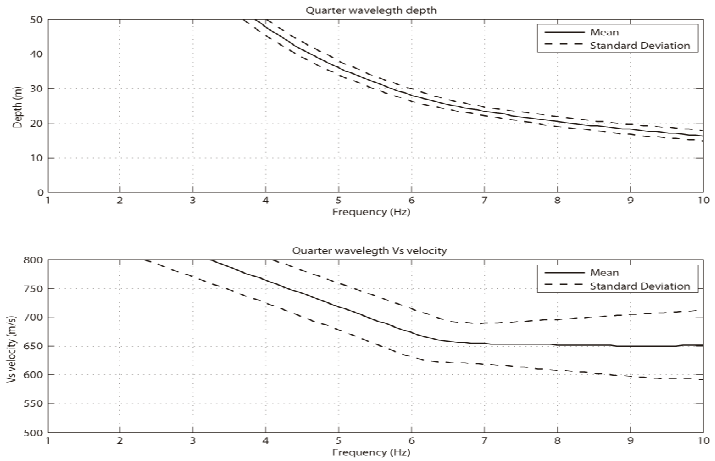

Figure A.14.3. Quarter wavelength velocity for site SLE obtained from MASW.

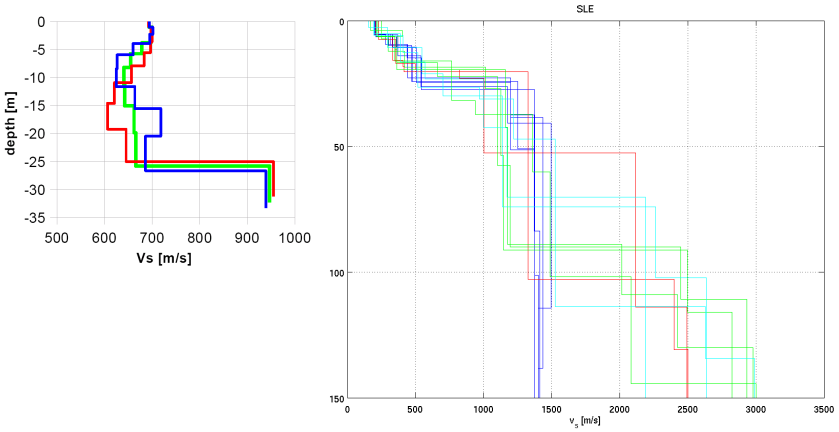

Figure A.14.4. Structural models close to site SLE obtained from MASW from the central part of the section (left), and ambient vibration array measurements (right). The ambient vibration array measurement was successful, however, the location of the array is not representative of the site of station SLE, due to its position above a thick layer of soft sediments not present at the station. The estimate of the S-wave velocity of the first 50m of non-weathered rock is in the range 1000-1500m/s.

A.15 Station STEIN

The sensor of station STEIN is located in a small cave in the flank of a hill. The sensor is several meters below the surface. The rock is composed mostly of sediments of the Upper Freshwater Molasse (OSM, Miocene). Surface material consists of unconsolidated, loose sediments. Geophysical techniques were applied at site STEIN although not directly at the station site. Seismic measurements were performed on 2 sections. The closest point of the first section is about 30m away from the sensor. The second section is about 100m away. In P-wave seismics softer layers are visible over the entire profile with thicknesses in the range 5 to 10m. Results from S-wave seismics agree with results obtained with P-wave seismics. The velocity profiles obtained from S-wave seismics and MASW are very similar. The S-wave velocity at the surface is around 200m/s and is increasing gradually to 500 m/s at a depth of 15-20m. Below this layer velocities are again gradually increasing. The results from the 96m arrays cannot resolve the first non-weathered rock layer.

The H/V spectral ratio at site STEIN has peaks at 0.7Hz, around 2Hz and 12 Hz (12Hz peak is shown in the figure). The H/V peaks are difficult to explain, because the rock layers cannot be resolved with MASW. The interpretation of the H/V peak at 2Hz would require a strong velocity increase at a depth of about 50-75m when assuming an average velocity of 400-600m/s in the upper layers.

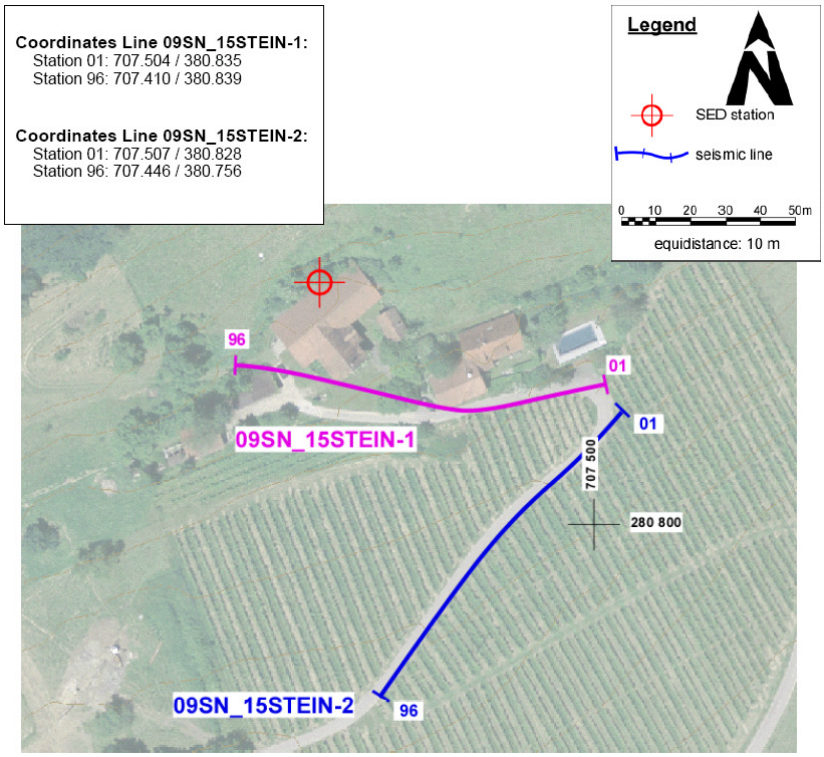

Figure A.15.1. Measurements at site STEIN.

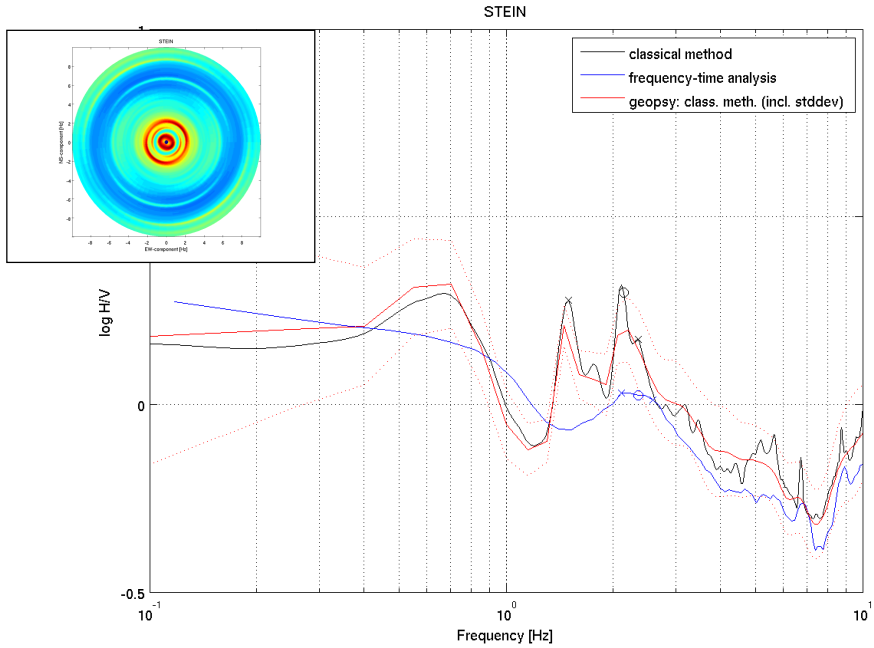

Figure A.15.2. H/V spectral ratios measured at the site of seismic station STEIN. The seismic instrument is located in a cave.

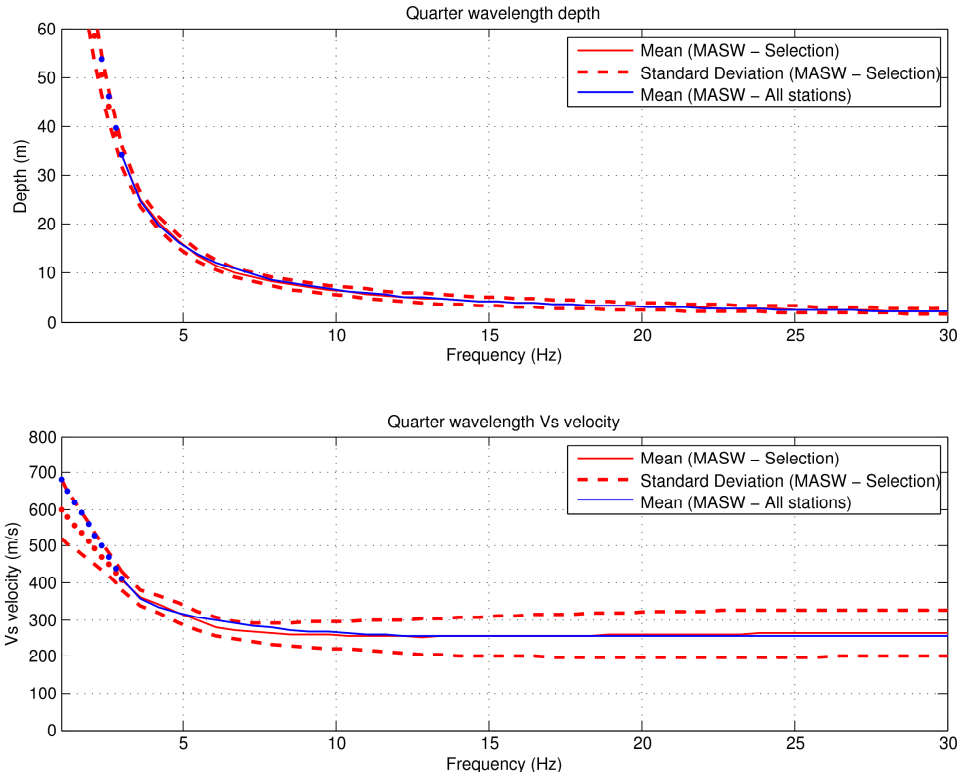

Figure A.15.3. Quarter wavelength velocity for site STEIN obtained from MASW, using the small receiver configurations from profiles 1 and 2 (red) and for the whole lines (blue). For the Vs5 to vs30 calculation the small profiles are taken.

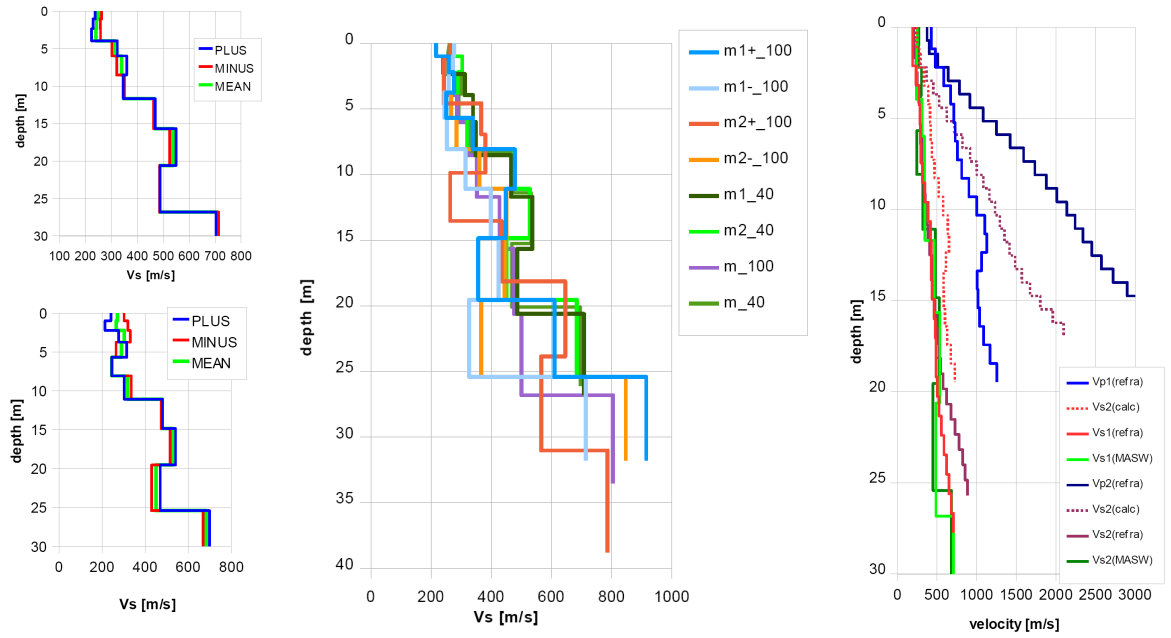

Figure A.15.4. Structural models close to site STEIN obtained from MASW and P- and S-wave seismics. For more details, see the report of GeoExpert related to the site STEIN.

a) b)

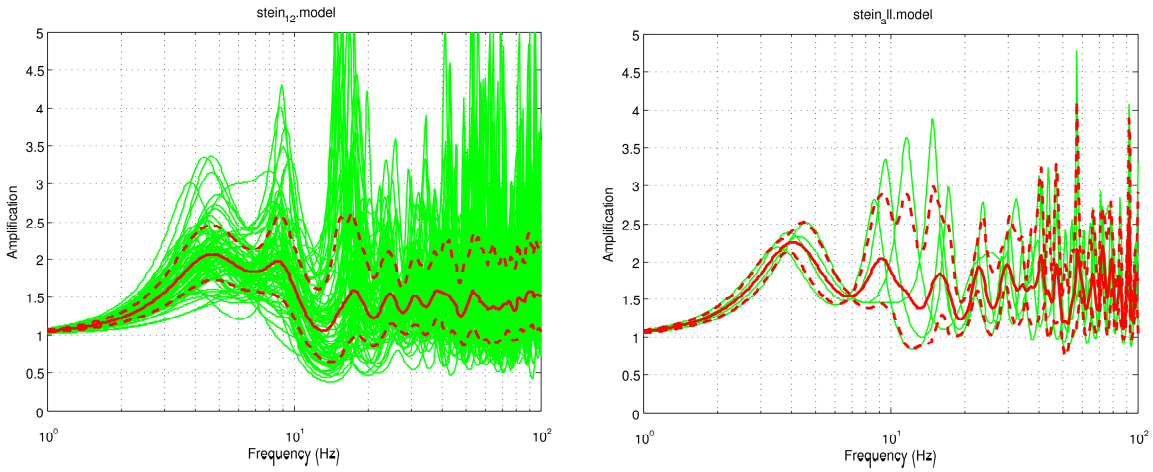

Figure A.15.5. SH amplification functions from Vs profiles obtained with the MASW technique, using small receiver configurations from profiles 1 and 2 (a) and the whole lines (b). The first is preferable, due to the reliability of the inverted profiles and the better statistics. Average values are in red solid lines, standard deviations in red dashed lines.

A.16 Station SULZ

The sensor of station SULZ is located in a small vault, about 2 m below the surface. Active S-wave measurements at this site were performed along two sections. Due to the topography at the site, the position of station SULZ is at the edge of the area where measurements were performed. As part of the validation test, ambient vibration array measurements were performed at the same site as the active seismic survey. The results from all techniques show that the bedrock is very close to the surface, and the measured velocities for the surface waves are around 1000m/s. MASW for the long profiles did not result in an improved resolution at depth when compared to the smaller profiles. There are two possibilities for interpreting the measured phase velocities at frequencies above 10 Hz. With the first interpretation the derived dispersion curves are assigned to the fundamental modes of Rayleigh and Love waves. MASW results were interpreted in this way, and therefore result in higher average shear-wave velocities in the structural models. The second interpretation is based on the result obtained with the SPAC method, with which it was possible to identify a relatively strong dispersive signal on the vertical component in the frequency band 1-3.5Hz. If we assume that the results from SPAC are reliable, then we only see a segment of the Rayleigh fundamental mode. In this case it is suggested that HRBF (High Resolution Beam Forming) and MASW provides parts of the dispersion curves of higher modes at higher frequencies, and almost no information for the fundamental mode is found above 10Hz (see the results for Love waves in Figure 12 and compare to Figure 7 in the report for SULZ in Appendix B). Inversion of the MASW results is based on the first interpretation, whereas the final result from ambient vibration array measurements takes the average of the two hypotheses. The results from MASW are confirmed by ambient vibration array measurements within the uncertainties of the methods.

The H/V spectral ratio at site SULZ has a peak around 0.8-0.9 Hz. Assuming an average S-wave velocity of 1100-1400 m/s, the thickness of the first bedrock layer is therefore in the range 340-440m. The velocity contrast to the deeper rock layer is not very strong.

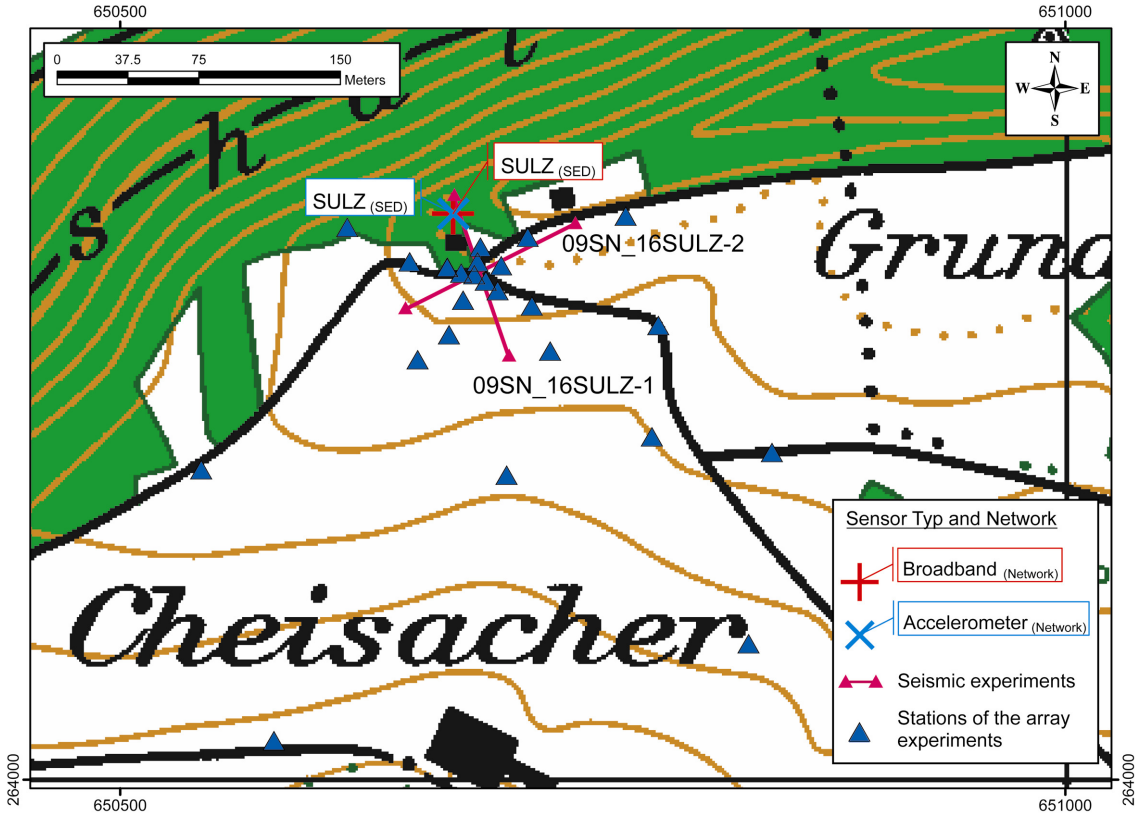

Figure A.16.1. Measurements at site SULZ.

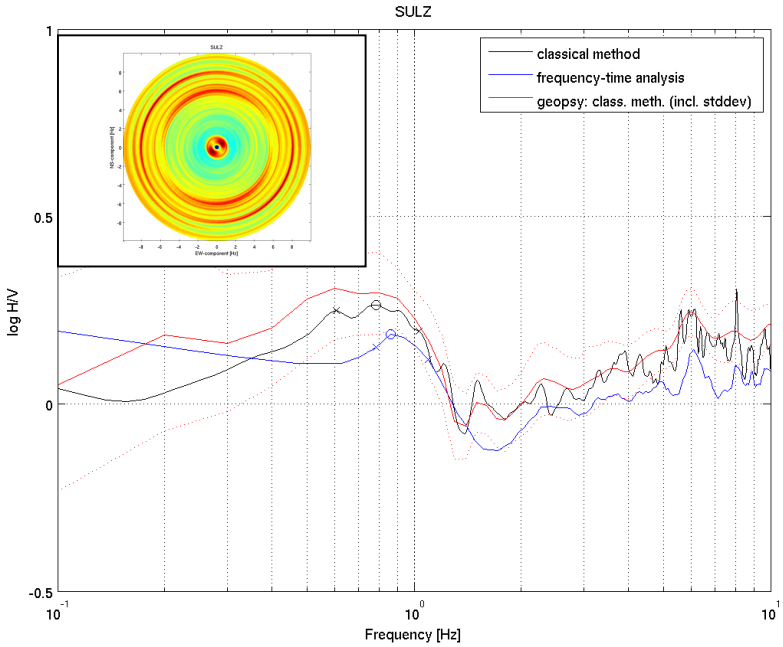

Figure A.16.2. H/V spectral ratios at the site of seismic station SULZ. The station is about 2m below the surface.

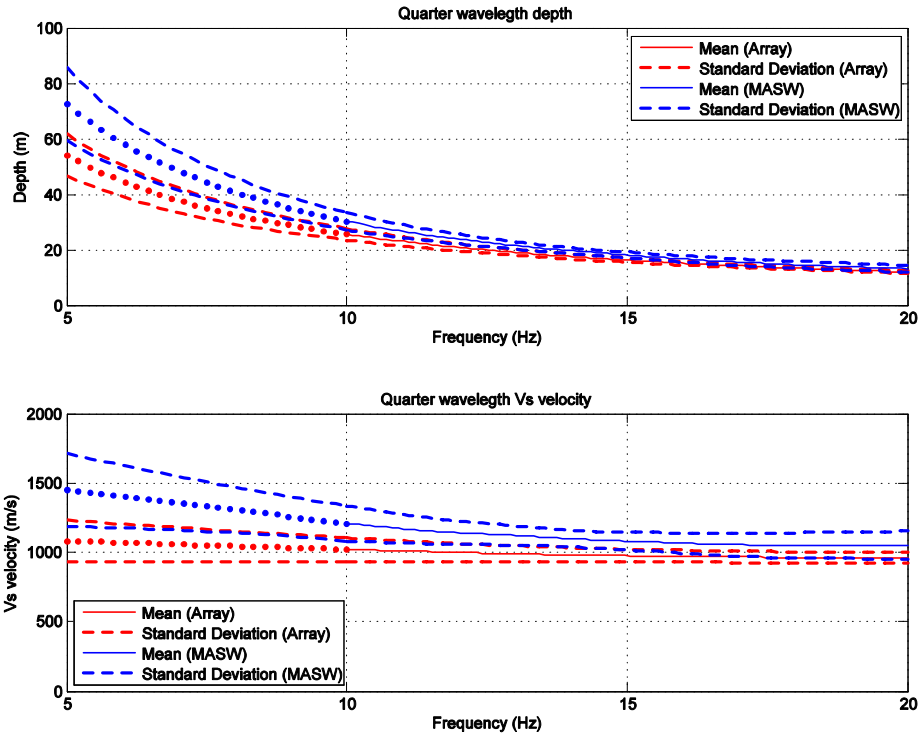

Figure A.16.3. Quarter wavelength velocity for site SULZ obtained with MASW and ambient vibration array techniques.

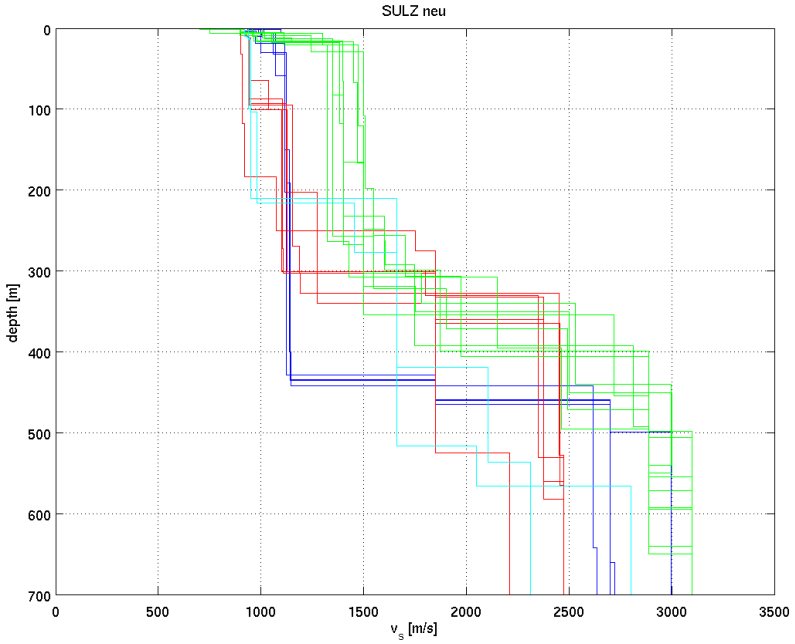

Figure A.16.4. Structural models at site SULZ. Green: the derived dispersion curves above 10 Hz are assigned to the fundamental modes of Rayleigh and Love waves. Other colors: Interpretation is based on the result obtained with the SPAC method, assuming higher modes at frequencies above 10Hz.

A.17 Station TORNY

The sensor of station TORNY is located in the basement of a bunker, about 4 m below the surface of the terrain. The surface layer is composed of loose moraine of some meters in thickness overlaying Upper Marine Molasses. S-wave measurements were performed on 2 sections with very clear dispersion curves derived from MASW. The nearest point of section 1 is less than 20m away from the sensor position, and for section 2 around 100m. On section 2, the seismic P- and S-wave profiles indicate a thinner sedimentary layer than on profile 1. Because section 1 is closer to the seismic station, the MASW results from this section were used to compute the values for vs5 to vs30. Section 2 is used for comparison. From the 100m arrays (useful seismic lines m1+, m1-, m2+) we can observe that the S-velocity of the non-weathered rock layer is increasing rapidly to 1400m/s or more. The results are confirmed by the S-wave refraction results.

The H/V spectral ratio at site TORNY has two peaks, a very weak (questionable) one at around 2 Hz and a larger peak in the frequency range of about 7-9 Hz. For section 1, the average value of the S-wave velocity in the uppermost layer is in the range 500-550m/s. The thickness of this layer is estimated to be about 16m. This can explain the H/V peak at 7-9Hz. From the average of the longer 100m arrays, it is difficult to explain the small peak in H/V at 2 Hz. Assuming an average S-wave velocity of 1500-1800 m/s, the thickness of the first bedrock layer would be in the range 180-225m.

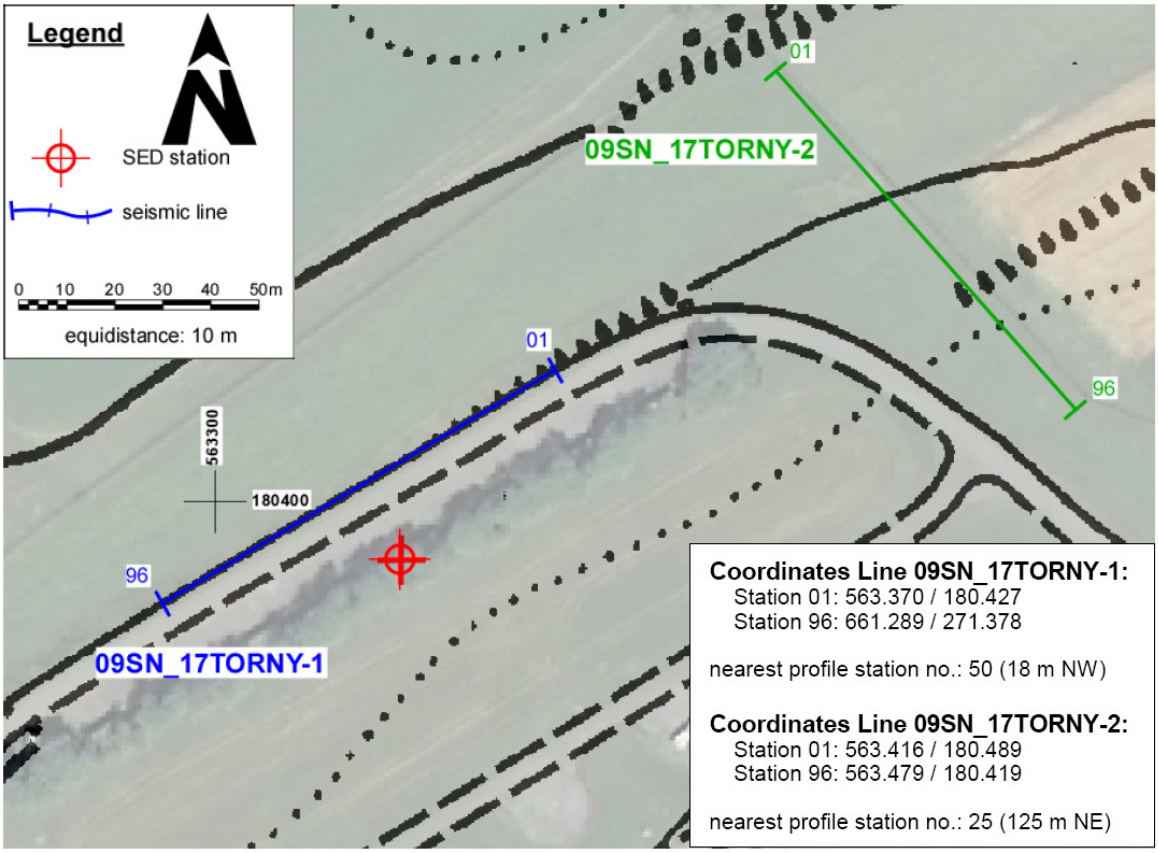

Figure A.17.1. Measurements at site TORNY.

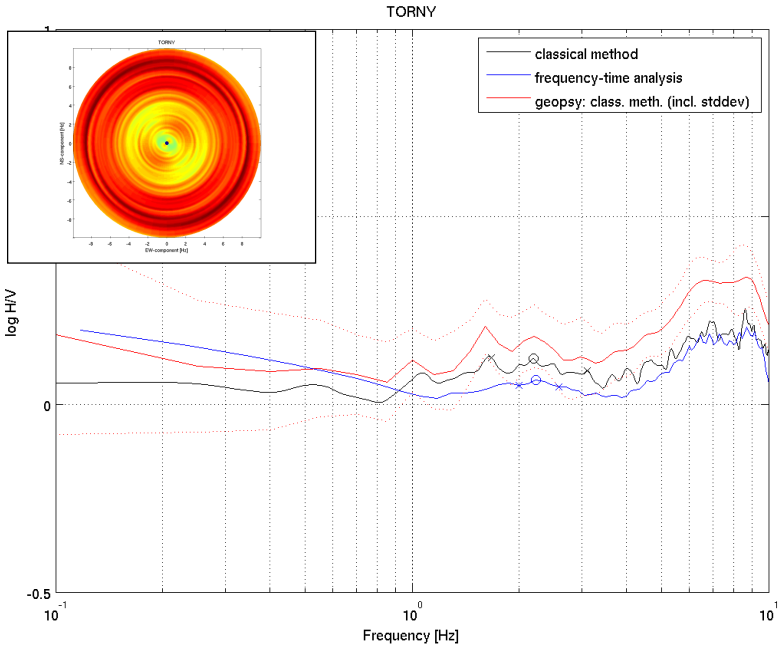

Figure A.17.2. H/V spectral ratios at the site of seismic station TORNY.

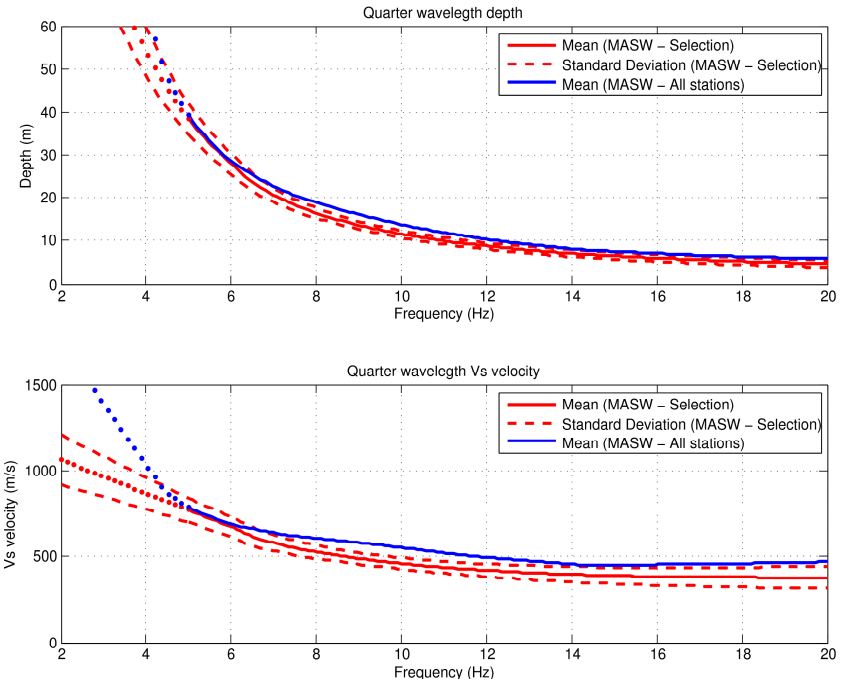

Figure A.17.3. Quarter wavelength velocity for site TORNY obtained with MASW (Section 1). Section 1 is used to derive vs5 to vs30 for the station site.

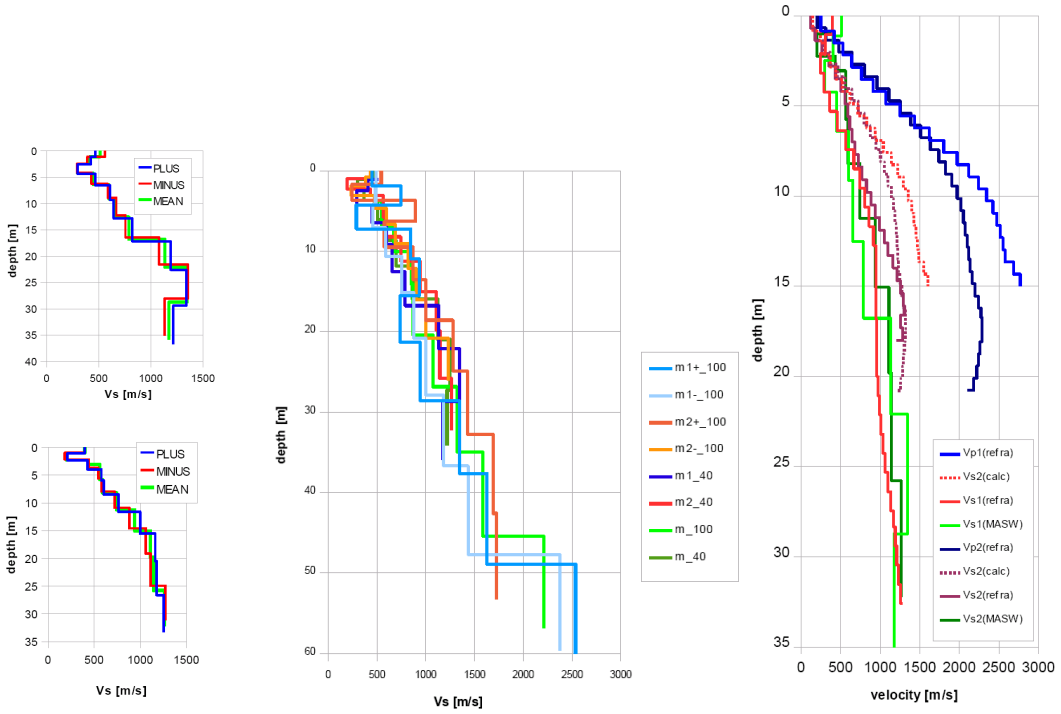

Figure A.17.4. Structural models at site TORNY obtained from MASW and seismic methods. For more details, see the report of GeoExpert related to the site TORNY.

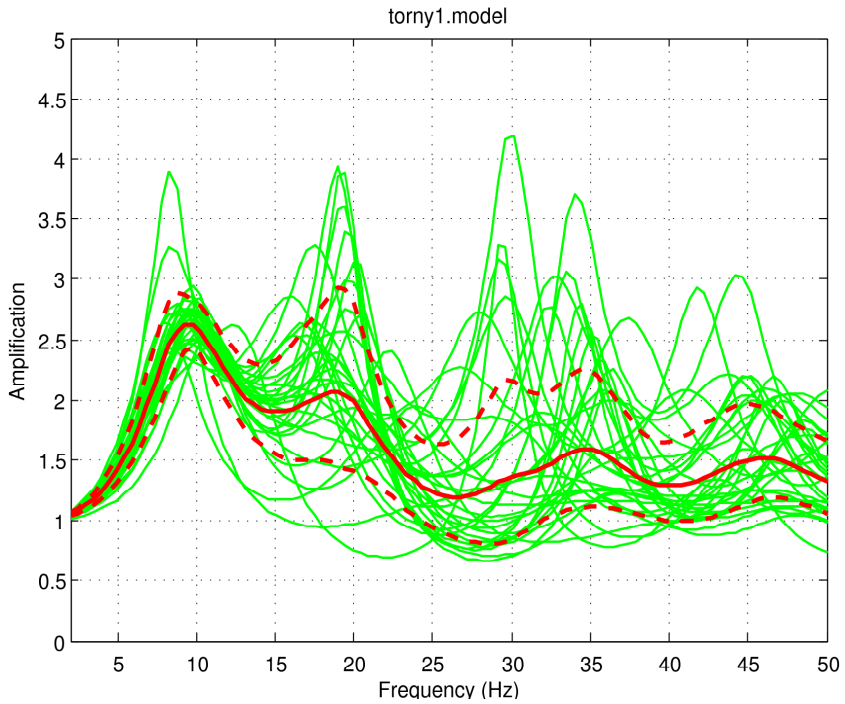

Figure A.17.5. SH mono-dimensional amplification function at site TORNY obtained from structures on Section 1 (MASW results). Mean in red solid line, standard deviation in red dashed line (log-normal statistic). The calculated fundamental frequency of resonance (around 9 Hz) has a good match with the one obtained from H/V ratios on ambient noise.

A.18 Station WEIN

The sensor of station WEIN is located in the basement of a small building. The sensor is coupled to the reinforced concrete basement structure of the building. The location of the building is on a slope of a Molasse sediment ridge (clastic Upper Freshwater Molasse, mainly conglomerate (Nagelfluh)). The Tertiary sediments are covered by glacial till. S-wave measurements were performed on 2 sections. The nearest point of section 1 is less than 10m away from the sensor, and for section 2 less than 20m. On section 1, the seismic P- and S-wave profiles indicate a thicker sedimentary layer closer to the seismic station. For this reason the results from the arrays in the southern part of section 1 were used to compute the values of vs5 to vs30. In section 2 thicker layers of sediments are observed in the western part of the S-wave seismic profile (but not in the P-wave profile). MASW results could not be interpreted in a larger part of the western part of profile 2. From this profile, we have therefore chosen the eastern part of the MASW profile for vs30 computations, being closer to the location of the seismic station WEIN.

The H/V spectral ratio at site WEIN has two peaks, a weak (questionable) one at around 0.7 Hz and a larger peak in the frequency range of about 4-5 Hz. For the selected parts of the section the average value of the S-wave velocity in the uppermost layer is in the range of 500-600m/s. The thickness of this first layer is estimated to be about 10m. Then the S-wave velocity is gradually increasing to 900-1400m/s at about 40m in depth. The scatter between the different profiles (40m and 100m) is high. In order to explain the H/V peak at 4-5Hz, a velocity contrast is required at around 40-50m. From the average of the longer 100m arrays (having large differences between the different profiles), no conclusive decision about the deeper layers can be made.

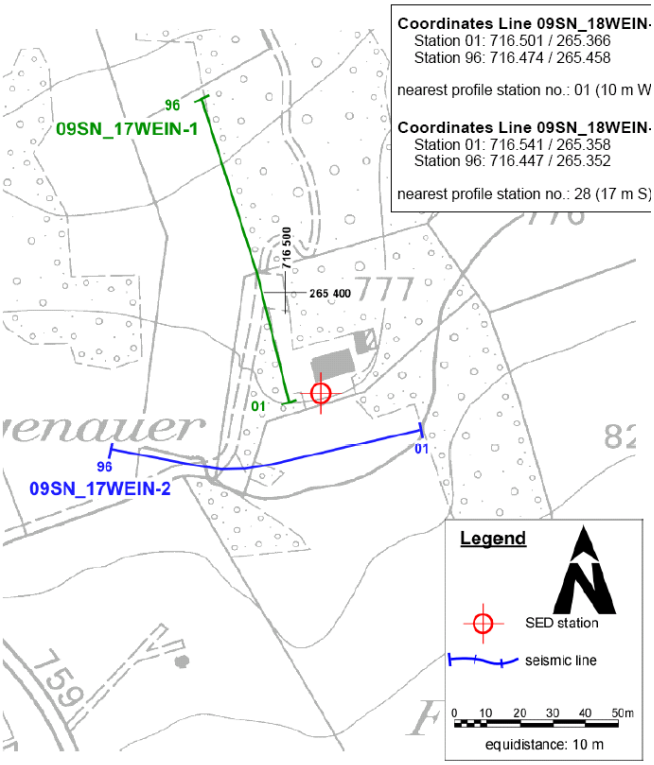

Figure A.18.1. Measurements at site WEIN.

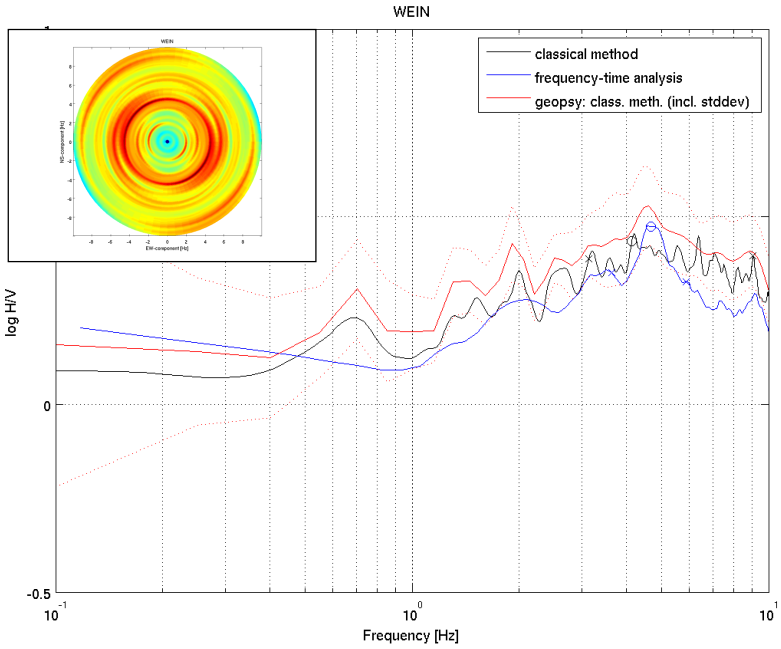

Figure A.18.2. H/V spectral ratios at the site of seismic station WEIN.

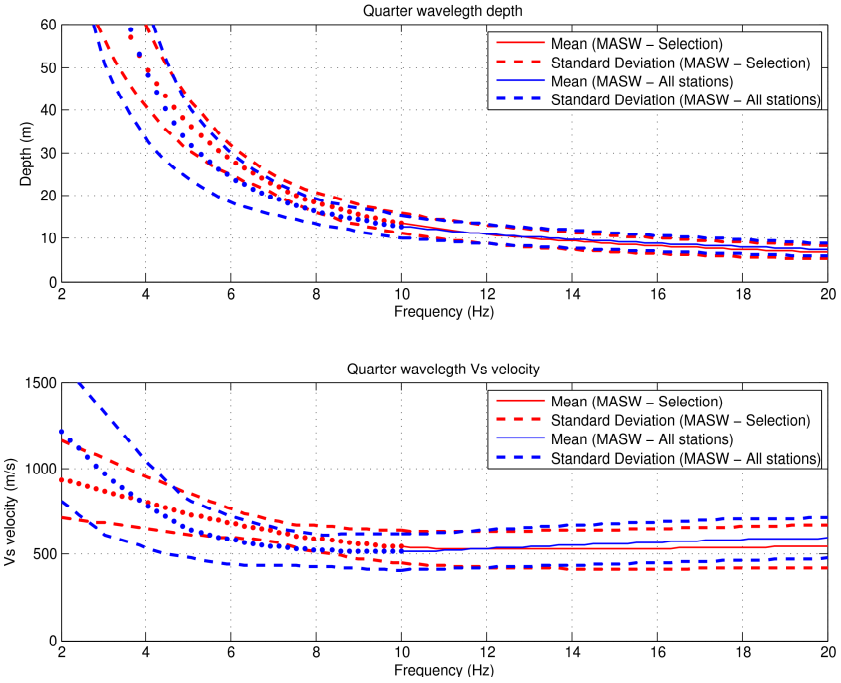

Figure A.18.3. Quarter wavelength velocity for site WEIN obtained with MASW. For the calculation of vs5 to vs30 the red curves are used.

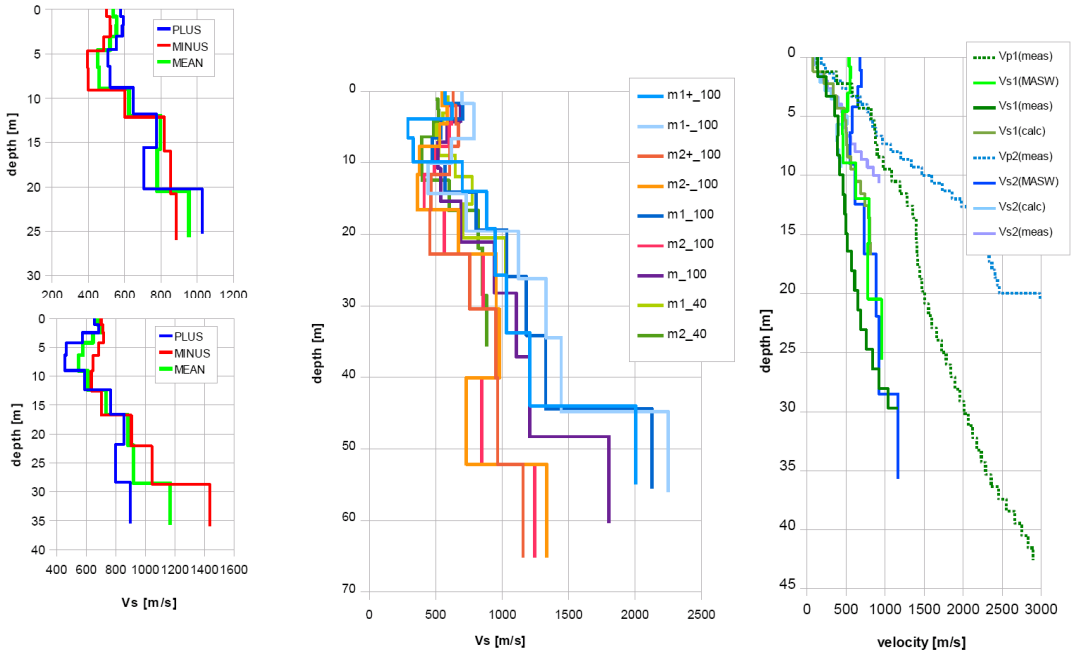

Figure A.18.4. Structural models at site WEIN obtained from MASW and seismic measurements. For more details, see the report of GeoExpert related to the site WEIN.

A.19 Station WILA

The sensor of station WILA is located in a bunker, about 4 m below the surface, on the top of a hill. The hill strikes in the NE-SW direction. The sediments are unsorted conglomerates (Nagelfluh) of the Hörnli alluvial fan (Upper Freshwater Molasse).

Active S-wave measurements were performed on two sections of the flank of the hill, both at a distance of about 20m from the station. The top of the hill, where the station is located, is at approximately the same height as seismic line 1, and about 20m higher than the closest part of seismic line 2. For the assessment of the S-wave velocity profile at station WILA, MASW results from the closest part of both sections are used. While on section 1 a thin surface layer of about 10m in thickness and with shear wave velocity of around 600m/s is seen, analysis of section 2 shows lower velocities of about 300-350m/s for the uppermost layer. Such a layer in section 2 would result in a fundamental frequency of about 7.5-9Hz, which is higher than the measured value at station WILA. The H/V spectral ratio at site WILA has a broad peak between 2 and 5 Hz. The peak at 5 Hz has a clear polarization perpendicular to the strike of the hill. An influence of the topography (2D resonance) might be possible due to the steep flanks of the hill. Explaining the H/V spectral ratio at site WILA using a layer of softer sediments would need some adjustment of the measured velocity structure. For instance, the adjustment could be justified by the difference in elevation between seismic line 2 and station WILA (i.e., an additional layer of softer material); however, we have no further reasons for such an adjustment. For the derivation of vs5 to vs30 we averaged the velocities of the structures obtained on the two closest parts of the sections.
The S-wave velocity of the first bedrock layer is 700-900m/s, with a layer thickness of about 10m. The S-wave velocity then increases to about 1000-1300m/s at a depth of around 30-40m. The 100m MASW profile on section 1 shows a phase at 700-900m/s that could be interpreted as the direct S-wave in the rock layer.

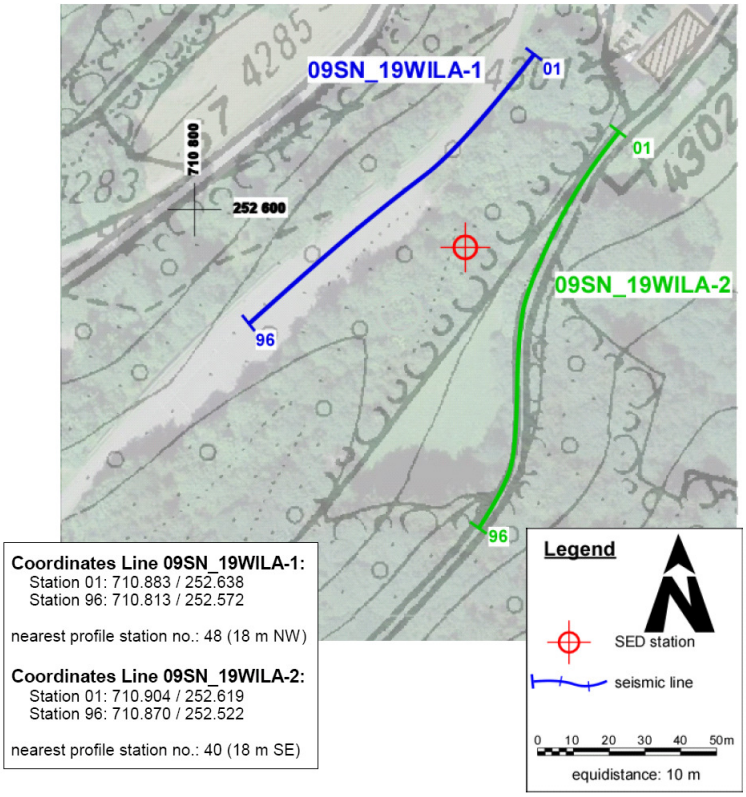

Figure A.19.1. Measurements at site WILA.

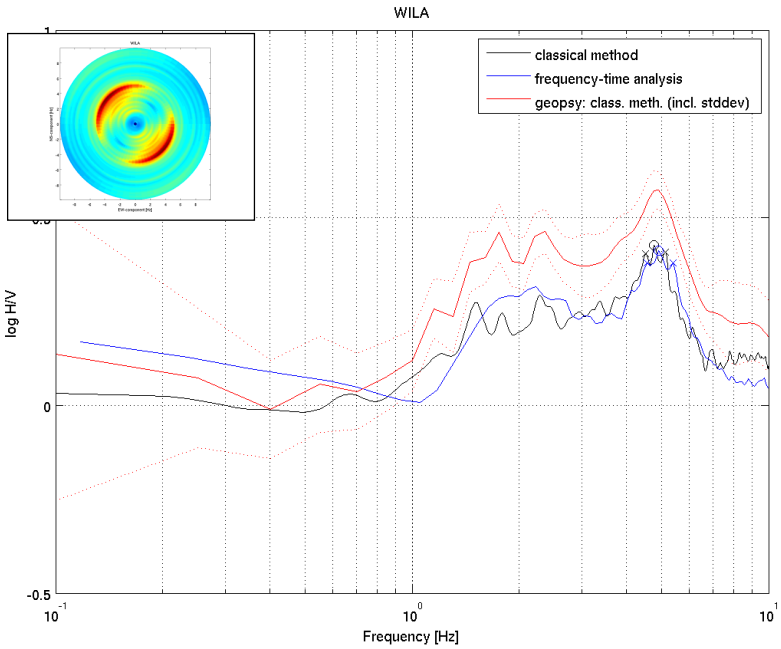

Figure A.19.2. H/V spectral ratio at the site of seismic station WILA. The H/V as a function of azimuth is also shown.

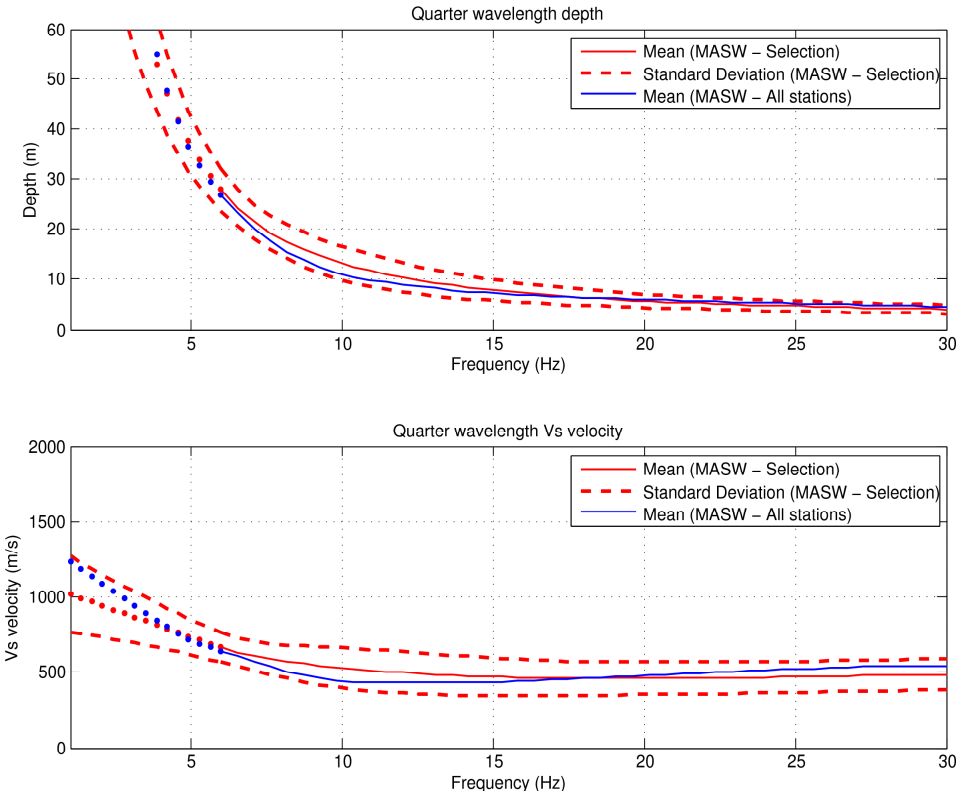

Figure A.19.3. Quarter wavelength velocity for site WILA obtained with MASW. Velocity profiles from line 1 and 2 are averaged in an offset range from 40m to 60m.

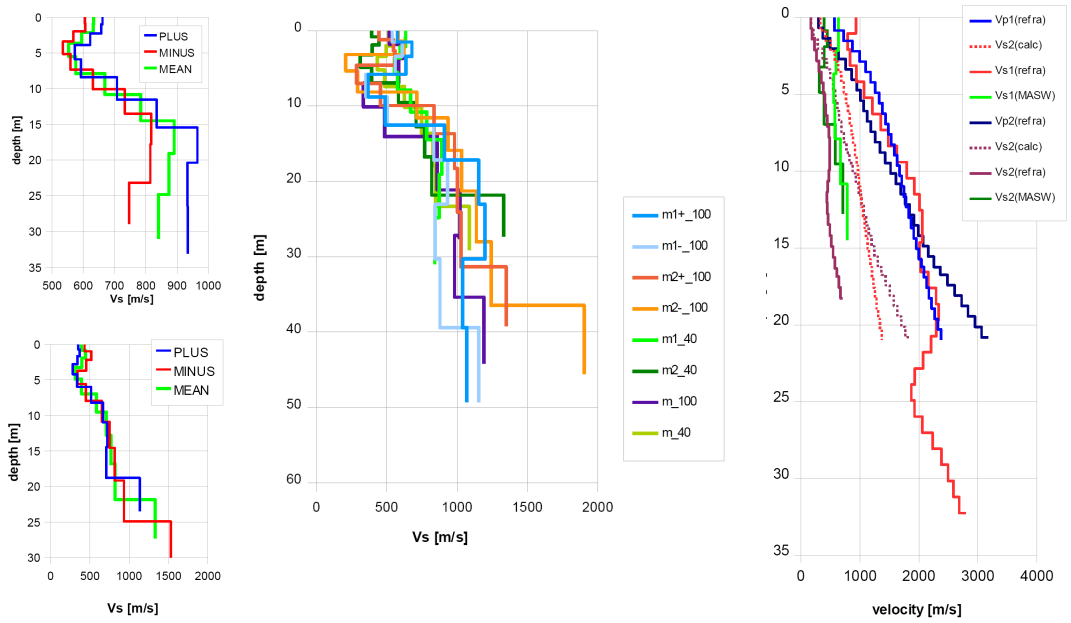

Figure A.19.4. Structural models close to site WILA obtained with MASW. The S-wave refraction results on profile 1 might be affected by wave conversions and is not compatible with the measured P-wave velocity. For more details, see the report of GeoExpert related to the site WILA.

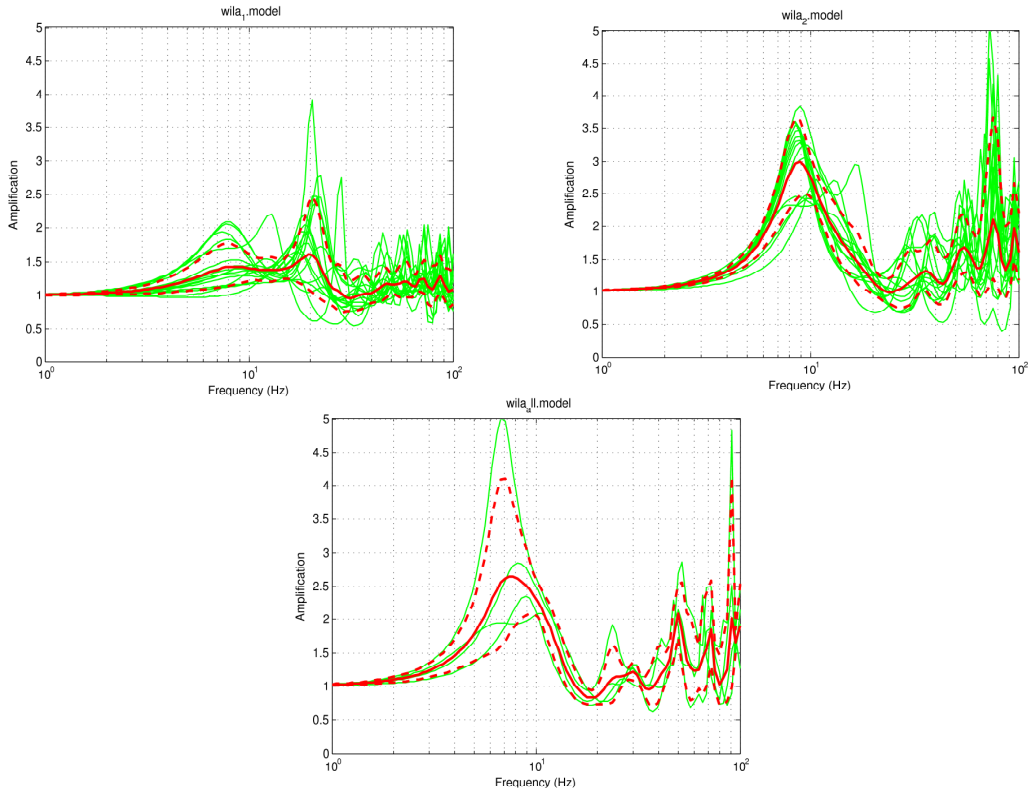

Figure A.19.5. SH amplification function for the two profiles using the short arrays (line 1 on top right, line 2 on top left), and for the long arrays including both profiles in the same graph (bottom). The amplification curves cannot explain the observed H/V ratio, which might also be caused by topographical effects. Input velocity profiles, moreover, are not well constrained below 20 m depth, limiting the resolution in the frequency band of interest.

A.20 Station WIMIS

Station WIMIS is located about 3m in horizontal direction from the surface in a bunker, in a steep rock face of massive Jurassic limestone (Malmkalk). The entrance area of the bunker is characterized by a complex geological setting with deep Quaternary deposits. It was not possible to perform the measurements at a rock location close to seismic station WIMIS. The seismic section in the area of the entrance of the bunker (Section 2) resulted in dispersion curves that are dominated by the influence of soft sediments (plus direction) or the dispersion plots are difficult to interpret (minus direction). In addition, the long profiles of 72 m length did not provide useful results. For these reasons we have not used the results obtained from profile 2. Profile 1 is more than 500m from the seismic station WIMIS, however it is located on outcropping bedrock. The results obtained from this profile are used to define vs5 to vs30. The measured dispersion curves vary considerable also along section 1, which resulted in the large standard deviation of the quarter wavelength velocity.
S-wave seismics resulted in S-wave velocities that increase from about 900 m/s to 1500 m/s in the first 5 m. These values are generally higher than the values obtained with MASW with which 1500m/s is measured at about 10m depth. Measured S-wave velocities from seismics and MASW are also consistent with S-wave velocities derived from measured P-wave velocities.

The H/V spectral ratio at site WIMIS has only a small and insignificant peak at about 1.4 Hz. The generally flat H/V curve is typical for rock sites.

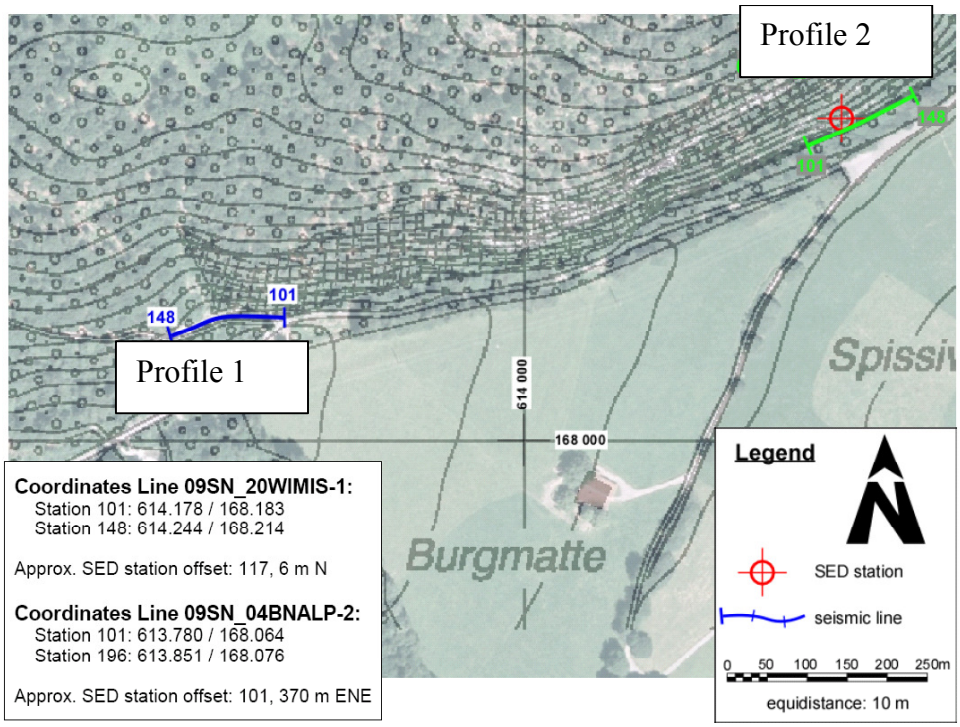

Figure A.20.1. Measurements at site WIMIS.

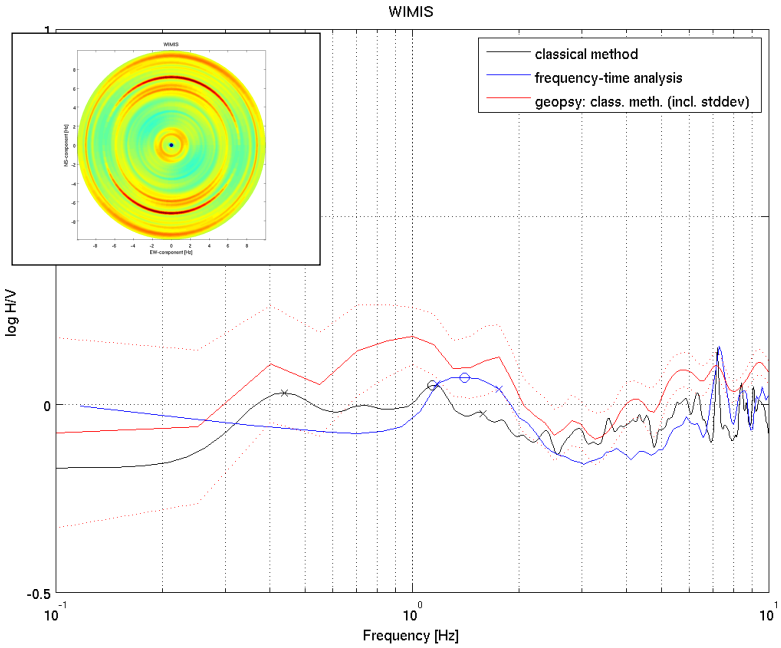

Figure A.20.2. H/V spectral ratios at the site of seismic stations WIMIS. The station is about 3m below the surface (in horizontal direction).

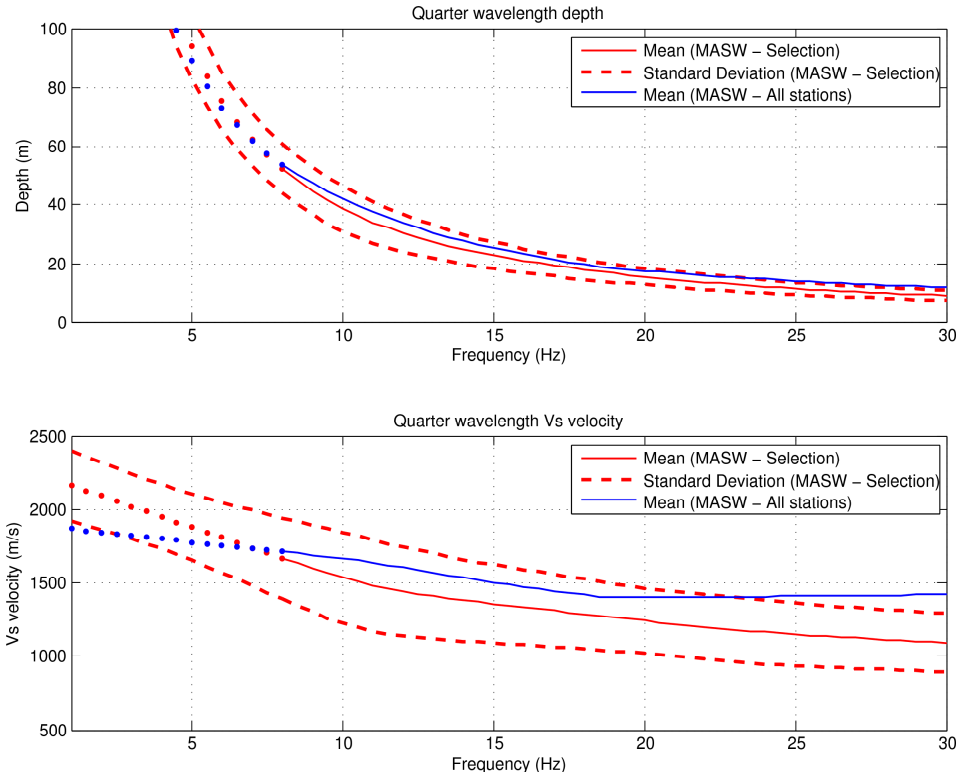

Figure A.20.3. Quarter wavelength velocity for site WIMIS obtained with MASW. For the vs5 to vs30 determination, the mean of the different MASW sections on profile 1 is used.

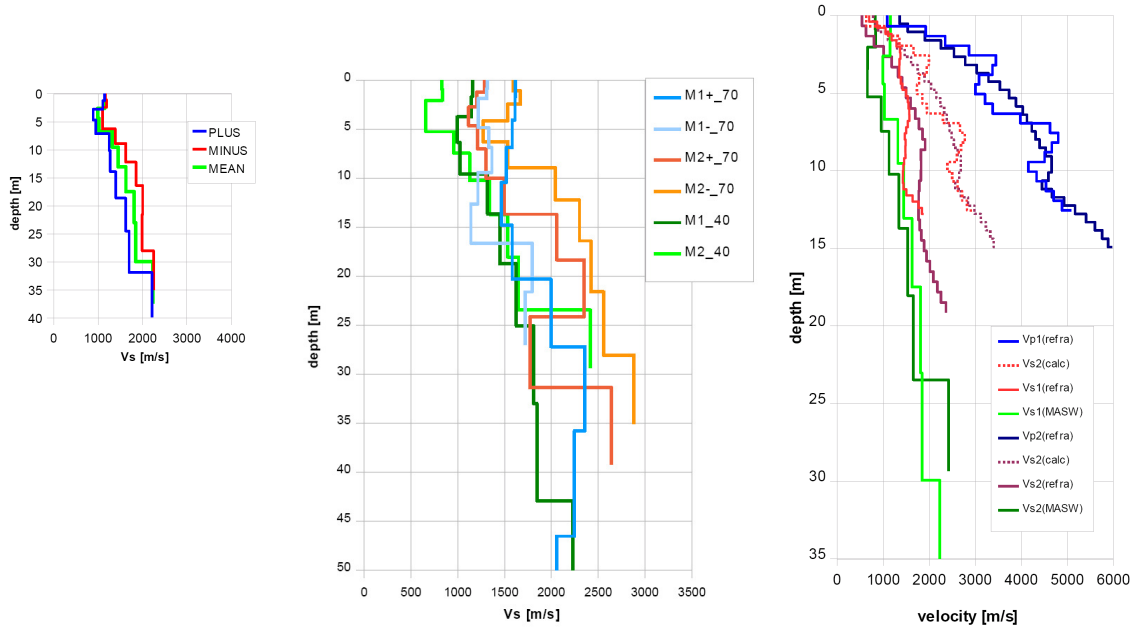

Figure A.20.4. Structural models at site WIMIS measured with MASW and seismic methods. For more details, see the report of GeoExpert related to the site WIMIS.

A.21 Station ZUR

The sensor of station ZUR is located in a vault, about 4.5 m below the surface in weathered sediments of the Molasse. Active S-wave measurements were performed on one section at a distance of about 100m from the station. Ambient vibration array measurements were performed closer to station ZUR. The position of the station ZUR is at the edge of the area of the array close to the "Erdbebenwarte". The peak in the H/V curve of the central station of the array is at 10Hz and indicates a surface layer of softer material, confirmed by the S-wave seismic measurements. The average velocity of this layer is around 400m/s (the S-wave seismics estimate was 320m/s), with a thickness of about 10m. The dispersion curves derived from active seismics indicate that the surface layer has S-wave velocities as low as 200m/s.

The H/V spectral ratio at site ZUR has a peak around 6 Hz, the entire H/V curve seems to be shifted by about 2-3 Hz when compared to that obtained for the central station of the array. This might also be due to the fact that the station ZUR is not at the free surface. Assuming an average S-wave velocity of 400 m/s, the thickness of the first layer with softer sediments at station ZUR can then be estimated in the range 12-15m. The S-wave velocity of the first bedrock layer is 900-1100m/s, with a layer thickness of about 20m. The S-wave velocity is then increasing to about 1300-1500m/s around a depth of 30-40m.

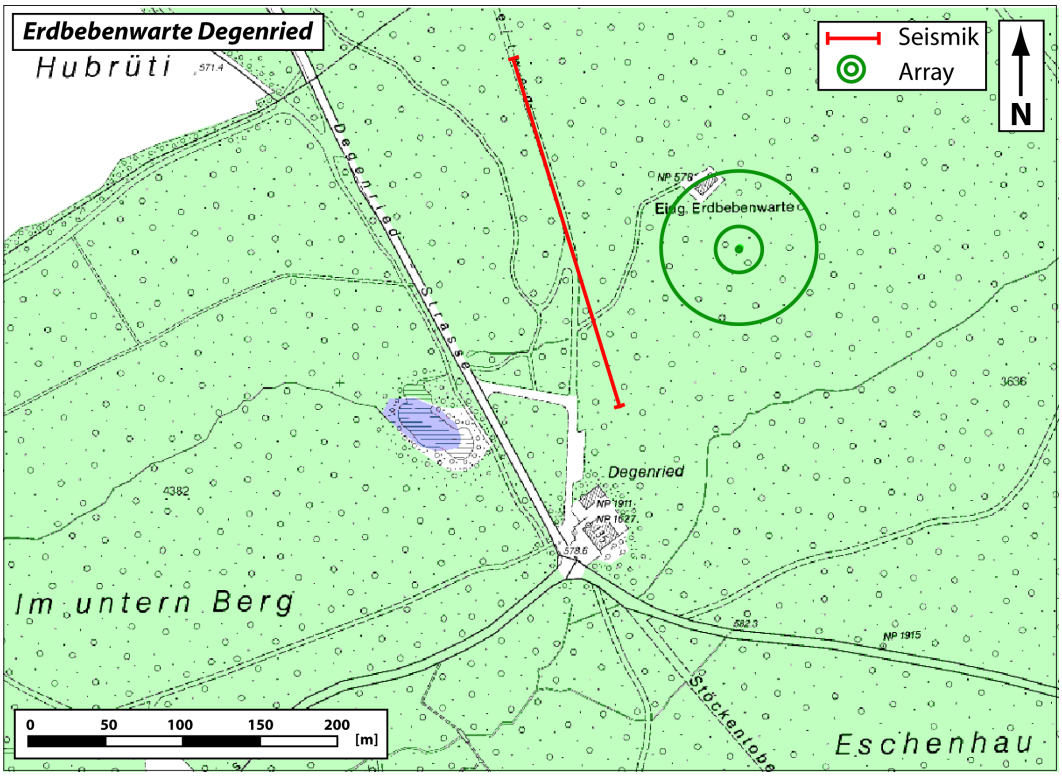

Figure A.21.1. Measurements at site ZUR.

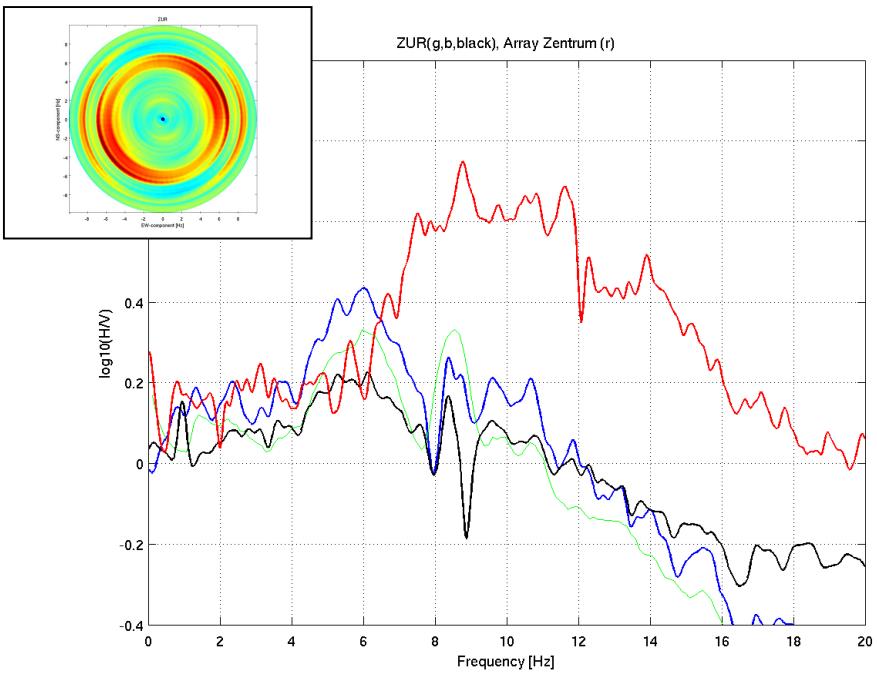

Figure A.21.2. H/V spectral ratios at the site of seismic station ZUR (blue, black and green curves). The H/V curve from the central stations of the array is given in red. The fundamental frequency of resonance seems to be shifted by about 2.5Hz when compared to the site of station ZUR. Station ZUR is about 4.5m below the surface, which might affect the amplitude of the H/V curve.

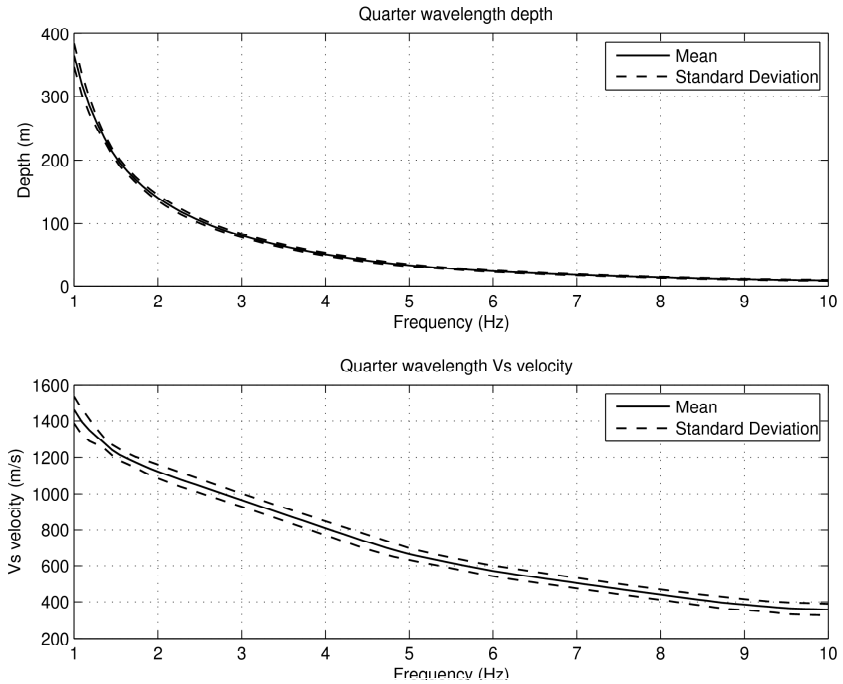

Figure A.21.3. Quarter wavelength velocity for site ZUR obtained with ambient vibration array techniques and corrected for the changes in the fundamental frequency of resonance.

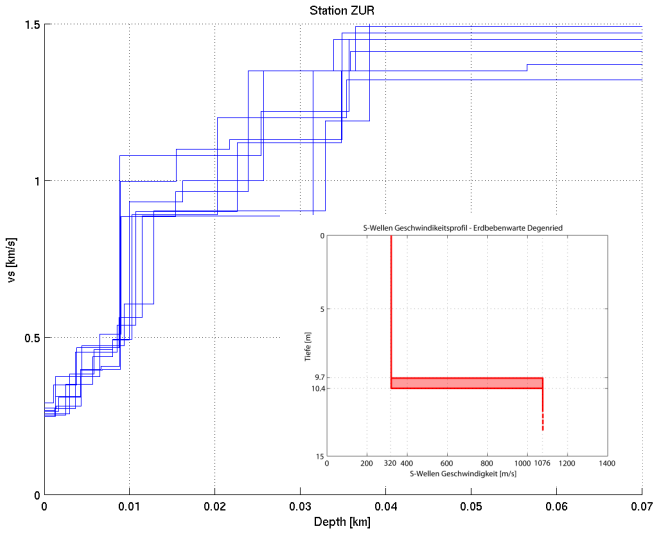

Figure A.21.4. Structural models close to site ZUR from the combined inversion of the Rayleigh wave phase velocity curve and ellipticity. The insert is the result from the more distant seismic profile.

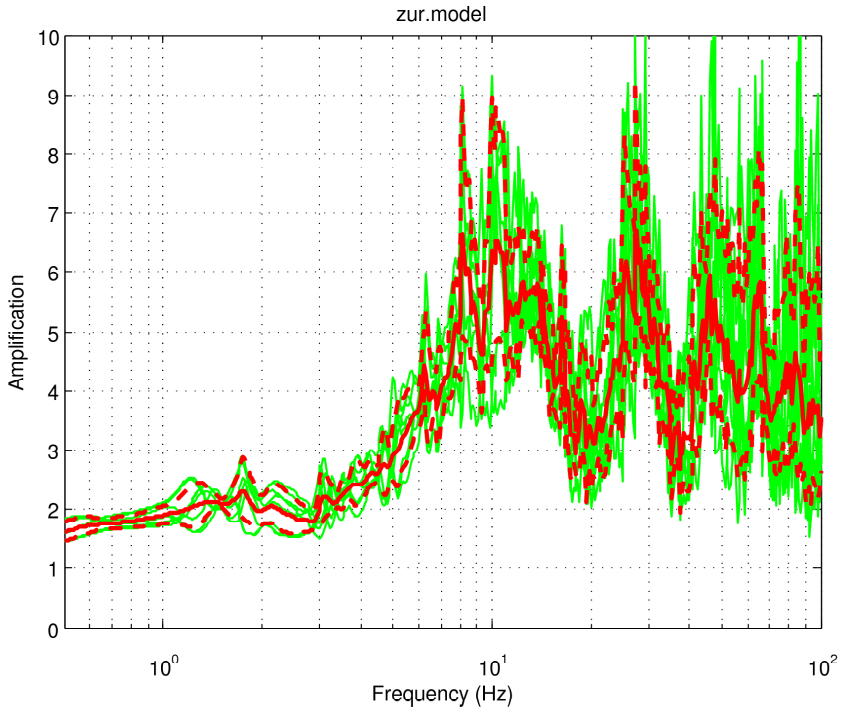

Figure A.21.5. SH amplification function obtained for the structural models in Figure A21.4.

Appendix B

B.1 Array-measurements at the broadband-site “SULZ”

G. Stamm, J. Burjanek, D. Fäh
Schweizerischer Erdbebendienst ETH Zürich

Location	Sulz (AG)
Seismic Station	SULZ
Method(s)	H/V-measurements
Array-measurements	
Date	27/08/2008
Measurements done by	Gabriela Stamm
Processing done by	Gabriela Stamm, Jan Burjanek

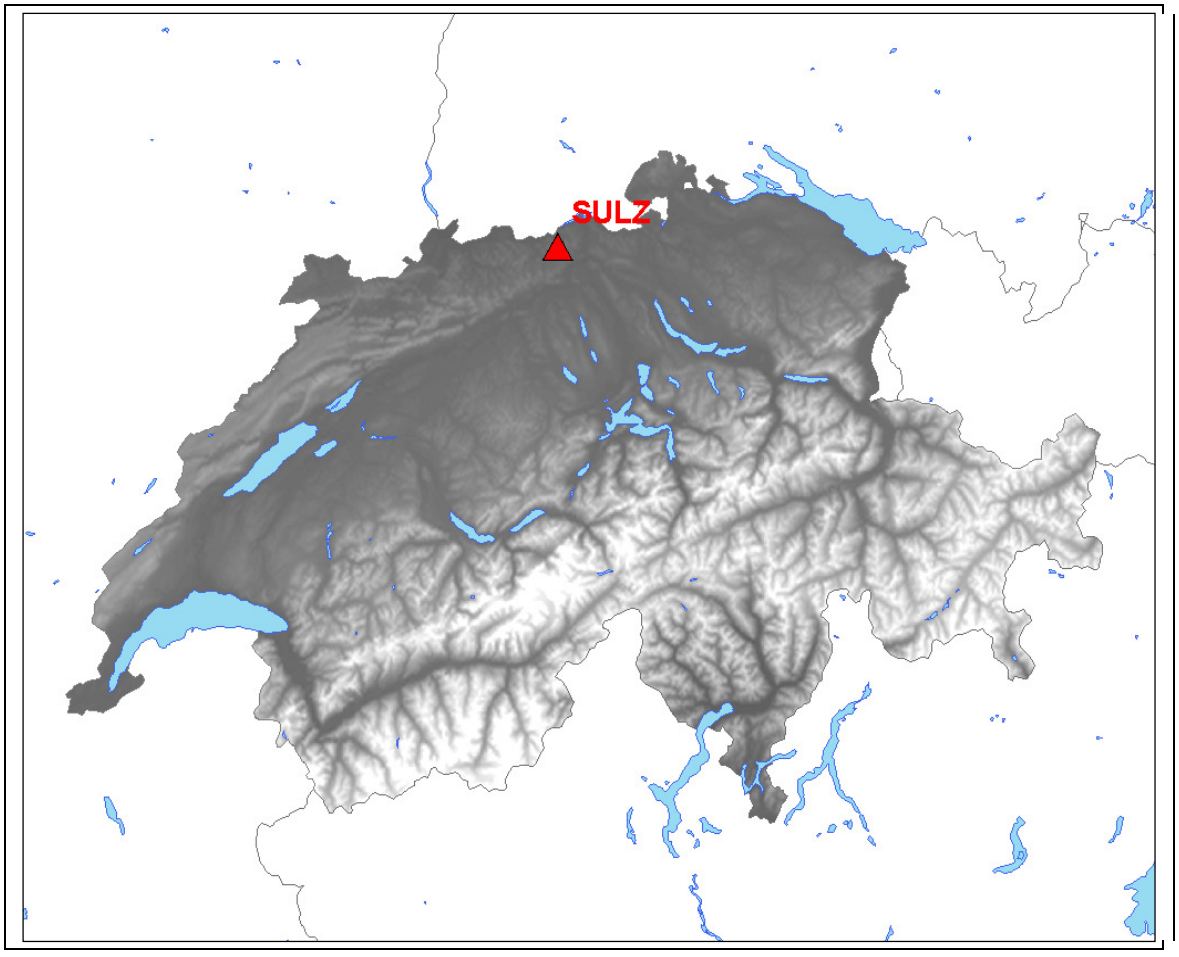

Figure1: Location of the broadband-site SULZ in Sulz (AG).

1. Method

1.1 H/V

To compute the H/V-ratios, two different methods were applied. The first one is the classical polarisation analysis in the frequency domain, where the polarisation is defined as the ratio between the quadratic mean of the Fourier spectra of the horizontal components and the spectrum of the vertical component. The second method tries to reduce the SH-wave influence by identifying P-SV-wavelets from the signal and taking the spectral ratio only from these wavelets. This is done by means of a frequency-time analysis of each of the three components of the ambient vibrations. Both methods are described in more detail in Fäh et al., 2001. To ensure that the measuring site can be handled as a "1D-case", the H/V-ratios of all array-points were compared together. All points showing differing curves were then excluded of the array-processing.

1.2 Array-processing

The first array method we use is based on the high-resolution beam-forming (HRBF) method. It was originally proposed by Capon (1969) but developed and applied to vertical recordings of ambient vibrations by Kind et al. (2005). We have extended this method to also analyse the horizontal components (Fäh et al., 2008). In general, sub-arrays with different apertures are set up for the measurement to optimise the capabilities in a certain frequency band. Small apertures are used to resolve the shallow part of a structure, and by increasing the aperture, deeper and deeper structures can be investigated. The final dispersion curve over a wide frequency-range is then composed of the parts obtained by the different sub-arrays. The limits of each sub-array are given by the aliasing at high frequencies and the loss of resolution at low frequencies.

In a second step the Spatial Autocorrelation (SPAC) method was applied. The SPAC method is another class of array processing techniques of ambient noise vibrations introduced by Aki (1957). Where both HRBF and SPAC methods have been applied to the same data, SPAC methods have been found to yield higher resolution at low frequencies (Asten, 2006, and references therein). Thus it gives a possibility to increase a bandwidth of the dispersion curves. We use a modified SPAC method for non-circular arrays (Bettig et al., 2001) implemented within the GEOPSY software package by Wathelet et al. (2005). Pairs of stations in the array are grouped along rings of certain diameters (the choice of the rings is upon the user). The spatial autocorrelation function is then evaluated for each ring and transformed to the frequency-velocity domain. The so-called dispersion density is then generated by stacking SPAC functions in frequency-velocity domain. High density regions should then correspond to dispersion curves.

1.3 Inversion

Our inversion scheme is based on a genetic algorithm that was developed by D. Carroll and is described in Fäh et al. (2001, 2003). It does not require explicit starting models but only the definition of parameter limits. To estimate the average S-wave velocity structure below our array, we use the combined H/V spectral ratios and phase velocity curves for Rayleigh- and Love-waves as input.

2. Array-Configuration

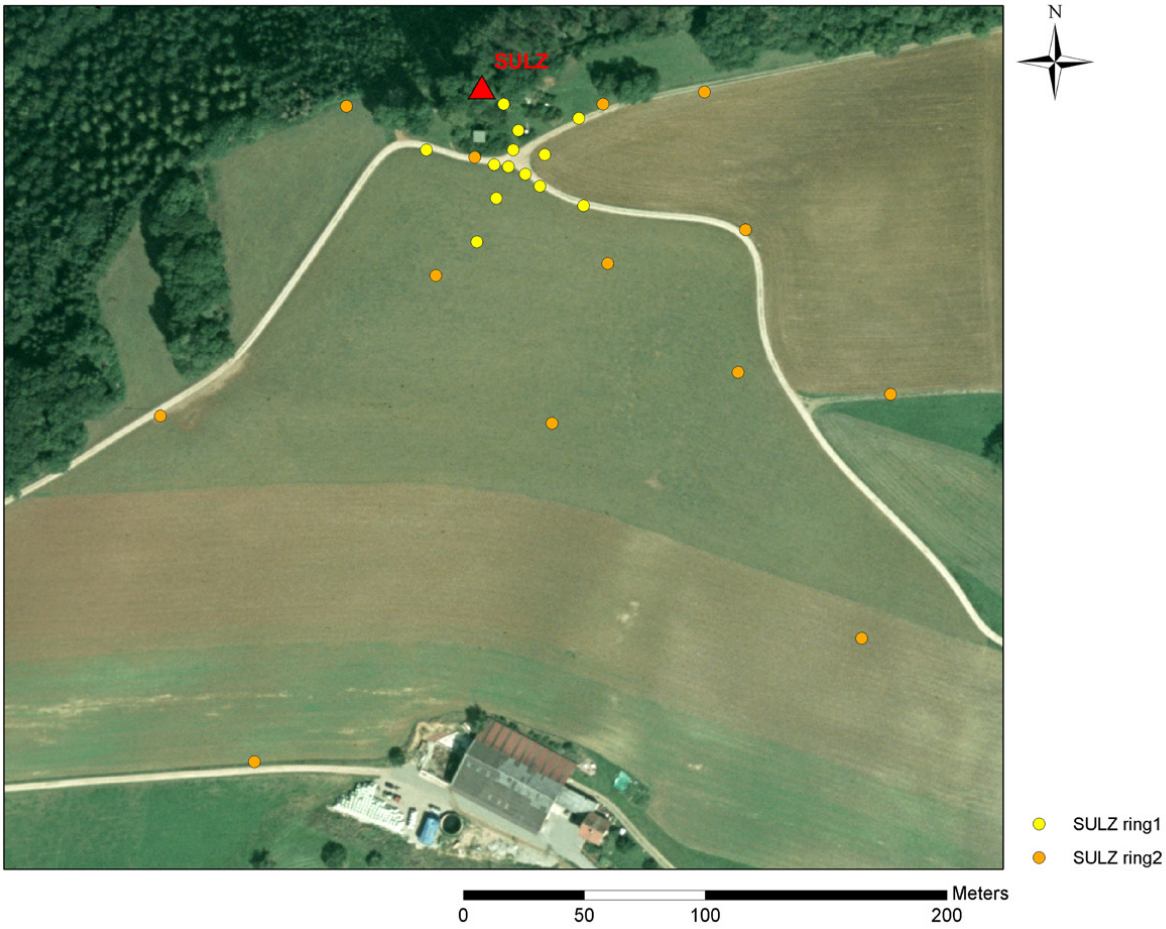

Figure 2: *Array-configuration for SULZ ring1 and ring2.*

Table 1: *Important parameters of the array set ups.*

	SULZ ring1	SULZ ring2
No. Sensors	14	13
max. Radius [m]	35	150
min. distance between two sensors [m]	~7	~70
max. distance between to sensors [m]	~70	~300

The broadband-station SULZ is situated on top of a hill, hence the array was set up on a gentle slope.

3. H/V

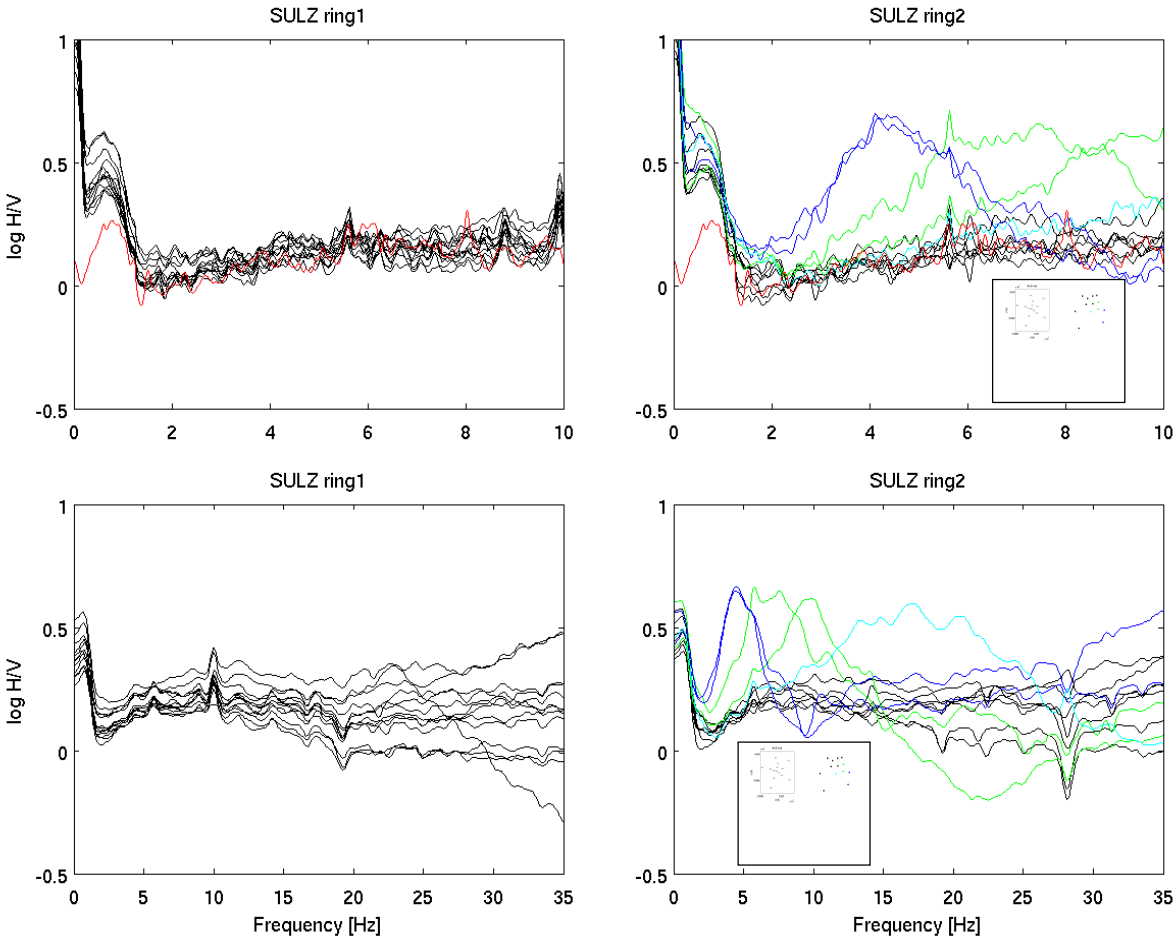

***Figure 3:** Comparison of the H/V-ratios of all points measured in SULZ ring1 and ring2 with that from the broadband-station SULZ (red).*

All H/V-ratios of the stations from ring1 are similar, so none of them had to be excluded from the array-processing. By looking at the H/V-ratios of ring2, a change in geology becomes visible. The five stations that are at the south-east of ring2 (see small plots of the array-configuration inside figure 3) show peaks at different frequencies. The further to the east that the stations were situated, the lower the frequency of the peak is. This indicated, that a layer of soft sediments is located to the east with increasing thickness of sediments.

4. Dispersion Curves

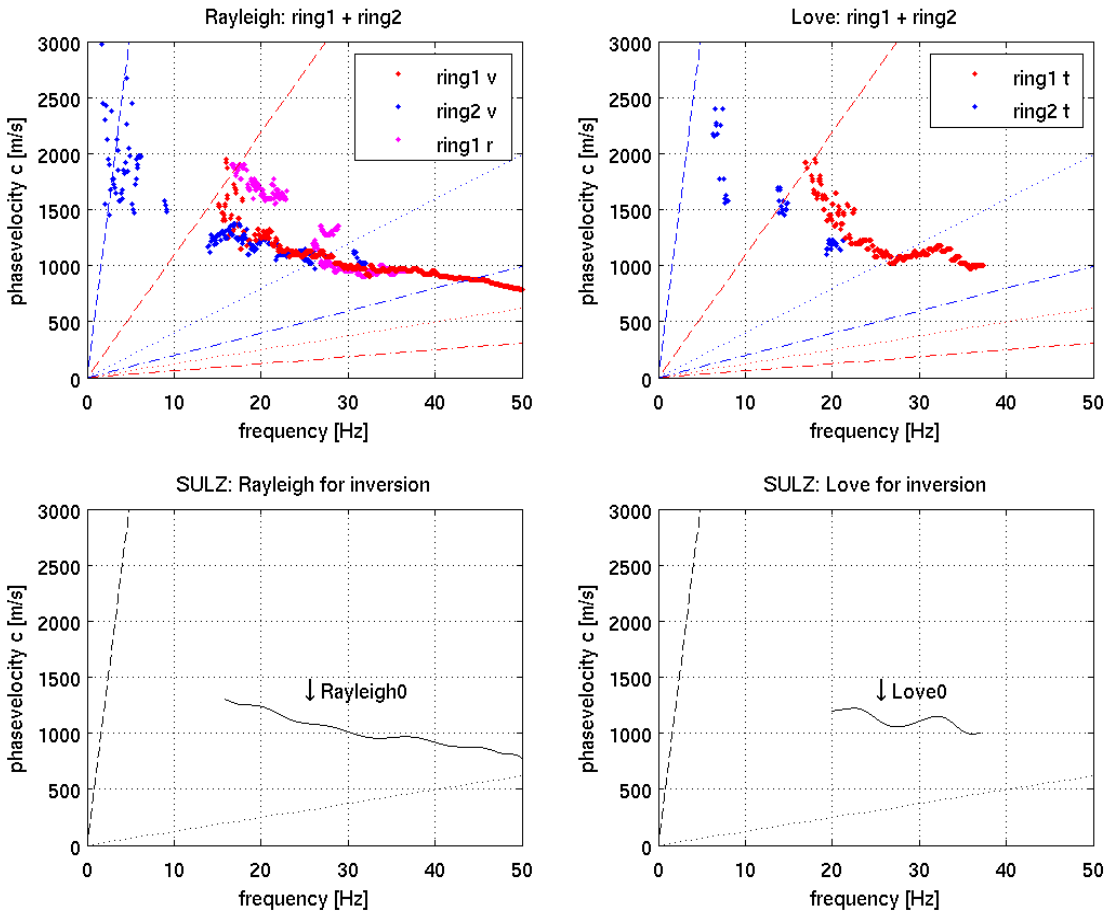

Figure 4: *Rayleigh- and Love-wave dispersion curves for SULZ ring1 and ring2. (v: vertical components, r: radial components, t: transverse components.)*

Dispersion curves were only clearly visible at frequencies higher then 15Hz. On the vertical components of ring1 and ring2 the fundamental mode of Rayleigh-waves is probably visible between 16 and 50Hz. On the radial components of ring1 parts of a higher mode can also be detected. The transverse components of ring1 and ring2 probably show a part of the fundamental mode of Love-waves.

5. Inverted Profiles

Table 1 gives a description of the type of models that were run for the site SULZ. The H/V-ratio was fit between 0.9-1.3 Hz, the Rayleigh fundamental mode between 16-30 Hz and the Love fundamental mode between 20-30 Hz. Figure 5 shows the obtained S-waves profiles. Figures 6 and 7 show the fit of the theoretical dispersion curves of the inverted models to the observed dispersion curves. The fit is generally good.

Table 1:

	H/V	Rayleigh fund. mode	Love fund. mode
type 1	0.9-1.3Hz	16-30Hz	20-30Hz

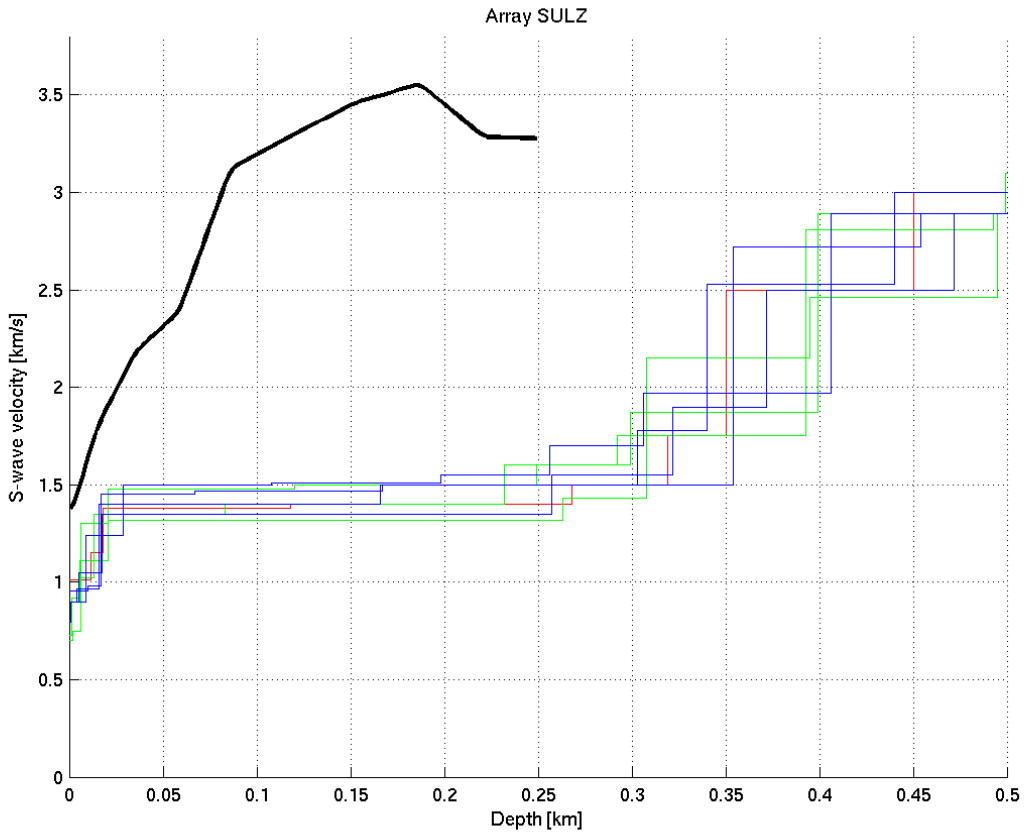

Figure 5: *Inverted S-wave profiles for the site SULZ (coloured curves). The black curve corresponds to the model obtained from seismic measurements by GGA.*

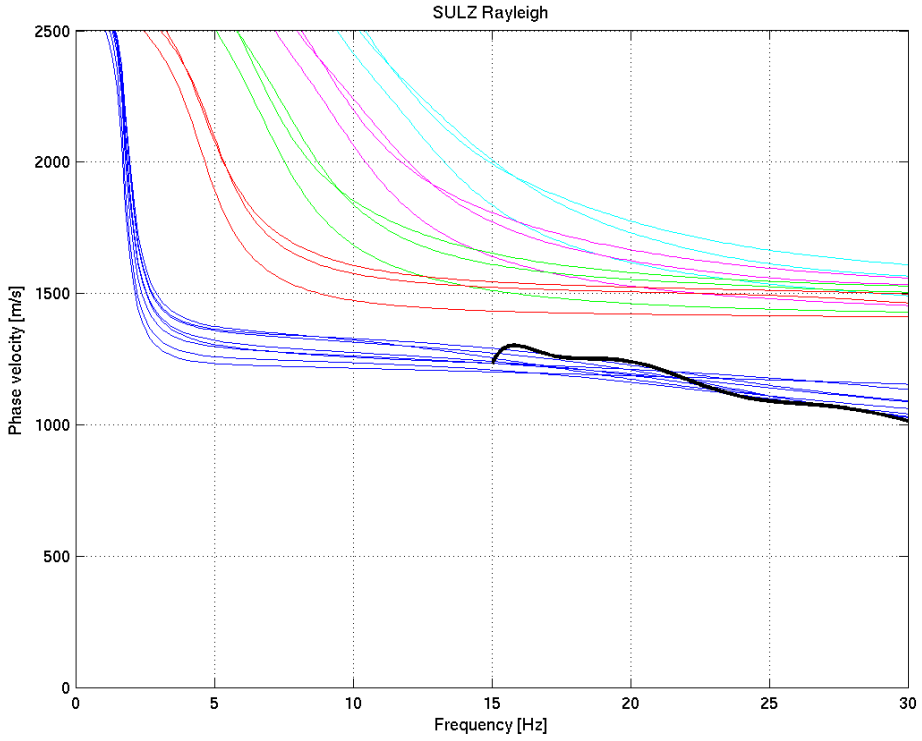

Figure 6: *Comparison between dispersion curves of the inverted structural models and measured curves for Rayleigh waves (colour). Different modes have different colours. The higher modes are not shown for all models.*

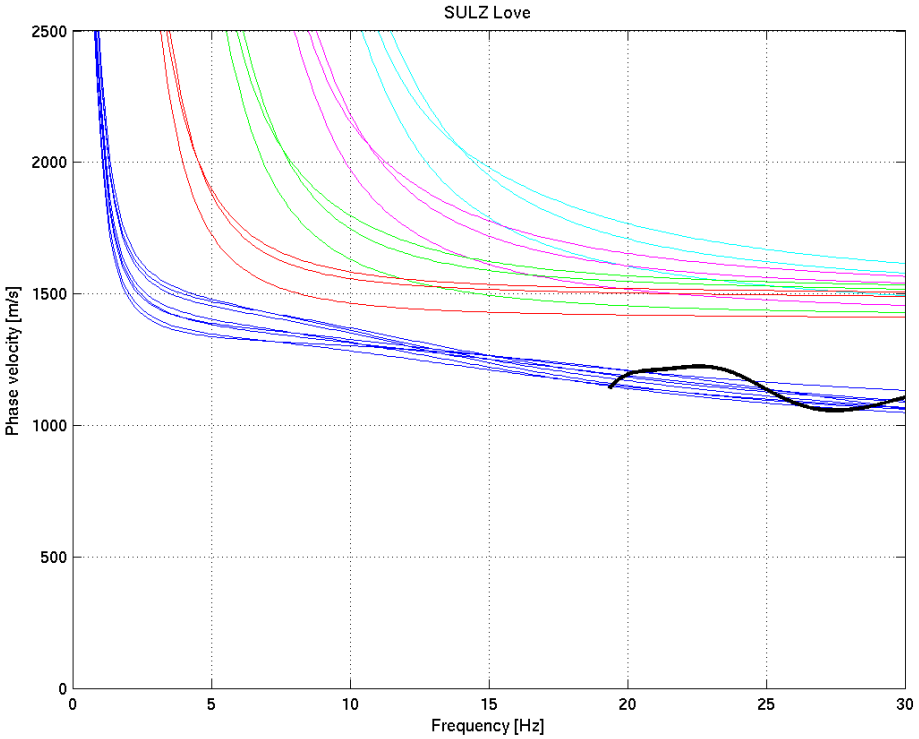

Figure 7: *Comparison between dispersion curves of the inverted structural models and measured curves for Love waves. Different modes have different colours. The higher modes are not shown for all models.*

At the same site S-wave reflection seismic measurements were performed in 2003 by the Institut für Geowissenschaftliche Gemeinschaftsaufgaben (GGA, Germany, unpublished data). The measured mean velocity profile is also shown in Figure 5. Figure 8 shows the measured S-wave velocity profile. The velocities obtained with seismic measurements are much higher than those from the ambient vibration array analysis. Such high velocities cannot explain the dispersion curves measured with ambient vibration array measurements.

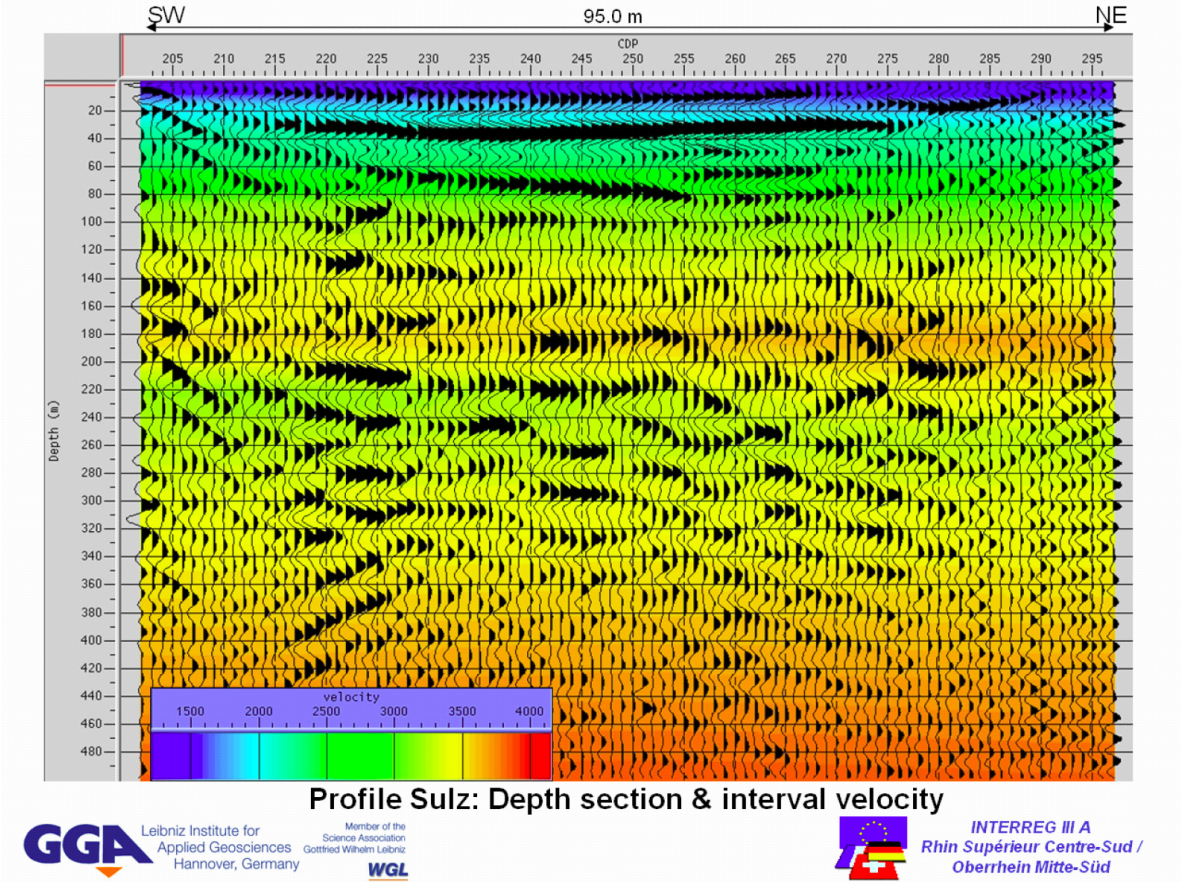

Figure 8: *S-wave velocity section obtained with S-wave reflection and refraction seismic measurement (Interreg III Project "Mikrozonierung am südlichen Oberrhein", U. Polom, unpublished results.*

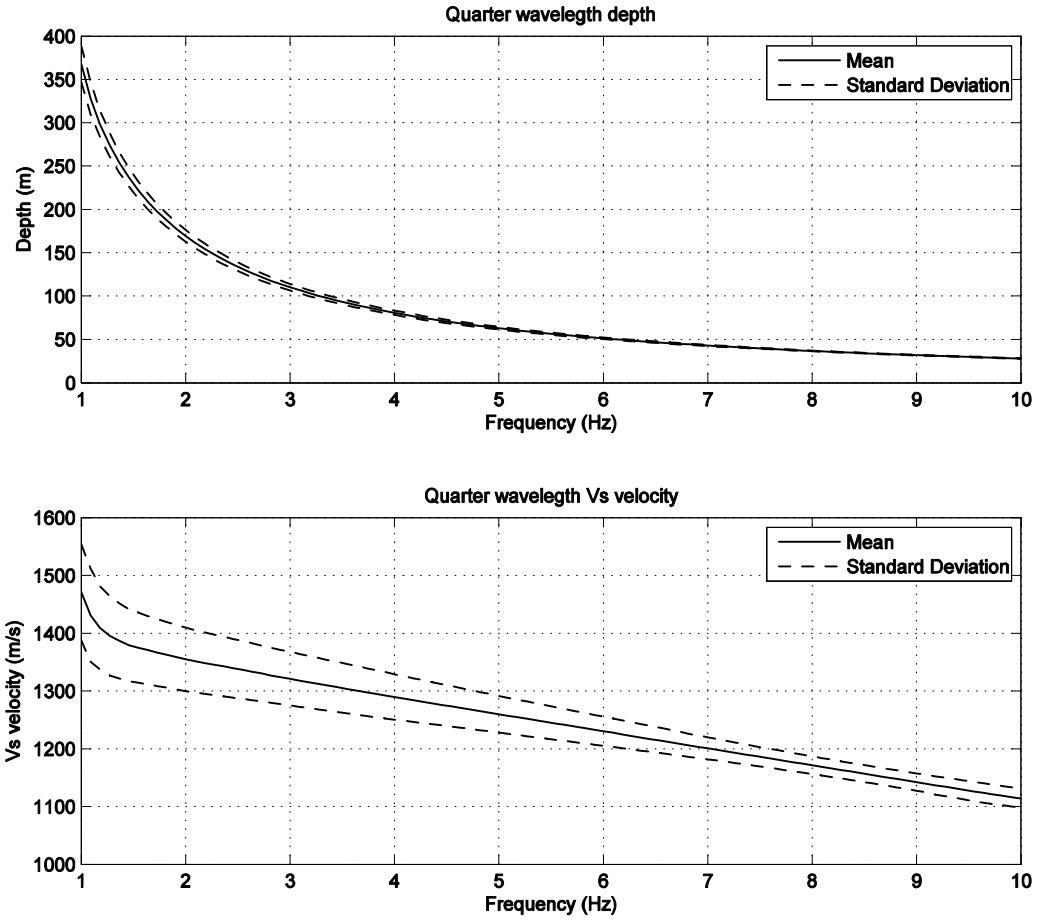

Figure 9: *Quarter wavelength and quarter-wavelength velocity as a function of frequency at the site of the arrays at SULZ.*

Finally Figure 9 provides the quarter-wavelength velocities and depth as function of frequency for the ambient vibration array measurements. The seismic station SULZ is located on rock. Table 2 summarizes the mean velocity for different thicknesses. The average velocity is computed in a way such that the travel-time in an average model corresponds to the sum of the travel times in the single layers:

$$\frac{1}{\bar{v}} = \frac{1}{H}\sum_{i=1}^{n}\frac{h_i}{v_i} \qquad \text{with} \qquad H = \sum_{i=1}^{n} h_i \,.$$

H [m]	Vs mean [m/s]	Vs stddev [m/s]
5	872	70
10	938	26
20	1040	22
30	1130	13
40	1188	15
50	1226	21
(100)	(1311)	(41)

Table 2: *Mean S-wave velocity at SULZ over the thickness H.*

6. Results obtained with SPAC

In case of SULZ, SPAC was applied to the vertical component of motion acquired at the larger subarray (334m aperture). The resulting dispersion density is depicted in Figure 10. The dashed line is the picked dispersion curve that is used for the subsequent inversion. The resolution limits were estimated from the scatter of the dispersion density plot and from the shape of the SPAC functions. Generally, a SPAC curve should follow a zero-order Bessel function. The scatter in the 1-3.5 Hz frequency band is relatively low. Two examples of SPAC curves are depicted in Figure 11. The contributions of SPAC functions to the dispersion density region specified by thin black lines (stable, well defined ridge in dispersion density plot, see Fig. 10) are denoted by black color. SPAC curves do not deviate from the shape of Bessel function in these intervals (especialy for ring 7). Several ring layouts were also tested with very similar results. Large scatter of dispersion density and SPAC functions, which do not fit Bessel's function preclude an estimation of dispersion curve at frequencies higher than 3.5Hz.
In summary, using SPAC it was possible to identify a relatively strong dispersive signal on the vertical component in the frequency band 1-3.5Hz.

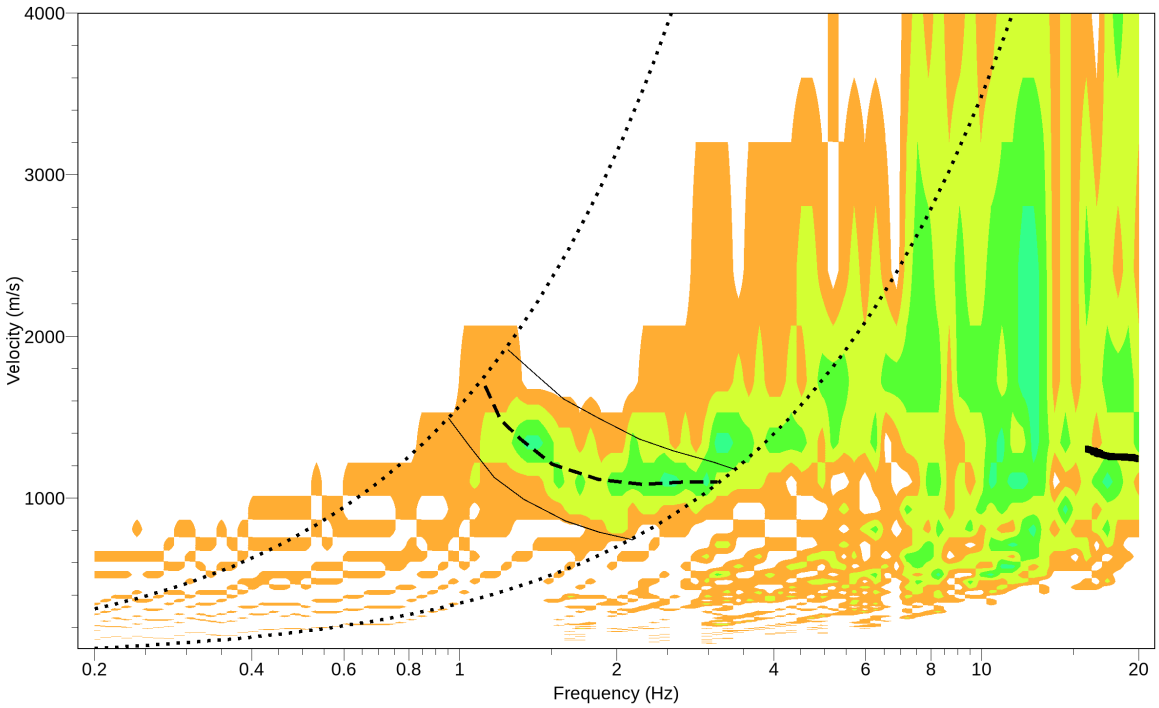

Figure 10: *Dispersion density grid (stack of dispersion solutions obtained from different rings) with picked dispersion curve (dashed line), and a chunk of the dispersion curve obtained from HRBF (thick solid line). A stable zone of higher dispersion density is delineated with thin black lines. The dotted lines represent the wave-number limits deduced from the observations.*

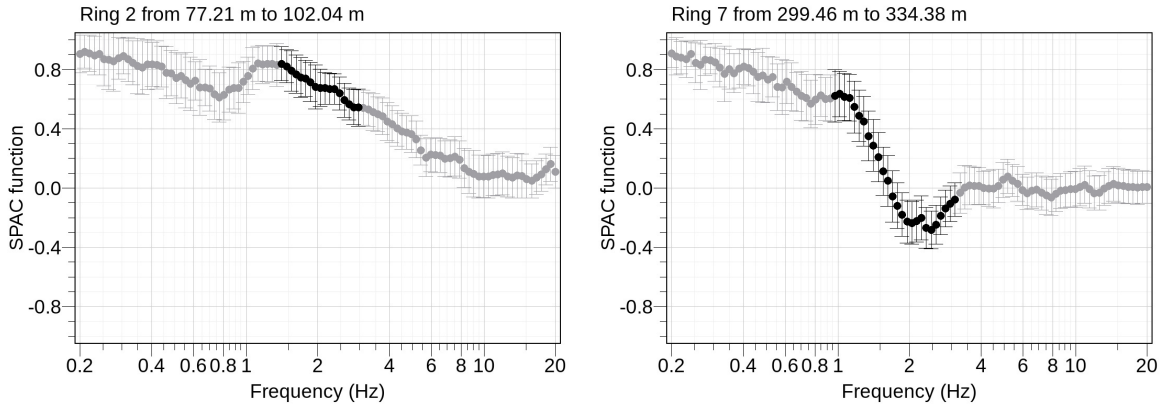

Figure 11: *An example of SPAC curves for two rings (small ring on the left, large ring on the right).*

If we assume that the results from SPAC are reliable, then we see a segment of the Rayleigh fundamental mode. In this case it is suggested that HRBF analysis provides parts of the dispersion curves of higher modes (see the results for Love waves in Figure 12 and compare to Figure 7), and almost no information for the fundamental mode. Assigning mode numbers to the different segments is difficult. However we have repeated the inversion using the results from SPAC, the H/V curve and assuming that one of the segments seen for Love waves belongs to the third or fourth higher mode. We also defined a range of possible velocities for the upper layer. The new inverted profiles are shown in Figure 13 (blue, cyan and red).

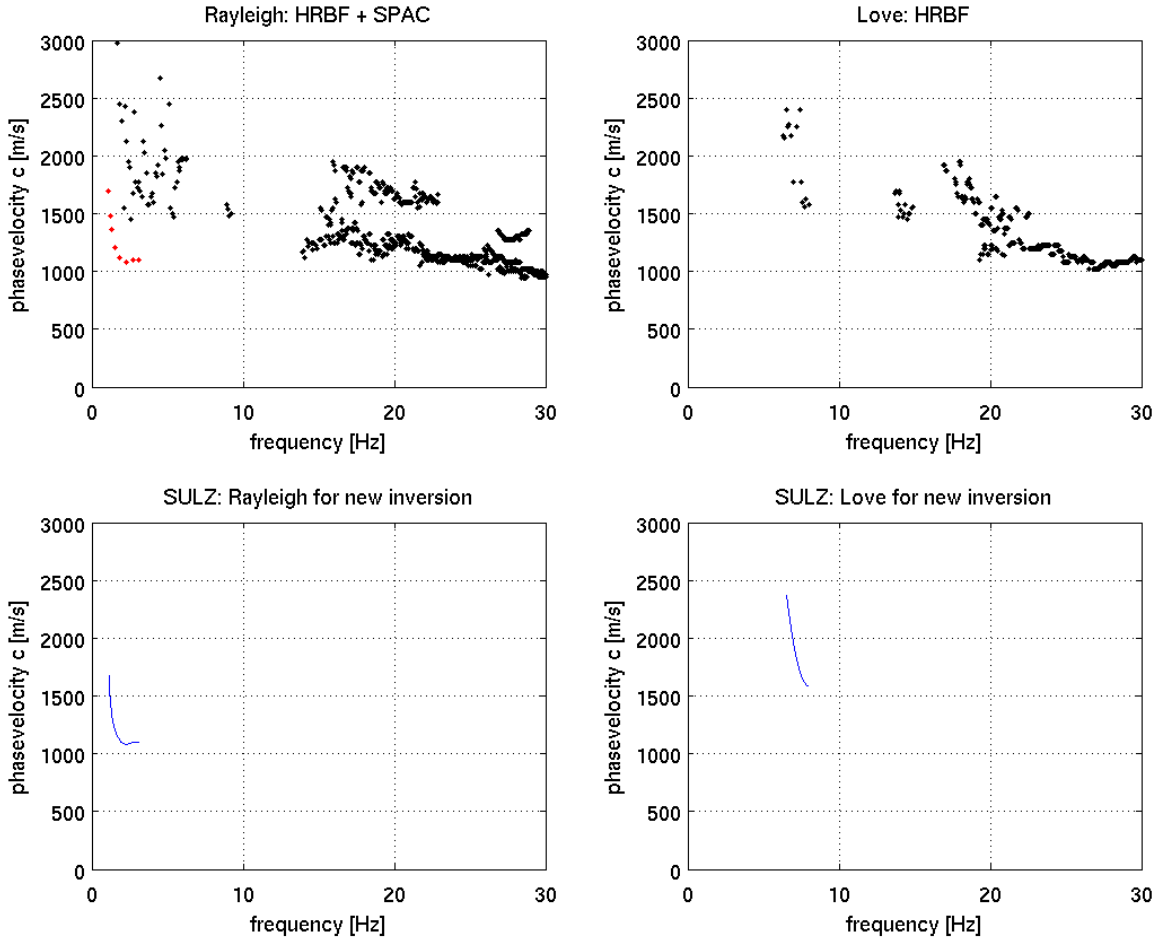

Figure 12: *The upper two pictures show the dispersion-curves obtained with HRBF (black) and SPAC (red). Below, the segments used for the new inversions are plotted in blue.*

In Figure 13, the inverted profiles using only the HRBF-results are shown in green. The new profiles using also the SPAC-results for the inversion are shown in blue (Love-segment was assigned to the fourth higher mode), cyan (Love-segment was also assigned to the fourth higher mode, very good fit of the Rayleigh fundamental mode segment) and red (Love-segment was assigned to the third higher mode).

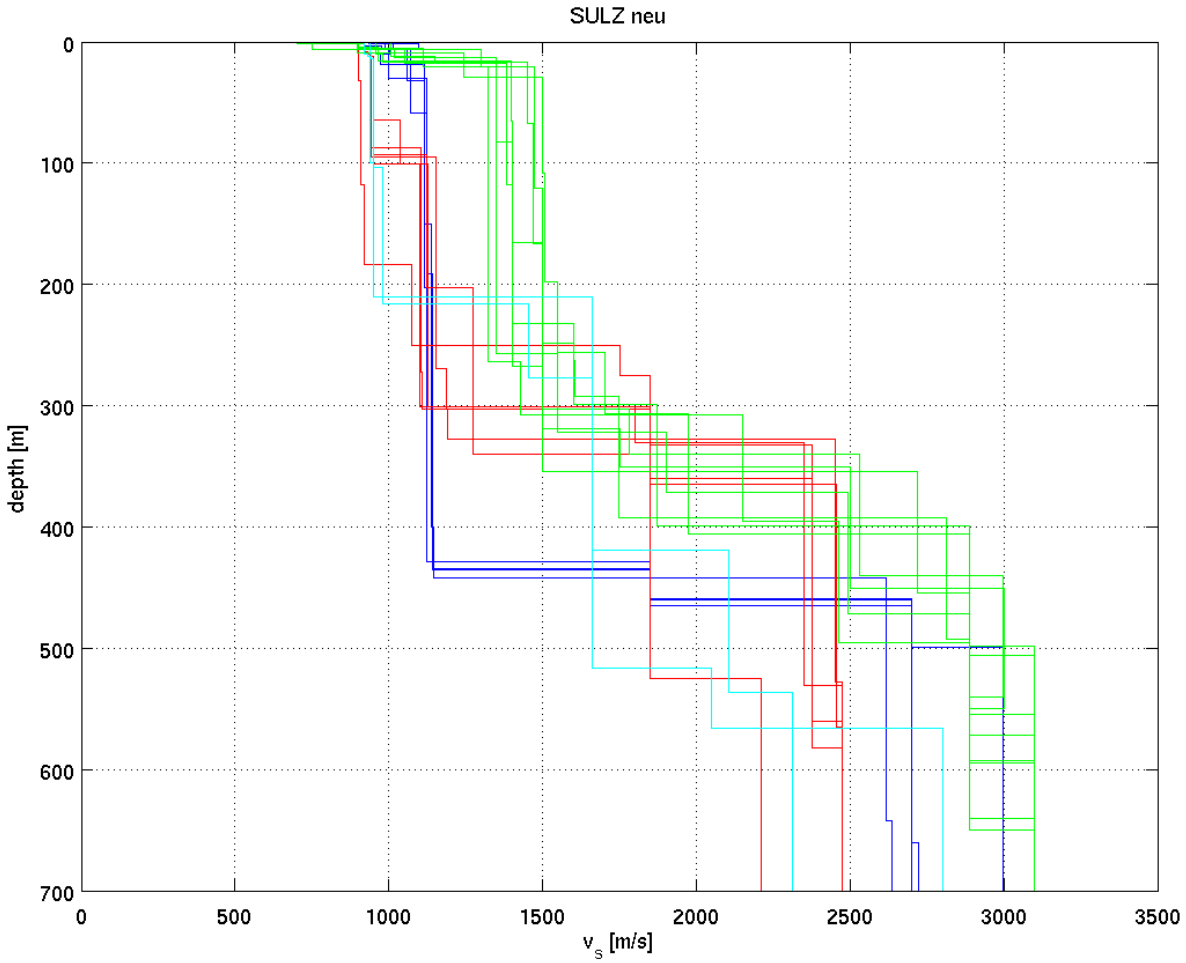

Figure 13: *inverted profiles using only the HRBF-results (green) as well as the new ones (blue, cyan and red). For all new models we assumed that the Rayleigh-segment obtained from SPAC is part of the fundamental mode. The Love-segment was once assigned to the third higher mode (red) and once to the fourth higher mode (blue and cyan). The cyan models show a very good fit to the Rayleigh fundamental mode segment.*

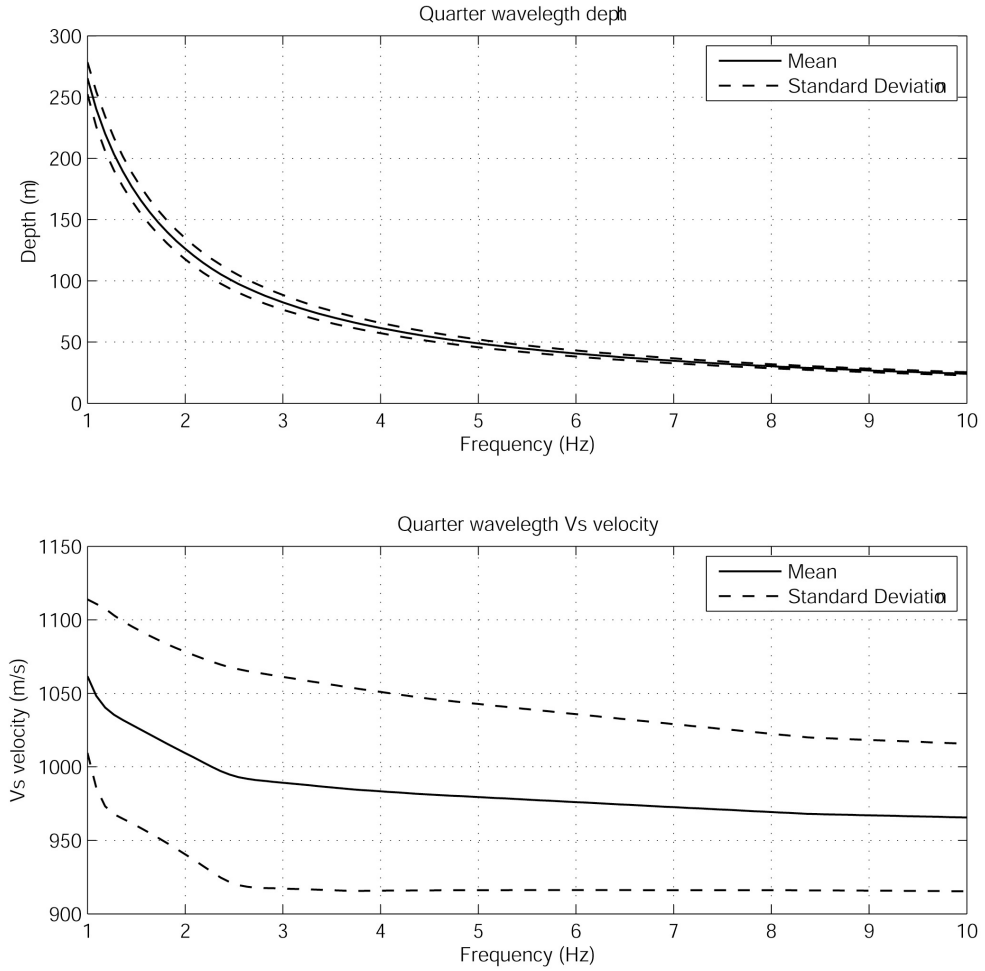

Figure 14: *Quarter wavelength and quarter wavelength velocity as a function of frequency at the site of the arrays at SULZ, using only the new inverted profiles obtained with the SPAC-results (blue, cyan and red in fig. 13).*

H [m]	Vs mean [m/s]	Vs stddev [m/s]
5	951	46
10	956	48
20	962	49
30	968	52
40	975	58
50	979	62
100	995	71
150	1020	66
200	1035	65
400	(1170)	(39)

Table 3: *Mean S-wave velocity at SULZ over the thickness H, when using only profiles obtained with the SPAC-results (blue, cyan and red in fig. 13).*

7. References

Aki K. (1957). Space and time spectra of stationary stochastic waves, with special reference to microtremors. Bull. Earthq. Res. Inst. 35, 415–456.

Asten, M.W. (2006). On bias and noise in passive seismic data from finite circular array data processed using SPAC methods, Geophysics, 71, 153-162.

Bettig, B., Bard, P. Y., Scherbaum, F., Riepl, J., Cotton, F., Cornou, C., and Hatzfeld, D., 2001, Analysis of dense array noise measurements using the modified spatial auto-correlation method (SPAC) Application to the Grenoble area: Bollettino di GeofisicaTeorica dApplicata, 42, 281–304.

Capon, J., (1969). High-resolution frequency-wave number spectrum analysis, Proc. IEEE, 57(8), 1408-1418.

Fäh, D., Kind, F. and Giardini, D. (2001). A theoretical investigation of average H/V ratios. Geophys. J. Int., 145, 535-549.

Fäh, D., Kind, F. and Giardini, D., (2003). Inversion of local A-wave velocity structures from average H/V ratios, and their use for the estimation of site-effects, J. Seismol., 7, 449-467.

Fäh, D., Stamm, G. and Havenith, H.-B., (2008). Analysis of three-component ambient vibration array measurements, Geophys. J. Int., 172, 199-213.

Kind, F., Fäh, D. and Giardini, D., (2005). Array measurements of S-wave velocities from ambient vibrations, Geophys. J. Int., 160, 114-126.

Wathelet M., Jongmans D., Ohrnberger M. (2005). Direct inversion of spatial auto correlation curves with the neighborhood algorithm. Bull. Seismol. Soc. Am. 95,1787–1800.

Yamanaka, H., Takemura, M., Ishida, H. and Niea, M. (1994). Characteristics of long-period micro-tremors and their applicability in exploration of deep layers. Bull. Seism. Soc. Am., 84, 1831-1841

B.2 Array-measurements at the broadband-site “SLE”

G. Stamm, D. Fäh
Schweizerischer Erdbebendienst ETH Zürich

Location	Schleitheim (SH)
Seismic Station	SLE
Method(s)	H/V-measurements
Array-measurements	
active source (Valerio Poggi)	
Date	SLE1 and SLE2: 30/05/2007
	SLE3: 15/08/2007
Measurements done by	Gabriela Stamm
Processing done by	Gabriela Stamm

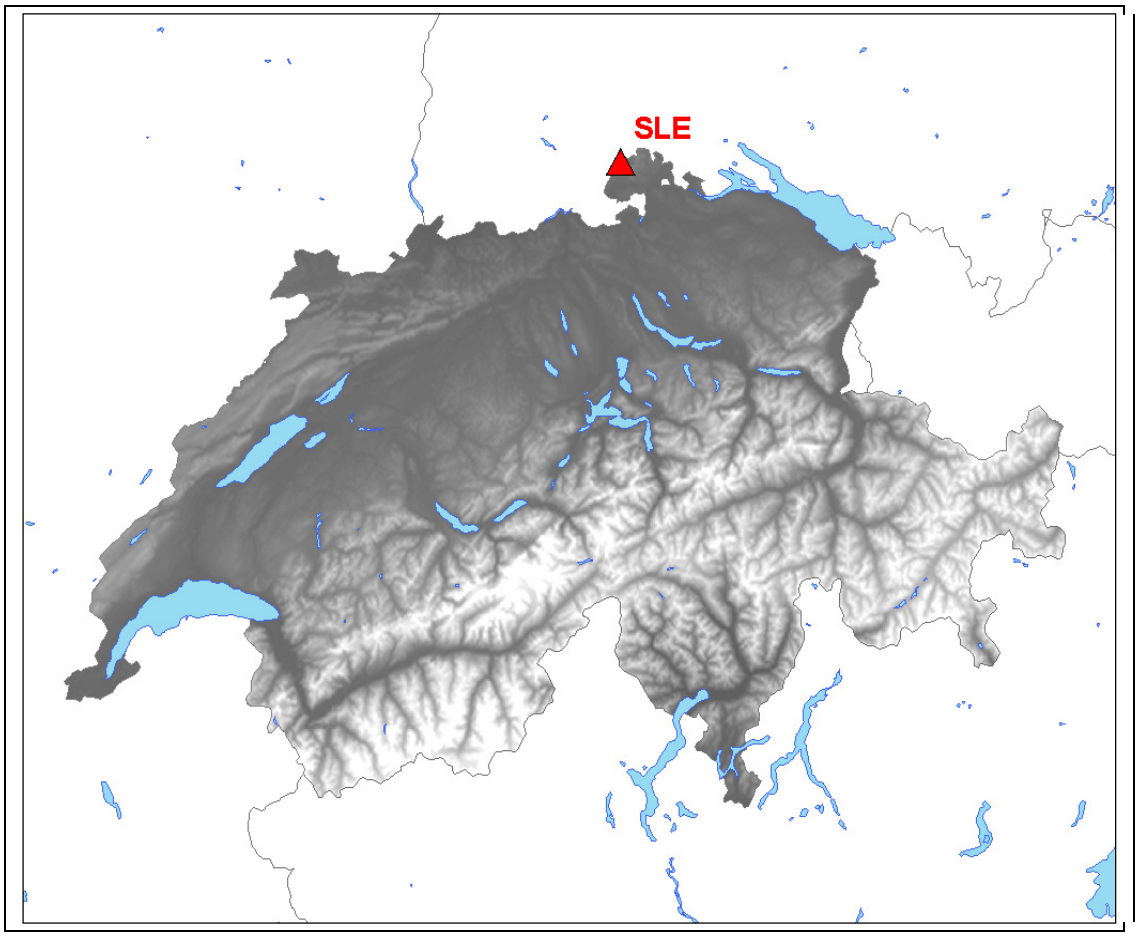

Figure 1: *Location of the broadband-site SLE in Schleitheim (SH).*

1. Method

1.1 H/V

To compute the H/V-ratios, two different methods were applied. The first one is the classical polarisation analysis in the frequency domain, where the polarisation is defined as the ratio between the quadratic mean of the Fourier spectra of the horizontal components and the spectrum of the vertical component. The second method tries to reduce the SH-wave influence by identifying P-SV-wavelets from the signal and taking the spectral ratio only from these wavelets. This is done by means of a frequency-time analysis of each of the three components of the ambient vibrations. Both methods are described in more detail in Fäh et al., 2001. To ensure that the measuring site can be treated as a "1D-case", the H/V-ratios of all array-points were compared with one another. All points showing differing curves were excluded of the array-processing.

1.2 Array-processing

The array method we use is based on the high-resolution beam-forming (HRBF) method. It was originally proposed by Capon (1969) but developed and applied to vertical recordings of ambient vibrations by Kind et al. (2005). We have extended this method to also analyse the horizontal components (Fäh et al., 2008).
In general, sub-arrays with different apertures are set up for the measurement to optimize the capabilities in a certain frequency band. Small apertures are used to resolve the shallow part of a structure, and by increasing the aperture, deeper and deeper structures can be investigated. The final dispersion curve over a wide frequency-range is then composed of the parts obtained by the different sub-arrays. The limits of each sub-array are given by the aliasing at high frequencies and the loss of resolution at low frequencies.

1.3 Inversion

Our inversion scheme is based on a genetic algorithm that was developed by D. Carroll and is described in Fäh et al. (2001, 2003). It does not require explicit starting models but only the definition of parameter limits. To estimate the average S-wave velocity structure below our array, we use the combined H/V spectral ratios and phase velocity curves for Rayleigh- and Love-waves as input.

2. Array-Configuration

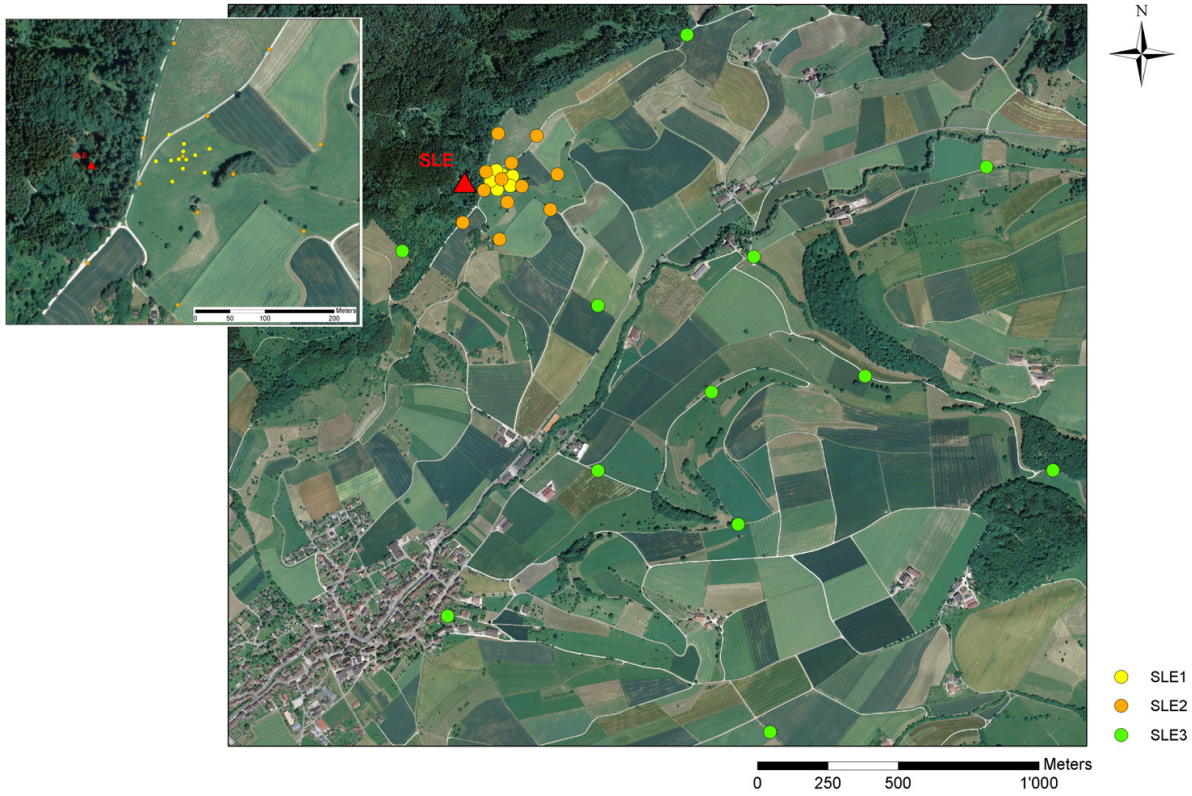

Figure 2: *Array-configuration for SLE1, SLE2 and SLE3.*

At the site SLE a total of three arrays were set up. SLE1 (diameter of 80m) and SLE2 (diameter of 400m) had the same central-station and therefore were processed together. The distance between their common central-station and the broadband-station is about 130m. It was not possible to go nearer to the broadband-station with our arrays due to the forest.
SLE3 was a large array with a diameter of 2.5km. Unfortunately however, it was not possible to retrieve any dispersion-curves from it.

Table 1: *Important parameters of the array set ups.*

	SLE1	SLE2	SLE3
No. Sensors	13	12	12
Max. Radius [m]	40	200	1200
min. distance between two sensors [m]	7	70	500
max. distance between to sensors [m]	80	390	2500

3. H/V

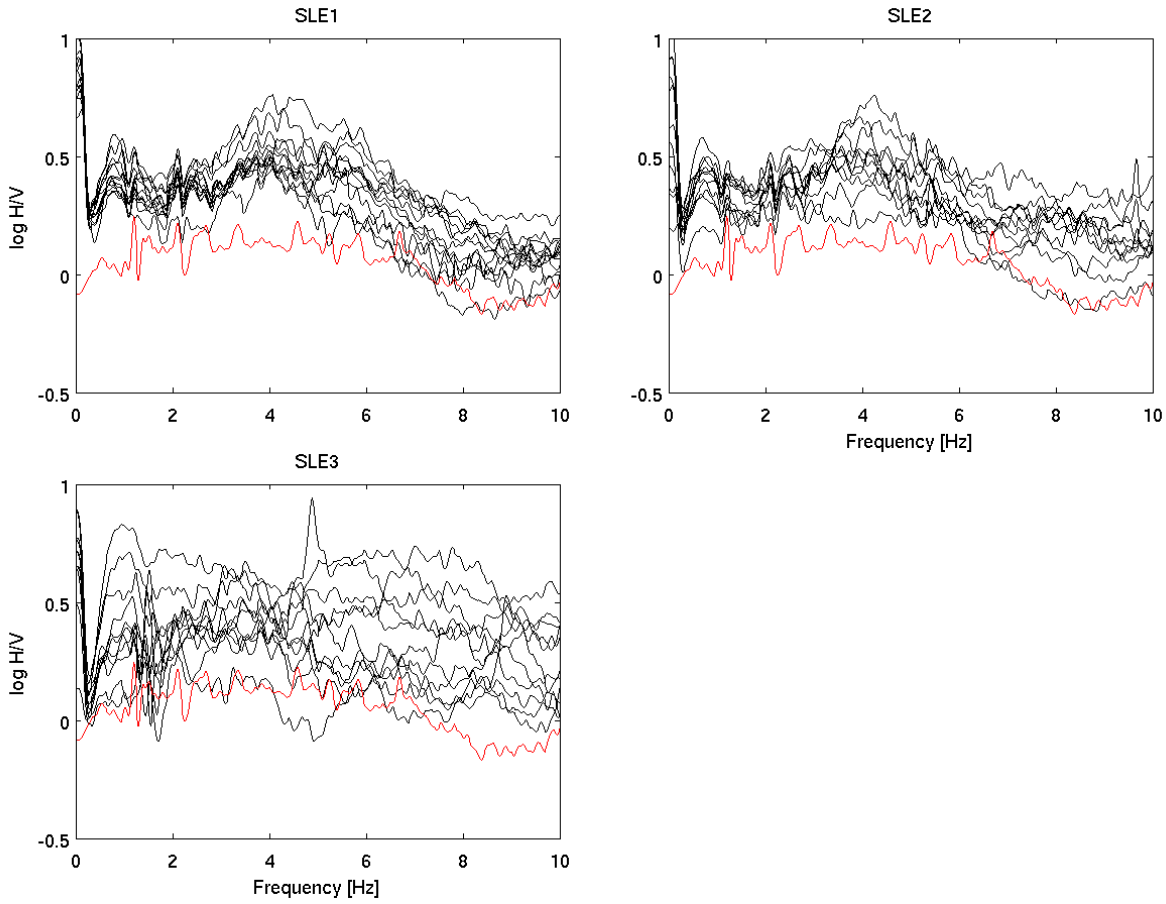

Figure 3: *Comparison of the H/V-ratios of all points measured in SLE1, SLE2 and SLE3 (black) with the one from the broadband-station SLE (red).*

SLE1 and SLE2 show similar H/V-ratios for all points of the array, therefore no stations had to be excluded for the array processing.
The H/V-ratio of the broadband-station shows no clear peak because the sensor is located in an old quarry, so the soft sediments are missing. A minimum in the H/V can be detected at about 8-10 Hz that is comparable to the minima in the H/V curves of stations in the arrays SLE1 und SLE2.

4. Dispersion curves

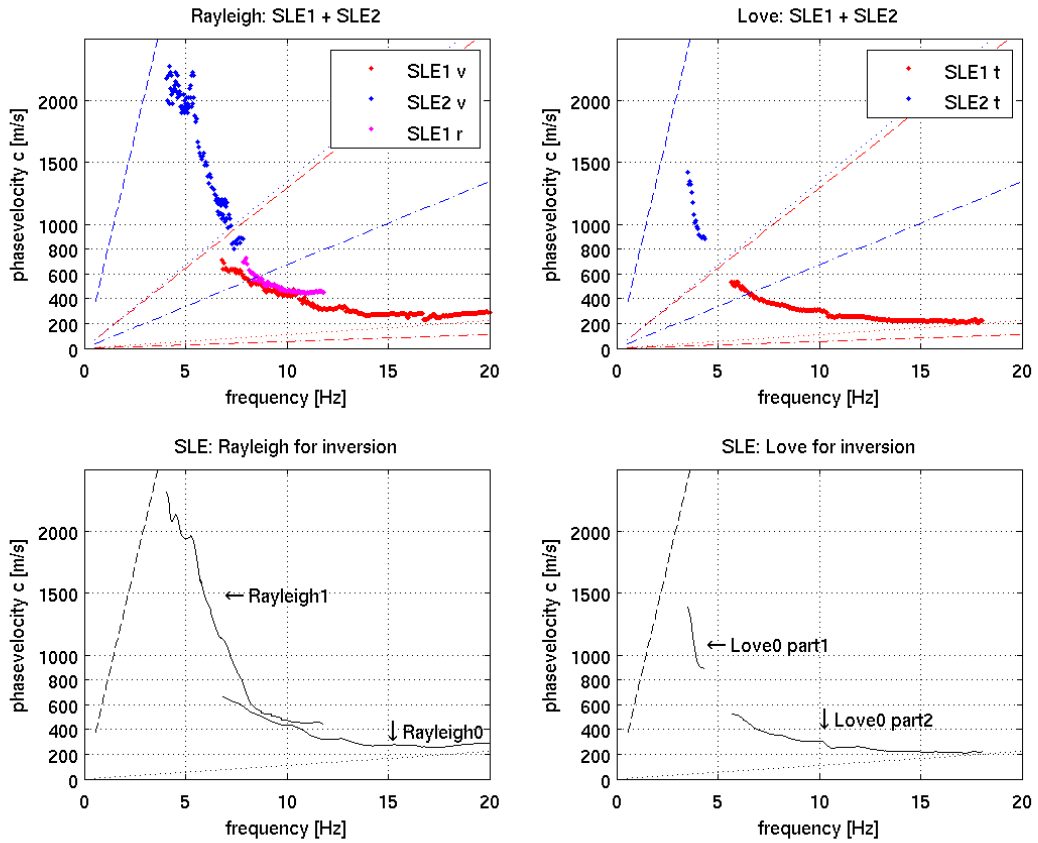

Figure 4: *Rayleigh- and Love-wave dispersion curves for SLE1 and SLE2. For SLE3 no results were obtained. (V: vertical components, r: radial components, t: transverse components.)*

On the vertical components of array SLE1, the fundamental mode of Rayleigh-waves is visible. The radial components of array SLE1 as well as the vertical components of SLE2 show part of the first higher mode of Rayleigh-waves. The fundamental mode of Love-waves is visible on the transverse components of SLE1 and SLE2.
The processing of SLE3 has not provided any dispersion curves when using the high-resolution beam-forming method.

5. Inverted Profiles

Four different types of models were inverted for the site SLE (see table 1). The parts of dispersion curves that were picked could be clearly assigned to either the fundamental ("0") or first higher ("1") mode of Rayleigh- or Love-waves. For the different types of models the inverted frequency-ranges were changed along with the frequency-range of the H/V-curve that was fit.

Table 1:

	H/V-Peak	Rayleigh fund. mode	Rayleigh 1. higher mode	Love fund. mode
type 1	0.8-1.1Hz	7-18Hz	8-11.2Hz	3.7-4.1 and 5.9-17.2Hz
type 2	5.6-8Hz	7-18Hz	8-11.2Hz	3.7-4.1 and 5.9-17.2Hz
type 3	5.6-8Hz	7-8 and 11-16Hz	5-7.5Hz	3.7-4.1 and 5.9-17.2Hz
type 4	not fitted	12-18Hz	6-11Hz	3.7-4.1 and 5.9-17.2Hz

Figure 5 shows the inverted S-wave profiles. The different types of models are given in different colours. Figures 6 and 7 show the fit of the theoretical dispersion curves of the inverted models to the observed dispersion curves. The fit is generally good. The models of type 1 (blue) show profiles that are clearly varying from the others below a depth of 100m. The reason for this is because of the lower H/V-peak we fit. The models of type 4 (cyan), where we did not fit the H/V-curve at all, show the largest variation of Vs for depths greater than 100m. The models that best fit the dispersion curves are obtained for the cyan models and one of the red models.

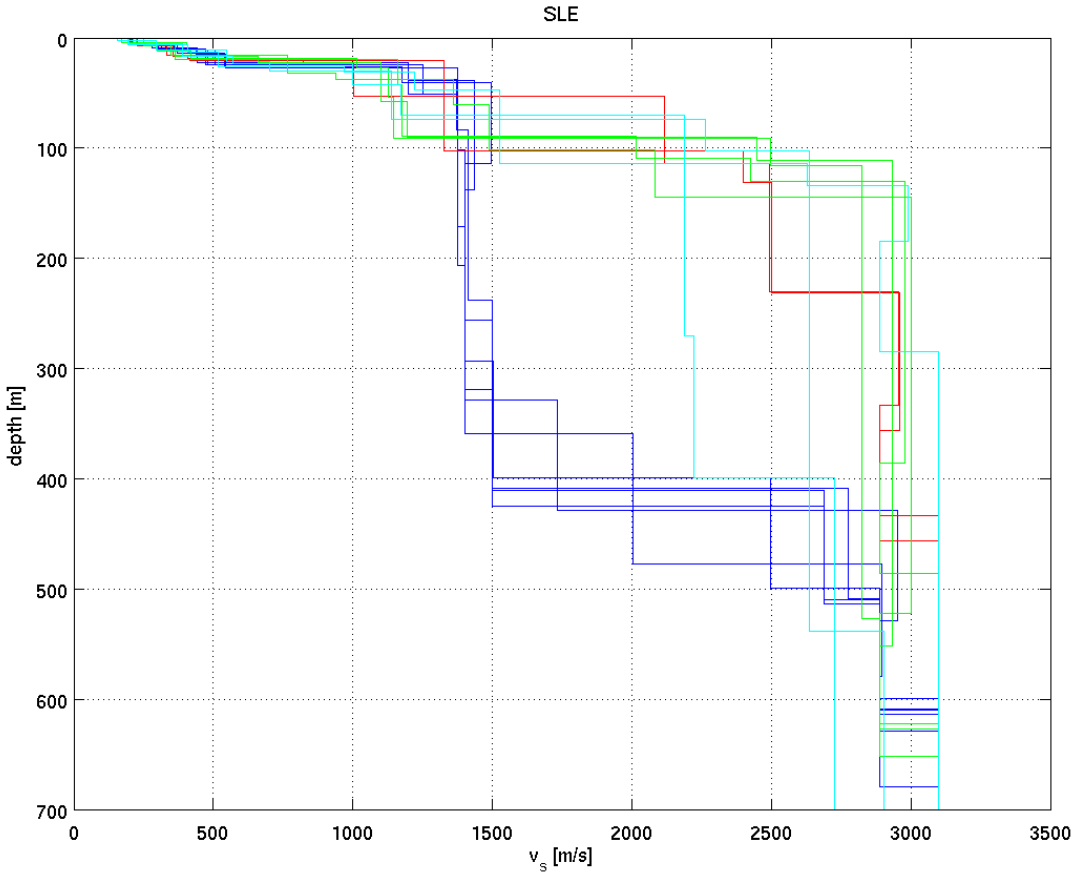

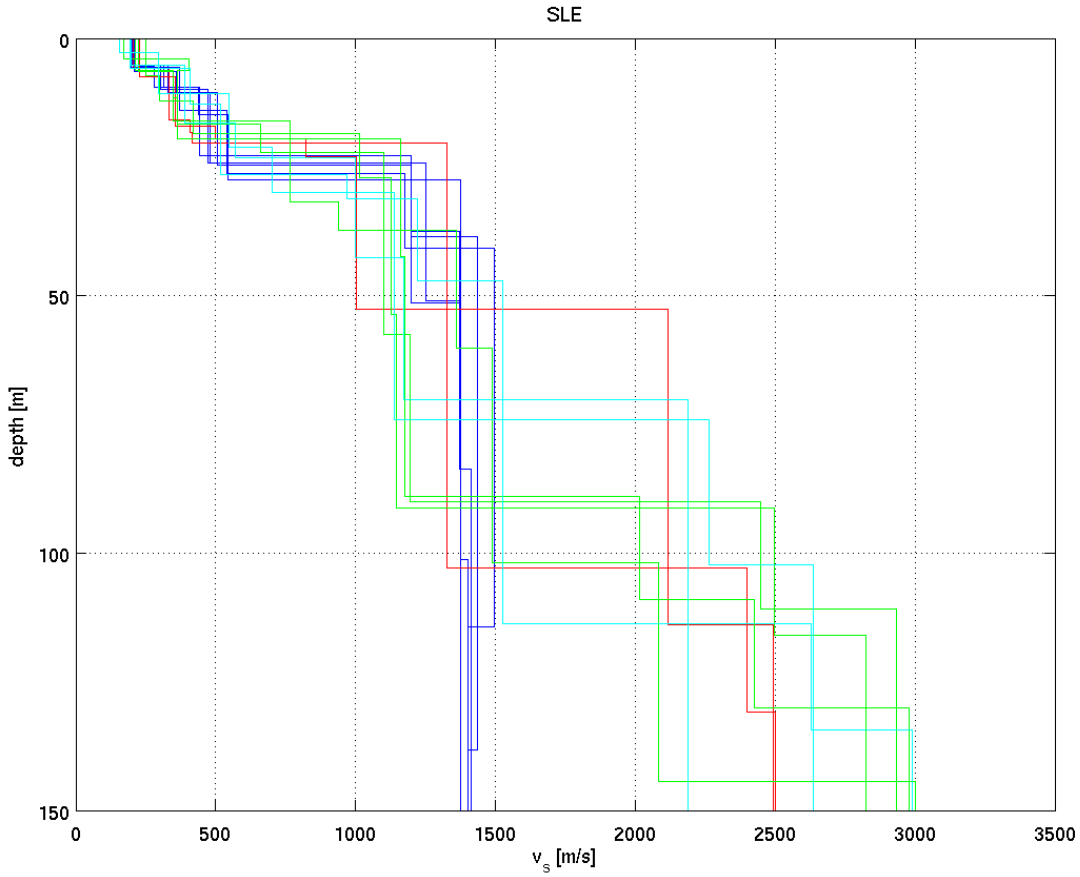

Figure 5: *Inverted S-wave profiles for the site SLE. The models of type 1 are shown in blue, type 2 in red, type 3 in green and type 4 in cyan. The preferred models are the cyan models and one of the red models.*

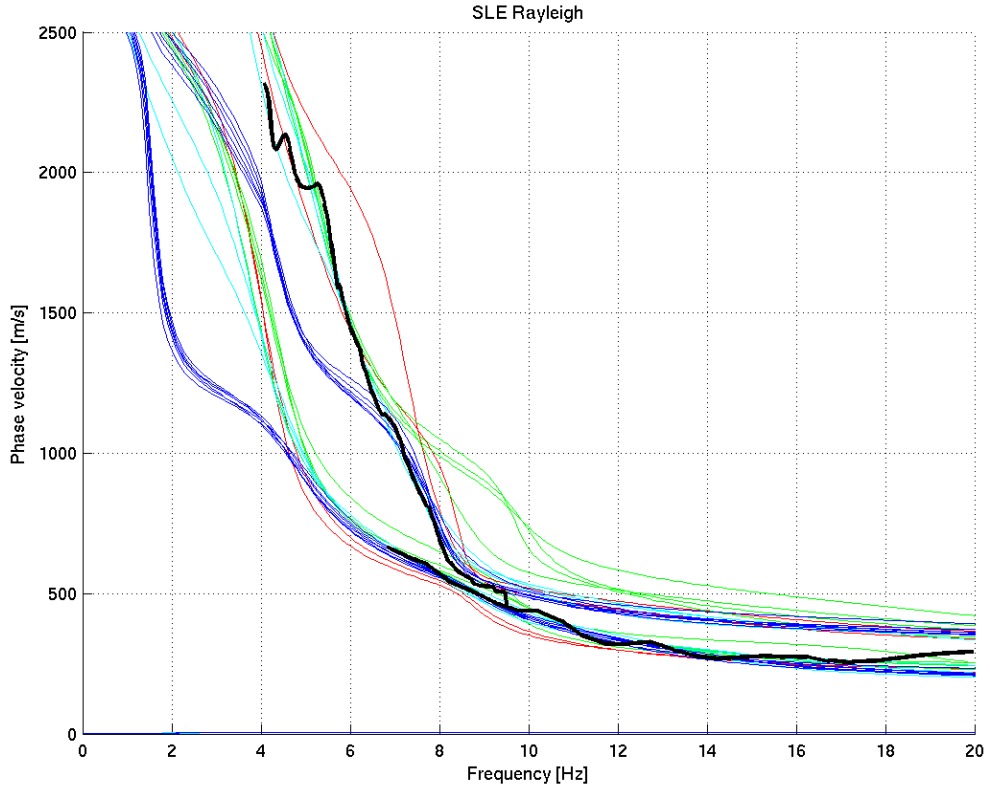

Figure 6: *Comparison between dispersion curves of the inverted structural models (colour) and measured curves for Rayleigh waves.*

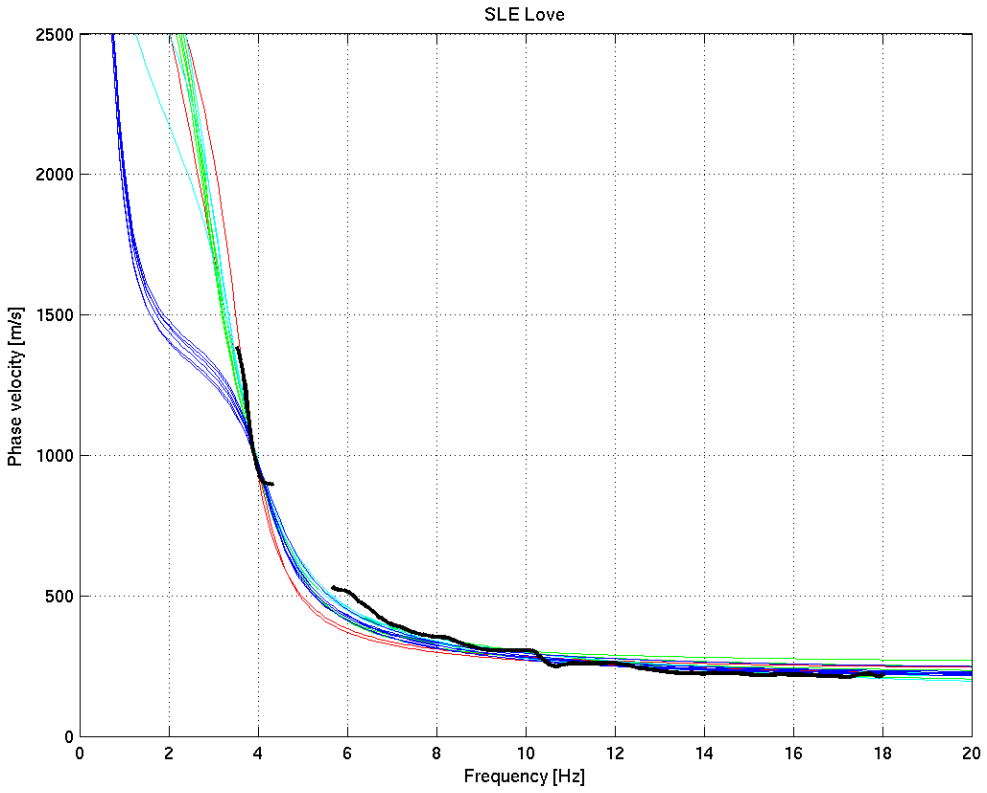

Figure 7: *Comparison between dispersion curves of the inverted structural models (colour) and measured curves for Love waves.*

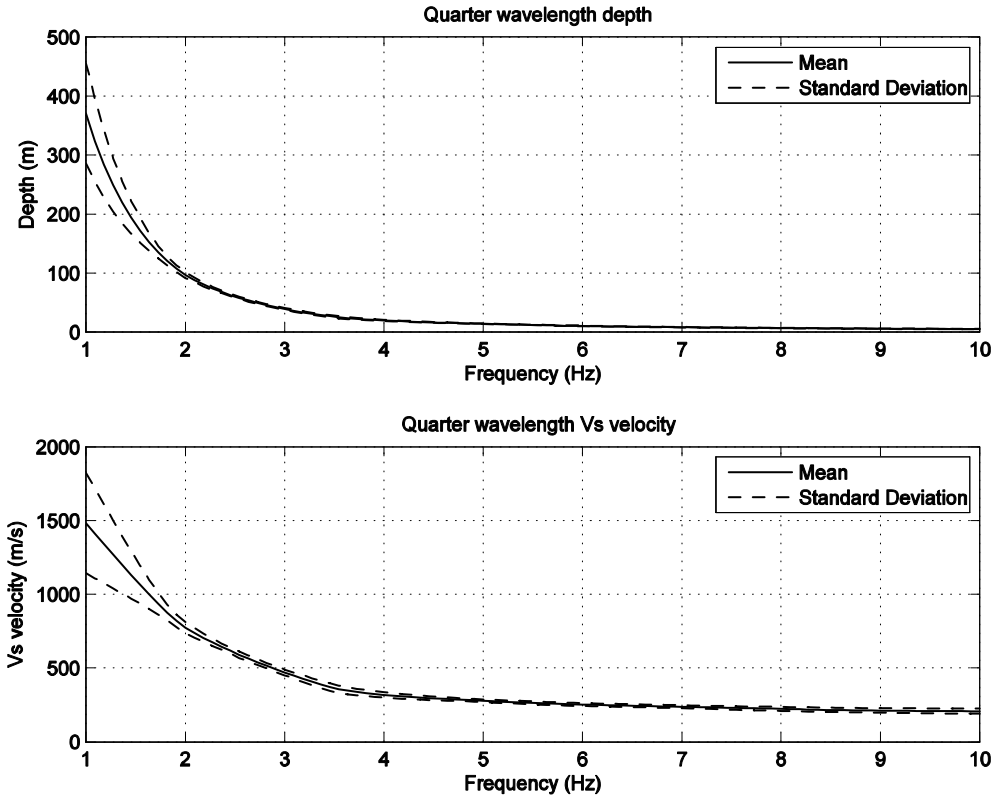

Figure 8: *Quarter wavelength and quarter wavelength velocity as a function of frequency at the site of the arrays SLE1 and SLE2. Notice that this structure is not representative for the site of the seismic station SLE.*

Figure 8 provides the quarter-wavelength velocity and depth as function of frequency. The seismic station SLE is located in a quarry on rock. The soft sediments that were identified with arrays SLE1 and SLE2 are therefore not present at the site of the seismic station SLE, and the surface-velocity structures in Figure 5 and quarter-wavelength velocities in Figure 8 are therefore not representative for the site SLE. We might assume that the deeper layers of the bedrock better represent the structure at the station site. The area around the seismic station SLE is therefore characterized by a structure with strong lateral changes, and the waves recorded at SLE are influenced by the entire complex velocity structure.

6. Possible structures for the array location close to seismic station SLE

The structural models correspond to the cyan models and one of the red models in Fig. 5.

Structure Nr.10 (red)

THICKNESS	DENSITY	P-WAVE VELOCITY	P-WAVE ATTENUATION	S-WAVE VELOCITY	S-WAVE ATTENUATION
THKNES(I)	RHO(I)	A1(I)	A2(I)	B1(I)	B2(I)
0.58514E-02	0.18000E+01	0.64996E+00	0.76927E-02	0.20391E+00	0.49042E-01
0.99981E-02	0.19000E+01	0.66926E+00	0.74710E-02	0.33463E+00	0.29884E-01
0.23807E-02	0.19000E+01	0.12018E+01	0.41606E-02	0.40912E+00	0.24442E-01
0.20906E-02	0.20000E+01	0.17505E+01	0.28564E-02	0.41407E+00	0.24151E-01
0.82502E-01	0.22000E+01	0.27669E+01	0.18071E-02	0.13250E+01	0.75473E-02
0.28161E-01	0.22000E+01	0.41565E+01	0.12029E-02	0.23997E+01	0.41671E-02
0.10050E+00	0.23000E+01	0.43300E+01	0.11547E-02	0.24999E+01	0.40001E-02

Structure Nr.16 (cyan)

THICKNESS	DENSITY	P-WAVE VELOCITY	P-WAVE ATTENUATION	S-WAVE VELOCITY	S-WAVE ATTENUATION
THKNES(I)	RHO(I)	A1(I)	A2(I)	B1(I)	B2(I)
0.27603E-02	0.18000E+01	0.40000E+00	0.12500E-01	0.15454E+00	0.64708E-01
0.79801E-02	0.19000E+01	0.60032E+00	0.83289E-02	0.29419E+00	0.33991E-01
0.10476E-01	0.19000E+01	0.10949E+01	0.45667E-02	0.54744E+00	0.18267E-01
0.87345E-02	0.20000E+01	0.15769E+01	0.31707E-02	0.70345E+00	0.14216E-01
0.44189E-01	0.22000E+01	0.19693E+01	0.25390E-02	0.11370E+01	0.87953E-02
0.28128E-01	0.22000E+01	0.39223E+01	0.12748E-02	0.22645E+01	0.44159E-02
0.43653E+00	0.23000E+01	0.45687E+01	0.10944E-02	0.26377E+01	0.37911E-02

Structure Nr.17 (cyan)

THICKNESS	DENSITY	P-WAVE VELOCITY	P-WAVE ATTENUATION	S-WAVE VELOCITY	S-WAVE ATTENUATION
THKNES(I)	RHO(I)	A1(I)	A2(I)	B1(I)	B2(I)
0.58109E-02	0.18000E+01	0.40038E+00	0.12488E-01	0.19375E+00	0.51614E-01
0.70064E-02	0.19000E+01	0.99357E+00	0.50324E-02	0.40876E+00	0.24464E-01
0.13682E-01	0.19000E+01	0.10327E+01	0.48415E-02	0.51637E+00	0.19366E-01
0.46336E-02	0.20000E+01	0.19377E+01	0.25803E-02	0.96887E+00	0.10321E-01
0.16058E-01	0.22000E+01	0.21159E+01	0.23631E-02	0.12216E+01	0.81861E-02
0.66549E-01	0.22000E+01	0.26405E+01	0.18936E-02	0.15245E+01	0.65595E-02
0.20703E-01	0.23000E+01	0.45499E+01	0.10989E-02	0.26269E+01	0.38068E-02

Structure Nr.18 (cyan)

THICKNESS	DENSITY	P-WAVE VELOCITY	P-WAVE ATTENUATION	S-WAVE VELOCITY	S-WAVE ATTENUATION
THKNES(I)	RHO(I)	A1(I)	A2(I)	B1(I)	B2(I)
0.51564E-02	0.18000E+01	0.40000E+00	0.12500E-01	0.19710E+00	0.50737E-01
0.11280E-01	0.19000E+01	0.77939E+00	0.64153E-02	0.38969E+00	0.25661E-01
0.67162E-02	0.19000E+01	0.11615E+01	0.43048E-02	0.57052E+00	0.17528E-01
0.19504E-01	0.20000E+01	0.19953E+01	0.25059E-02	0.99763E+00	0.10024E-01
0.27616E-01	0.22000E+01	0.20290E+01	0.24643E-02	0.11714E+01	0.85367E-02
0.19989E+00	0.22000E+01	0.37905E+01	0.13191E-02	0.21884E+01	0.45695E-02
0.12902E+00	0.23000E+01	0.38496E+01	0.12988E-02	0.22226E+01	0.44993E-02

7. References

Capon, J., (1969). High-resolution frequency-wave number spectrum analysis, Proc. IEEE, 57(8), 1408-1418.

Fäh, D., Kind, F. and Giardini, D. (2001). A theoretical investigation of average H/V ratios. Geophys. J. Int., 145, 535-549.

Fäh, D., Kind, F. and Giardini, D., (2003). Inversion of local A-wave velocity structures from average H/V ratios, and their use for the estimation of site-effects, J. Seismol., 7, 449-467.

Fäh, D., Stamm, G. and Havenith, H.-B., (2008). Analysis of three-component ambient vibration array measurements, Geophys. J. Int., 172, 199-213.

Kind, F., Fäh, D. and Giardini, D., (2005). Array measurements of S-wave velocities from ambient vibrations, Geophys. J. Int., 160, 114-126.

Yamanaka, H., Takemura, M., Ishida, H. and Niea, M. (1994). Characteristics of long-period micro-tremors and their applicability in exploration of deep layers. Bull. Seism. Soc. Am., 84, 1831-1841

B.3 Array-measurements at the broadband-site “BOURR”

G. Stamm, J. Burjanek, D. Fäh

Location	Bourrignon (JU)
Seismic Station	BOURR
Method(s)	H/V-measurements
Array-measurements	
Date	BOURR1: 29.09.2008
	BOURR2: 24.10.2008
Measurements done by	Gabriela Stamm
Processing done by	Gabriela Stamm, Jan Burjanek

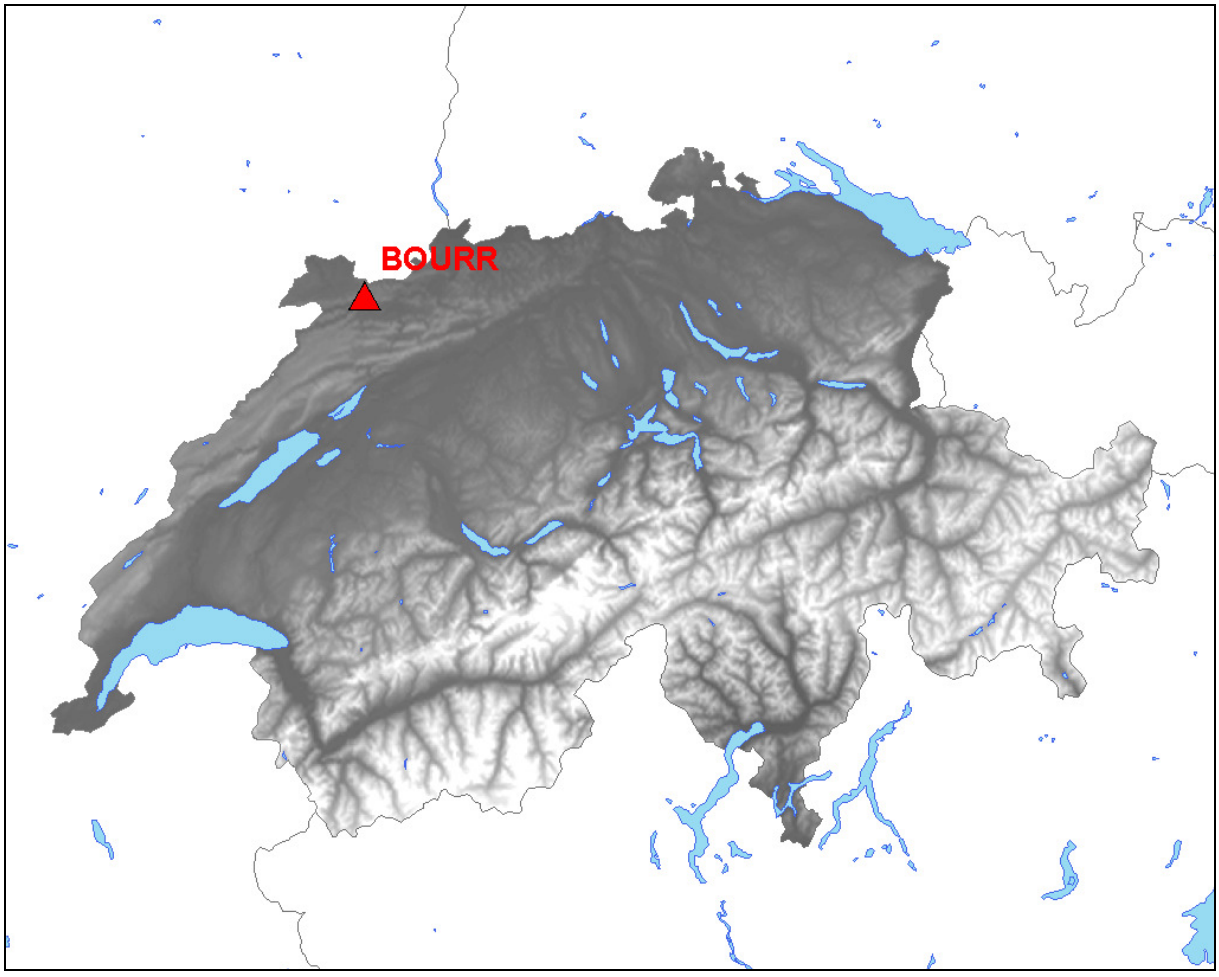

Figure1: *Location of the broadband-site BOURR in Bourrignon (JU).*

1. Method

1.1 H/V

To be sure that the measuring site can be handled as a "1D-case", the H/V-ratios of all array-points were compared together. All Points showing differing curves were then excluded of the array-processing. To compute the H/V-ratios, two different methods were applied. The first one is the classical polarization analysis in the frequency domain, where the polarization is defined as the ratio between the quadratic mean of the Fourier spectra of the horizontal components and the spectrum of the vertical component. The second method tries to reduce the SH-wave influence by identifying P-SV-wavelets from the signal and taking the spectral ratio only from these wavelets. This is done by means of a frequency-time analysis of each of the three components of the ambient vibrations. Both methods are described in more detail in Fäh et al., 2001.

1.2 Array-processing

The array method we use is based on the high-resolution beam-forming (HRBF). It was originally proposed by Capon (1969) but developed and applied to vertical recordings of ambient vibrations by Kind et al. (2005). We have extended this method to analyse also the horizontal components (Fäh et al., 2008).
In general, sub-arrays with different apertures are set up for the measurement to optimise the capabilities in a certain frequency band. Small apertures are used to resolve the shallow part of a structure, and by increasing the aperture, deeper and deeper structures can be investigated. The finale dispersion curve over a wide frequency-range is then composed of the parts obtained by the different sub-arrays. The limits of each sub-array are given by the aliasing at high frequencies and the loss of resolution at low frequencies.

1.3 Inversion

Our inversion scheme is based on a genetic algorithm that was developed by D. Carroll and is described in Fäh et al. (2001, 2003). It does not require explicit starting models but only the definition of parameter limits. To estimate the average S-wave velocity structure below our array, we use as input the combined H/V spectral ratios and phase velocity curves for Rayleigh- and Love-Waves.

2. Array-Configuration

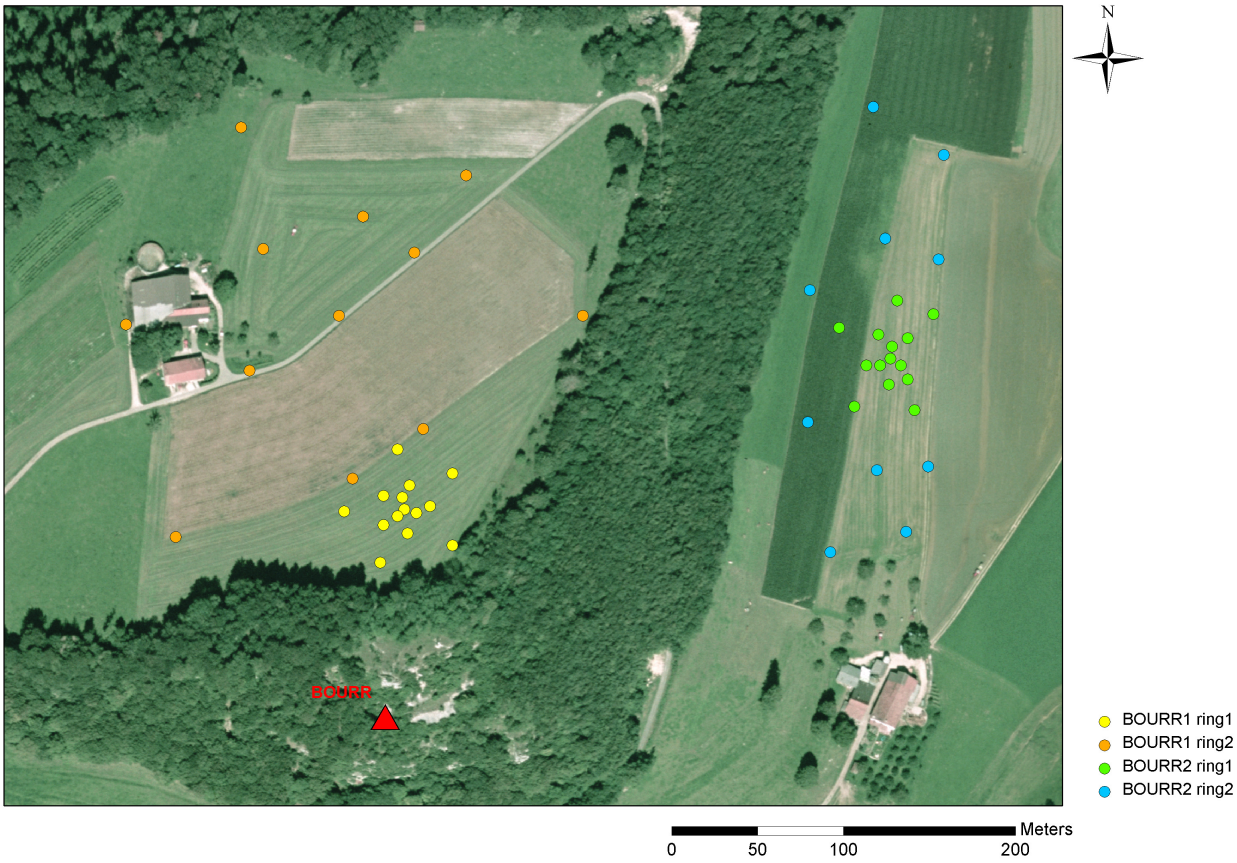

Figure 2: *Array-Configuration for BOURR1 and BOURR2.*

The site BOURR is located at a Jurassic hill range with two terraces. We set up two arrays, one on each terrace. The array BOURR1 is some tens of meters above the altitude of the broadband-station BOURR, the array BOURR2 is located at lower altitude.

Table 1: *important parameters of the array-setups.*

	BOURR1 ring1	BOURR1 ring2	BOURR2 ring1	BOURR2 ring2
# Sensors	14	13	14	11
max. Radius [m]	35	150	35	120
min. distance between two sensors [m]	7	60	7	65
max. distance between to sensors [m]	70	270	65	240

3. H/V

The comparison of the H/V-ratios of all stations from BOURR1 ring1 and ring2 show only one outlier in ring1. This station was then excluded from the array-processing. For BOURR2 ring2 we had to exclude four stations (those shown in green).

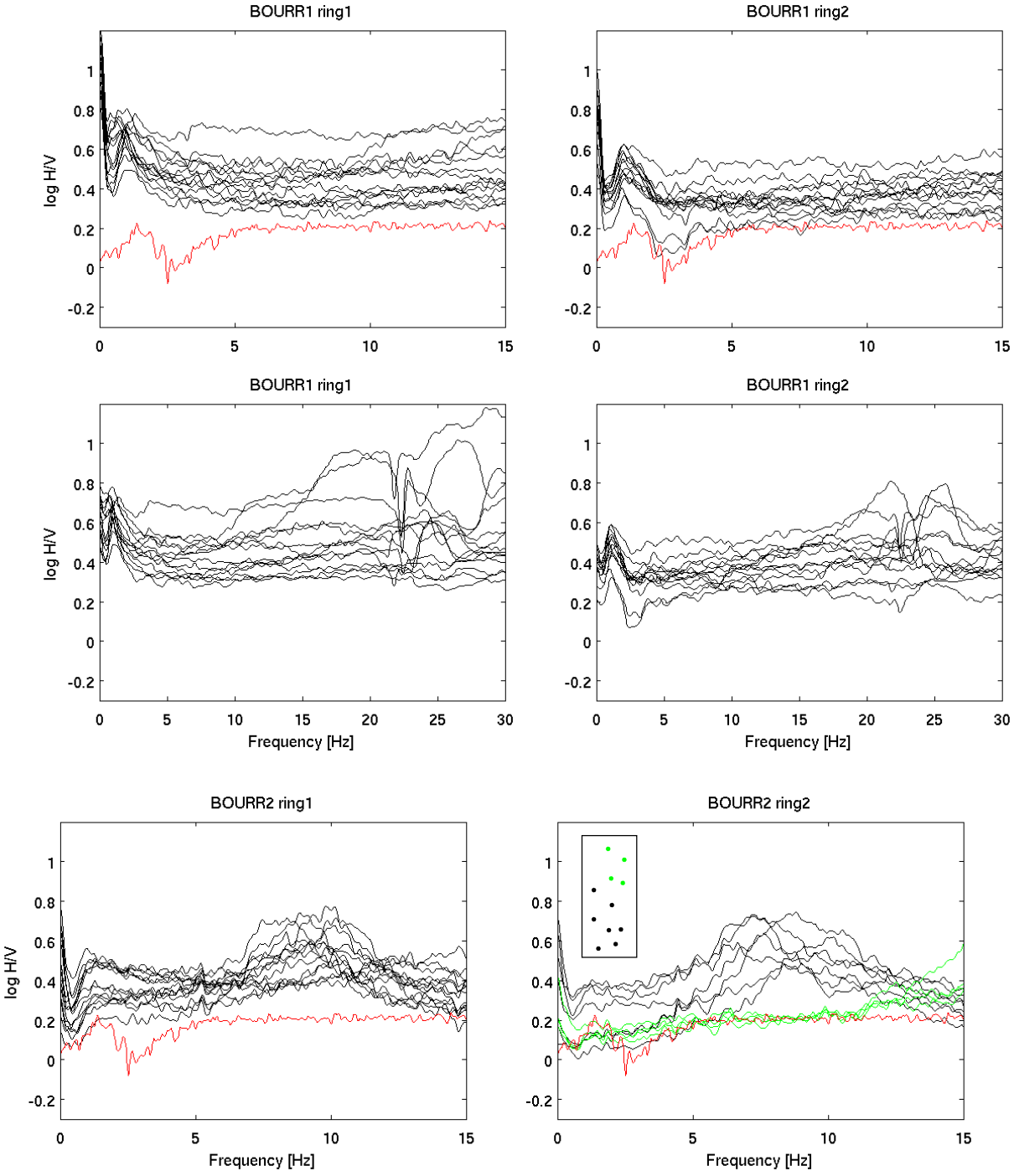

Figure 3: *Comparison of the H/V-ratios of all points measured in BOURR1 and BOURR2 (black) with that from the broadband-station BOURR (red). For BOURR2 ring2 some points (northern part of the array) are plotted in green because they show a differing H/V-ratio.*

4. Dispersion curves

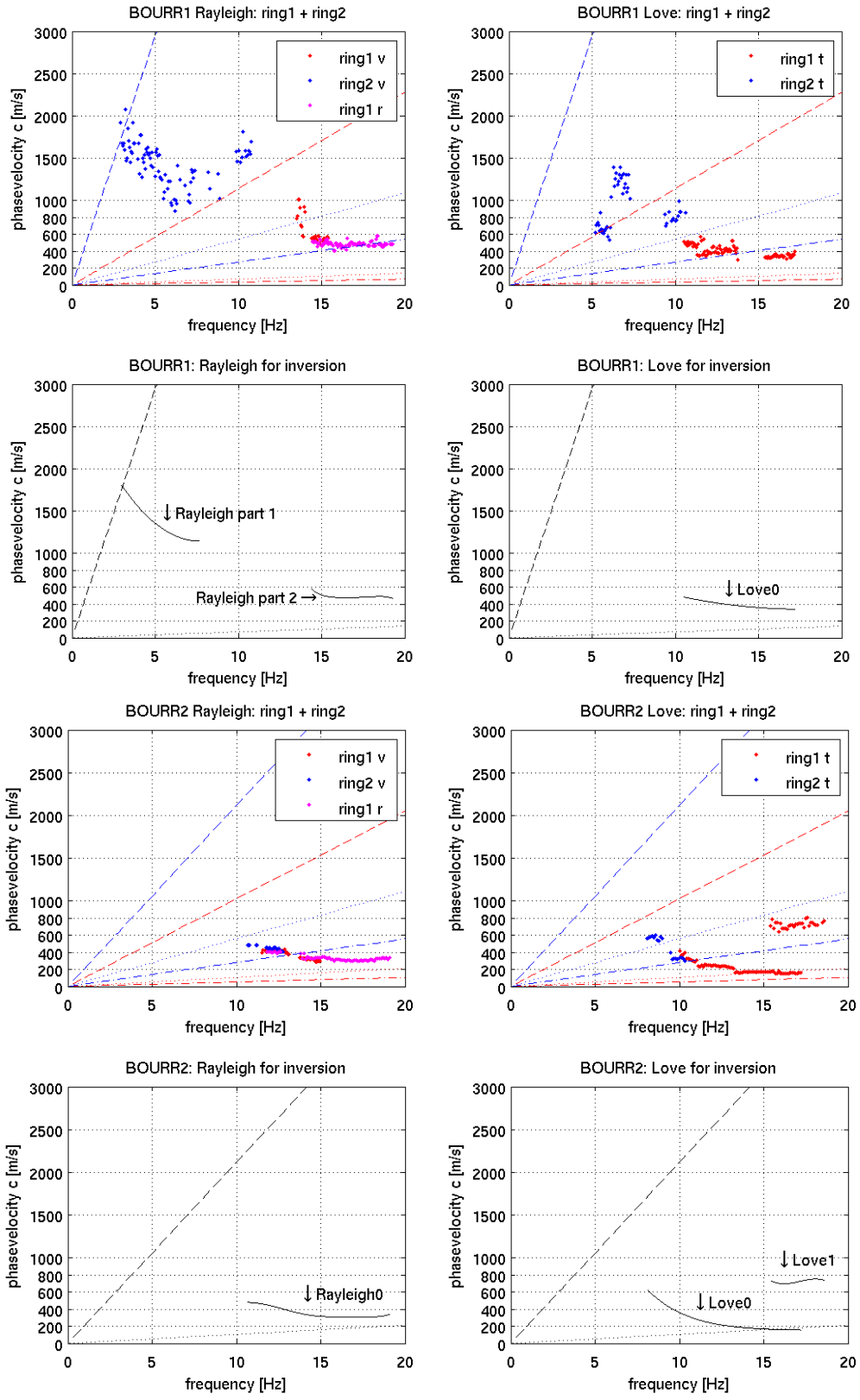

Figure 4: *Rayleigh- and Love-Dispersion curves for BOURR1 and BOURR2. (v: vertical components, r: radial components, t: transverse components.)*

For BOURR1 the processing of ring1 provides parts of the fundamental modes of Rayleigh- and Love-waves for frequencies above 10Hz. On the vertical components of ring2 the picked points are quite scattered, but nevertheless we considered it either as a part of the first higher mode or as the fundamental mode of Rayleigh-waves.
For BOURR2, parts of the fundamental modes of Rayleigh- and Love-waves were clearly visible, and also a part of the first higher mode of Love-waves could be found.

5. Inverted Profiles

BOURR1:
Table 2 gives the description of three different types of models that were run for the site BOURR1. For all models, the Love wave dispersion curve between ~11-17Hz was fit as part of the fundamental mode. The two parts of Rayleigh wave dispersion curve were once fit both as fundamental mode (type 2), and then part 1 as fundamental mode and part 2 as first higher mode (type 3) and vice versa (type 1). Only for the type 1 models we tried to fit also the H/V curve between 1 and 1.9Hz. However, because the fit was poor we did not repeat this for the two other types of model. The different assignments of Rayleigh modes take into account the large scatter of the picked phase velocities at low frequencies.
In Figure 5 the inverted S-wave profiles are shown. The different types of models for BOURR1 are given in different colour. The models of type 1 are printed in blue, type 2 in red and those of type 3 in green. The biggest differences between the different types are visible between a depth of 25m and 150m due to the assignment to a mode number and the loss of resolution below a certain depth.

Table 2:

	H/V	Rayleigh fund. mode	Rayleigh 1. higher mode	Love fund. mode
type 1	1-1.9Hz	14.5-18.5Hz	3.1-7.5Hz	11-17Hz
type 2	not fitted	3-8.5Hz and 14-19Hz	-	11-17Hz
type 3	not fitted	3.2-8Hz	14-19Hz	11-16.5Hz

BOURR2:
For the site BOURR2, only one type of model was inverted (see Table 3). After the experience with the inversion at site BOURR1 we did not try to fit the H/V-curve for the site BOURR2 (the peak is also less clear at the site BOURR2). The picked parts of dispersion curves could be assigned to the fundamental or first higher mode. Due to the restricted information contained in the dispersion curves, and the measured low velocities, the measurements are not useful to characterize the site of the instrument (the station is in a bunker, presumably in rock). The location of the array BOURR2 is on a site with very soft sediments (vs around 200 m/s). For BOURR2 only one type of model was inverted for (see Figure 5).

Table 3:

	H/V	Rayleigh fund. mode	Love fund. Mode	Love 1. higher mode
Type 1	not fitted	11-17Hz	8.2-15.5Hz	16-18Hz

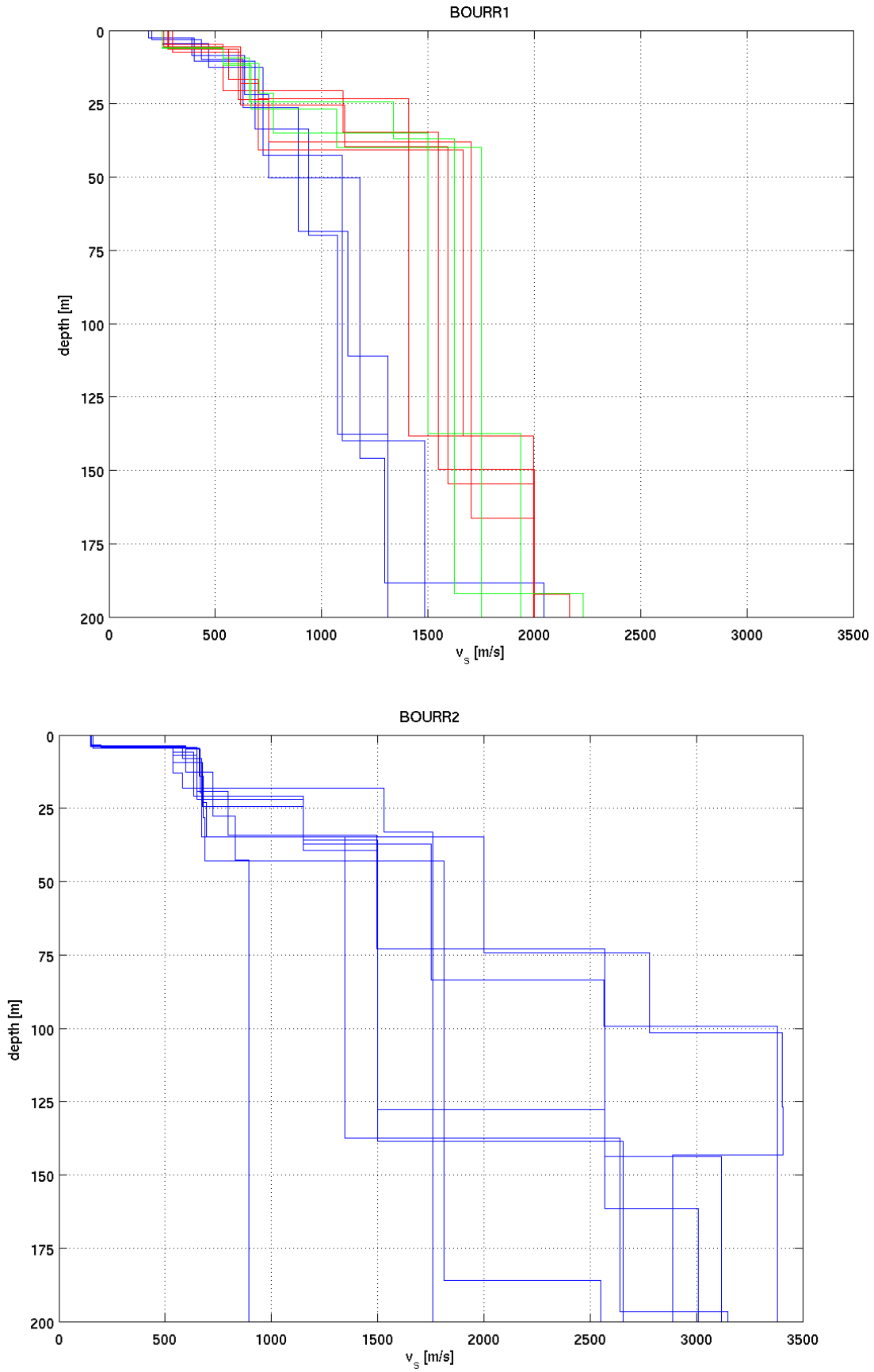

Figure 5: *Inverted S-wave profiles for the sites BOURR1 and BOURR2.*

Figures 6 and 7 show the fit of the theoretical dispersion curves of the inverted models to the observed dispersion curves for site BOURR1. The fit is generally good except for the type 3 models (green curves) and Love waves in Figure 7.

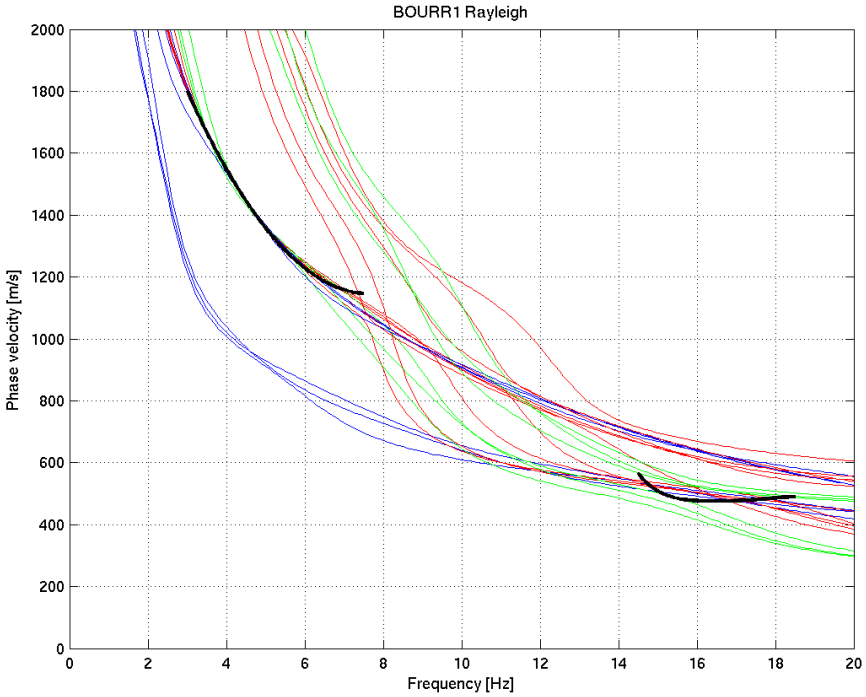

Figure 6: *Comparison between dispersion curves of the inverted structural models (black) and measured curves for Rayleigh waves (colour). The different types of models for BOURR1 are given in different colours according to Table 2. The fundamental and first higher modes are shown for all models.*

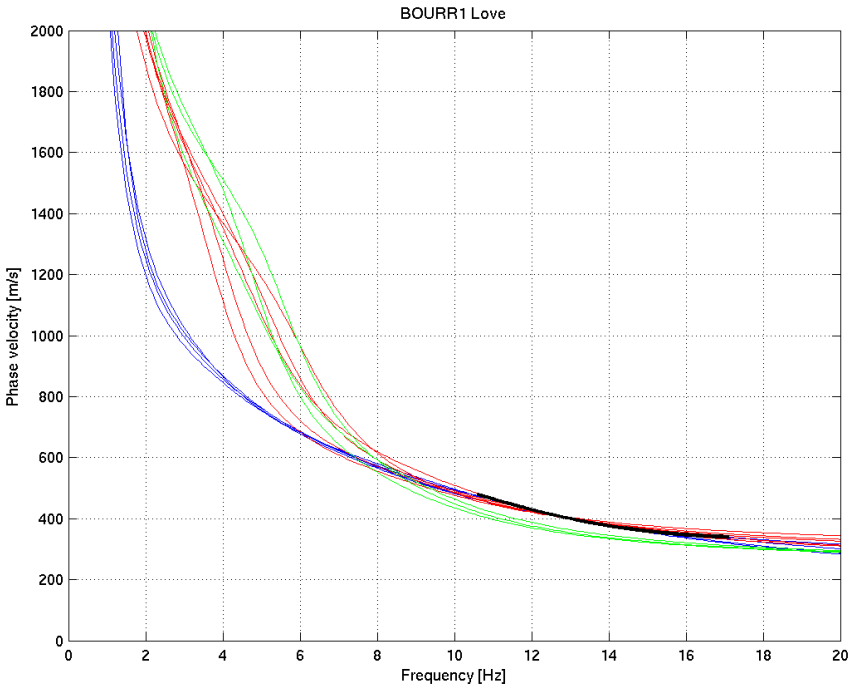

Figure 7: *Comparison between dispersion curves of the inverted structural models and measured curves for Love waves. The different types of models for BOURR1 are given in different colours according to Table 2. Only the fundamental mode is shown for each model.*

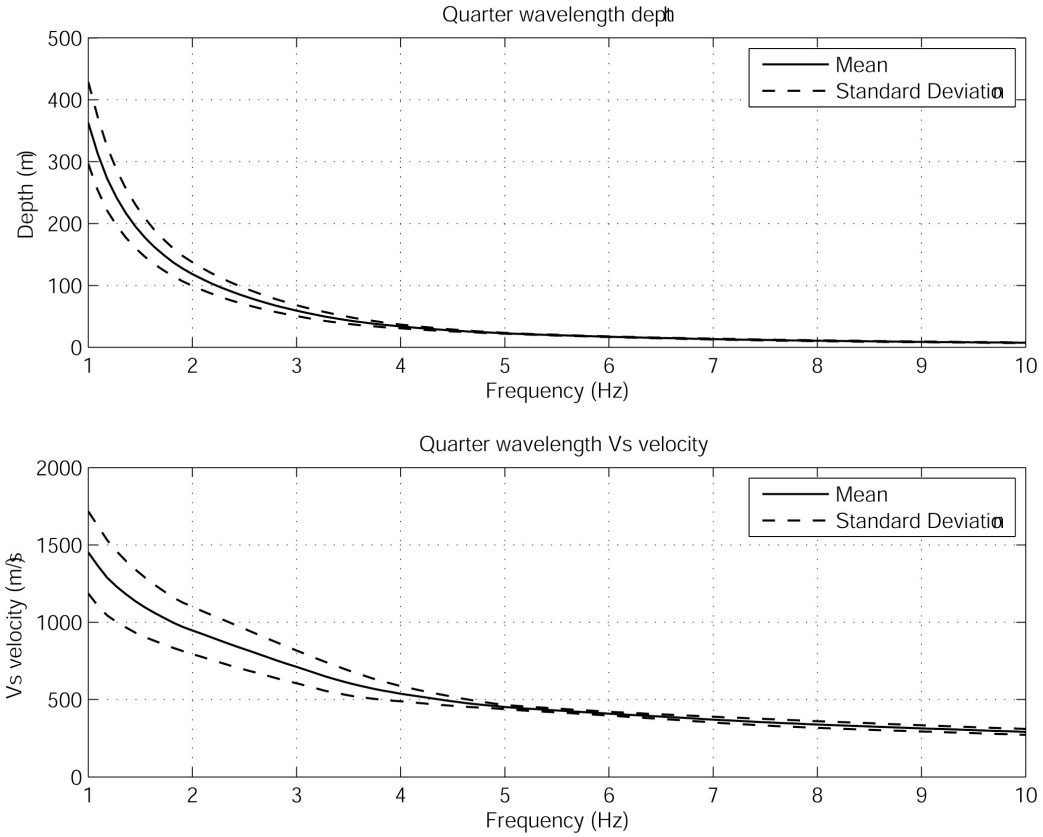

Figure 8: *Quarter wavelength and quarter-wavelength velocity as a function of frequency at the site of the arrays at BOURR1.*

Finally Figure 8 provides the quarter-wavelength velocities and depth as function of frequency for the ambient vibration array measurements. The seismic station BOURR1 is located in a bunker on rock. Table 4 summarizes the mean velocity for different thicknesses from the free surface of the upper terrace (Figure 2). The average velocity is computed in a way such that the travel-time in an average model corresponds to the sum of the travel times in the single layers:

$$\frac{1}{\bar{v}} = \frac{1}{H}\sum_{i=1}^{n}\frac{h_i}{v_i} \qquad \text{with} \qquad H = \sum_{i=1}^{n} h_i \,.$$

Table 4: *Mean S-wave velocity at BOURR1 over the thickness H.*

H [m]	Vs mean [m/s]	Vs stdev [m/s]
5	262	16
10	331	13
20	433	9
30	508	18
40	577	36
50	648	51
100	886	94
150	1022	118
200	1138	137

6. References

Capon, J., (1969). High-resolution frequency-wave number spectrum analysis, Proc. IEEE, 57(8), 1408-1418.

Fäh, D., Kind, F. and Giardini, D. (2001). A theoretical investigation of average H/V ratios. Geophys. J. Int., 145, 535-549.

Fäh, D., Kind, F. and Giardini, D., (2003). Inversion of local A-wave velocity structures from average H/V ratios, and their use for the estimation of site-effects, J. Seismol., 7, 449-467.

Fäh, D., Stamm, G. and Havenith, H.-B., (2008). Analysis of three-component ambient vibration array measurements, Geophys. J. Int., 172, 199-213.

Kind, F., Fäh, D. and Giardini, D., (2005). Array measurements of S-wave velocities from ambient vibrations, Geophys. J. Int., 160, 114-126.

Yamanaka, H., Takemura, M., Ishida, H. and Niea, M. (1994). Characteristics of long-period micro-tremors and their applicability in exploration of deep layers. Bull. Seism. Soc. Am., 84, 1831-1841.